CORA Cork Open Research Archive
Cartlann Taighde Oscailte Chorcaí

Title	The impact of variation in freezing and thawing process parameters on the critical quality attributes of a monoclonal antibody
Authors	Day, Neil
Publication date	2019-09-23
Original Citation	Day, N. B. 2019. The impact of variation in freezing and thawing process parameters on the critical quality attributes of a monoclonal antibody. MRes Thesis, University College Cork.
Type of publication	Masters thesis (Research)
Rights	© 2019, Neil Day. - https://creativecommons.org/licenses/by-nc-nd/4.0/
Download date	2026-11-03 01:28:02
Item downloaded from	https://hdl.handle.net/10468/9969

UCC
University College Cork, Ireland
Coláiste na hOllscoile Corcaigh

Ollscoil na hÉireann, Corcaigh

National University of Ireland, Cork



The Impact of Variation in Freezing and Thawing Process Parameters on the Critical Quality Attributes of a Monoclonal Antibody

Thesis presented by

Neil Day, B.Sc., CChem MRSC

for the degree of

Master of Science

in

Pharmacy – Pharmaceutics

at

University College Cork

School of Pharmacy

Head of School: Professor Stephen Byrne B.Sc. (Pharm.), Ph. D., M.P.S.I

Supervisors: Dr Sonja Vucen MPharm., Ph D.,

Dr. Abina Crean B.Pharm., Ph. D., M.P.S.I

Table of Contents

Declaration iii
Acknowledgements iv
List of Acronyms v
Abstract vi
1.0 Introduction 1
1.1 Therapeutic Proteins 1
1.2 Monoclonal Antibody Manufacturing Process 3
1.3 Destabilisation and Aggregation of Therapeutic Proteins 4
1.4 Analytical Techniques to Determine Protein Degradation 6
1.5 Freeze/Thaw-Induced Protein Aggregation 7
1.5.1 Cryo-Concentration 8
1.5.2 Solute Crystallisation 10
1.5.3 Low Temperature Destabilisation 11
1.5.4 pH Shifts 11
1.5.5 Exposure to Liquid-Air Interface 12
1.5.6 Polar Interactions 12
1.6 Freeze/Thaw Studies of Therapeutic Proteins 13
1.6.1 Scalability 15
1.7 Aims and Objectives 19
2.0 Equipment, Materials and Methods 20
2.1 Equipment 20
2.2 Materials 20
2.2.1 Drug Substance Technical Overview 22
2.2.2 Bulk Manufacturing of Protein Y 22
2.2.3 Formulation of the Product 23
2.3 Methods 23
2.3.1 Formulation Characterisation Studies 23
2.3.1.1 Differential Scanning Calorimetry (DSC) 24
2.3.1.2 Freeze Drying Microscopy (FDM) 24
2.3.1.3 Evaluation of pH Change in Dilution Buffer 24
2.3.2 Protein Y Characterisation Studies 25
2.3.2.1 Differential Scanning Calorimetry (DSC) 25
2.3.2.2 Size Exclusion Chromatography (SEC) 25
2.3.2.3 Dynamic Light Scattering (DLS) 26
2.3.2.4 Circular Dichroism Spectroscopy (CD)/UV-Absorbance 27
2.3.2.5 Fluorescence Spectroscopy 28
2.3.3 Freeze-Thaw Studies 29
2.3.3.1 Experimental Design of Experiments (DoE) 29
2.3.3.2 Thawing of Bulk FDS 33
2.3.3.3 Freeze/Thawing Experimental Procedure 33
3.0 Results 35

3.1 Formulation Characterisation 35
3.1.1 Modulated Differential Scanning Calorimetry (DSC) 35
3.1.2 Freeze Drying Microscopy (FDM) 36
3.1.3 Evaluation of pH Change in Dilution Buffer upon Freezing 38
3.2 Protein Y Characterisation Studies 39
3.2.1 Differential Scanning Calorimetry (DSC) 39
3.2.2 Dynamic Light Scattering (DLS) 41
3.2.3 Circular Dichroism Spectroscopy (CD)/UV-Absorbance 45
3.2.4 Fluorescence Spectroscopy 47
3.3 Freeze-Thaw Studies 48
3.3.1 Temperature Profile Results 51
3.3.1.1 Freezing 52
3.3.1.2 Thawing 57
3.3.2 DoE Results – Post Thaw 60
3.3.2.1 Cryo-Concentration 60
3.3.2.2 Protein Unfolding 62
3.3.2.3 Protein Tertiary Structure 63
3.3.2.4 Protein Aggregation 69
3.3.3 Stability Studies 71
3.3.3.1 Protein Unfolding 71
3.3.3.2 Protein Tertiary Structure 72
3.3.3.3 Protein Aggregation 78
3.4 Scalability of the Data 82
4.0 Discussion 87
4.1 Analytical Methods 87
4.2 Freeze-Thaw DoE 88
4.2.1 Influence of process parameters on freeze/thaw profiles and Protein Y cryo-concentration 88
4.2.2 Protein Y structural changes during freeze/thaw processes 90
4.2.3 Protein Y aggregation during freeze/thaw processes 92
4.2.4 Protein Y structural changes during post-thaw stability study 92
4.2.5 Protein Y aggregation during post-thaw stability study 93
4.3 Validity of the Small-Scale Model to Understand the Behaviour of the Respective Full-Scale Commercial Process 93
5.0 Proposals for Future Work 97
6.0 Conclusions 101
7.0 Bibliography 102

DECLARATION

This thesis is submitted to the National University of Ireland, University College Cork by Neil Day for examination in the degree of Master of Science (Pharmacy – Pharmaceutics). This thesis has not been submitted for any other purpose or degree offered by this or any other university. The material presented in this thesis is entirely the author's own original work, except where duly noted and acknowledged. This thesis was authored by Neil Day with supervision and editorial advice from my supervisors, Dr Sonja Vucen and Dr Abina Crean.

Signature: Date:

ACKNOWLEDGEMENTS

I would like to offer sincere thanks to my manager at Sanofi; Maureen McLaughlin for supporting my efforts with this research project and allowing me the opportunity to understand protein science in further depth.

I would also like to thank all the members of the Sanofi Waterford Manufacturing Sciences team who accommodated me in the laboratory and made me feel part of the team. In particular, special thanks to; Tim McCoy, Sean Cullen, Evin Allen, Kumar Khamar and Kevin O'Connor for giving of their time to provide me with invaluable help and advice.

Sincere thanks to my UCC supervisors; Abina Crean and Sonja Vucen for their encouragement, guidance and support throughout the project. I'm especially grateful to Sonja for her patience and guidance in review of the earlier drafts of this thesis and Abina for ensuring I stayed focused on the aims of the project.

I would like to thank my parents; Barry and Janet, who have always encouraged my education through my school life and helped me get to where I am today.

I would also like to acknowledge the love and support of my wife Eileen; you helped me believe in myself and keep me focused in the tougher moments of this project.

Lastly, I would like to dedicate this work to my children; Caleb, Muireann and Óran, who are all in different stages of their own educational journeys. You have inspired me to rekindle my own curiosity and realise we're learning something new every day.

LIST OF ACRONYMS

CD – circular dichroism

CQA – critical quality attribute

DLS – dynamic light scattering

DoE – Design of Experiments

DSC – differential scanning calorimetry

FDM – freeze drying microscopy

FDS – formulated drug substance

HPLC – high performance liquid chromatography

mAb – monoclonal antibody

Phen - phenylalanine

SEC – size exclusion chromatography

Trp – tryptophan

Tyr – tyrosine

UV - ultraviolet

λ - lambda

λ_{max} – lambda maximum

ABSTRACT

Therapeutic proteins or biopharmaceuticals have been playing an ever-increasing role in the treatment of human diseases over last 40 years. One of the main challenges with manufacture of these proteins is the stabilization of both the finished product and its processing intermediates during storage. Freezing and frozen storage is widely applied to improve stability of the bulk drug substance. The process of freezing a protein results in stresses that can cause protein degradation and subsequent aggregation.

The aim of this project was to evaluate the effect of parameters involved with freezing and thawing of a formulated monoclonal antibody solution in polycarbonate bottles and to assess the scalability of these experiments to the respective full-scale commercial process.

Initial experiments were performed to characterise the formulation and develop analytical methods that can detect change in unfolding and aggregation of a fully human IgG1 monoclonal antibody ('Protein Y'). A designed set of experiments were then executed to understand the effect of parameters involved in freezing and thawing steps of a formulated therapeutic protein solution on protein aggregation and perturbations in tertiary structure. Results showed that the processing parameters studied caused significant variation in freeze and thaw process times, with the factors causing slower rates of freeze and thaw also shown to cause changes in the tertiary structure of Protein Y. Despite the observed changes in tertiary structure, the effect on aggregation was less pronounced, with only a significant change noted for the polydispersity index (PdI), as measured by dynamic light scattering (DLS).

1.0 INTRODUCTION

1.1 Therapeutic Proteins

Therapeutic proteins are a subset of biopharmaceuticals which have been playing an ever-increasing role in the treatment of human diseases over the last 40 years. These protein therapies have made great advances in the treatment and prevention of many rare and severe diseases including diabetes, cancer, anaemia, autoimmune and inflammatory diseases (Lamanna et al., 2018).

There are several variant classes of therapeutic protein, including vaccines, hormones, enzymes, monoclonal and polyclonal antibodies and fusion proteins. Over 370 biopharmaceutical drug products using protein molecules were approved to date for human therapeutic use in the European Union (EU) and United States of America (USA). The most dominant sub-class within therapeutic proteins are monoclonal antibodies, which have comprised over half (53%) of first time approvals from 2015 to July 2018 (Walsh, 2018).

However, based on the multi-dimensional nature of these therapeutic proteins relative to small molecule therapies, the increased effectiveness in treatment comes with added complexity to ensure that protein critical quality attributes (CQAs) are maintained. The biological function and activity of these therapeutic proteins are defined by their specific three-dimensional structure and shape, which can be broken down into primary, secondary, tertiary and sometimes quaternary structure. Protein folding and unfolding are crucial ways of regulating biological activity and targeting proteins to different cellular locations. Only correctly folded proteins have long-term stability in crowded biological environments and the failure of proteins to fold correctly, or to remain correctly folded, is the origin of a wide variety of pathological conditions (Dobson, 2003).

Antibodies are a type of immunoglobulin made by B-cells in the body when the cell encounters its matching antigen. B-cells mature in the bone marrow and activation occurs in lymphoid tissues. Each mature B-cell makes a specific antibody that recognises a specific antigen. Antibodies contain two identical heavy polypeptide chains and two identical light polypeptide chains as illustrated in **Figure 1-1**. Furthermore, each chain contains a variable region and a constant region. The variable regions of the heavy and light chains come together to form two antigen binding sites (the 'tips' of the Y), known as the Fab region. The opposite end of the chains form, the constant region, which encodes effector functions that destroy whatever is bound by the Fab region. The chains are connected together by disulphide bonds and non-covalent forces (Vermeer and Norde, 2000).

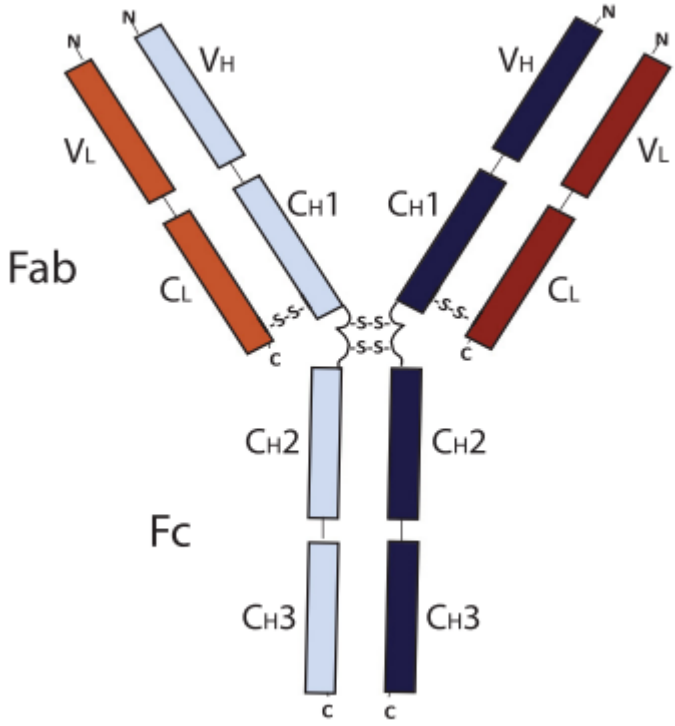


Figure 1-1: Illustration of a monoclonal antibody structure (Shah et al., 2018)

1.2 Monoclonal Antibody Manufacturing Process

The nature of the commercial monoclonal antibody manufacturing process means it can take a few months to manufacture one batch of formulated drug substance solution (FDS). The host cells undergo weeks of scale-up through upstream cell culture processes followed by several purification operations. In addition, as the proteins are expressed biologically from inside a host cell there is inherent variability linked with the expression based on the cell line, between different clones derived from the same parental cell line and even between proteins produced by the same cell (Vulto and Jaquez, 2017). The process of manufacturing therapeutic proteins expressed from mammalian cells typically follows a common process flow with subtle product specific variation.

The first step of the process is to extract cells from a cell bank for initiation of cell culturing in growth media. This is usually started in shaker flasks at sub-one litre levels. The cell culture is scaled up until a sufficient cell density is reached to perform harvest of the expressed protein. Clarification is then performed to remove cell debris from the solution. This is typically done by depth filtration or centrifugation. The protein solution is then purified via a number of chromatography steps. Removal of viruses occurs through filtration. The protein solution is concentrated to the correct content via ultrafiltration and diafiltration, followed by further filtration to ensure sterility and formulation to ensure drug product stability. The formulated drug substance solution is then aseptically filled into the primary container closure system for dosing to patients. The container closure system can be a vial, pre-filled syringe or cartridge for insertion into an injector pen. Furthermore, FDS filled into vials may be lyophilised (freeze-dried) to ensure drug product stability is maintained (Jagschies et al., 2018).

With the rapid growth of the biologic drug pipeline, new challenges have arisen with regards to formulating and processing of such products. One of the main challenges is the stabilization of biologics, both as a finished product, as well as processing intermediates during storage. Besides lyophilisation, a well-established process often used for finished products (i.e. FDS) is freezing. Frozen storage is widely applied to improve stability of bulk drug substance or clinical trial formulations. In addition to increased quiescent storage stability, both lyophilized and frozen products are less sensitive to mechanical stress experienced during transport (Radmanovic et al., 2013). In the case of liquid formulations, mechanical stress during transport (e.g. shaking) results in significant changes to protein critical quality attributes, necessitating extensive transport studies. A further advantage of frozen storage is a significant reduction of microbial growth, which is especially relevant in the case of bulk drug substance storage. All these considerations result in a significant interest in frozen storage of biologic products.

1.3 Destabilisation and Aggregation of Therapeutic Proteins

Degradation of protein refers to a physical or chemical change from the native conformation that may result in inactivity and/or aggregation. Degradation is usually a prelude to aggregation, where aggregation refers to the association of two or more protein molecules. Protein aggregates can cause immune responses resulting in adverse effects in patients ranging from skin rashes to anaphylaxis (Wang and Roberts, 2010). Therefore, it is critical to understand these mechanisms of aggregation and therefore prevent them occurring prior to patient administration.

There are a number of external factors to which protein molecules are subjected during manufacturing that could induce degradation. Aggregation and related particle formation is a dominant degradation pathway of antibodies and can occur during all

stages of protein therapeutic processing and storage (Singh and Nema, 2010). Antibody aggregation is complex and can proceed through covalent or non-covalent association that is highly dependent on the solution conditions, including pH, ionic strength, and excipients. The covalent associations can be due to disulphide or non-disulphide covalent bonds, while the non-covalent associations usually appear as a result of hydrophobic or electrostatic interactions (Singh and Nema, 2010).

Figure 1-2 describes different protein aggregation pathways and shows that pathways can lead to reversible and non-reversible aggregation. Covalent aggregates are generally irreversible and occur as the result of a chemical modification such as oxidation. Reversible aggregation can include the association of the hydrophobic patches of two proteins that are partially unfolded caused by the physical stresses of processing. Partially unfolded proteins aggregate easier than fully unfolded proteins due to the optimal exposure of hydrophobic patches. As aggregates increase in size they precipitate from the solution, becoming visible. Precipitated aggregates or flocculation are generally irreversible (Wang et al., 2010).

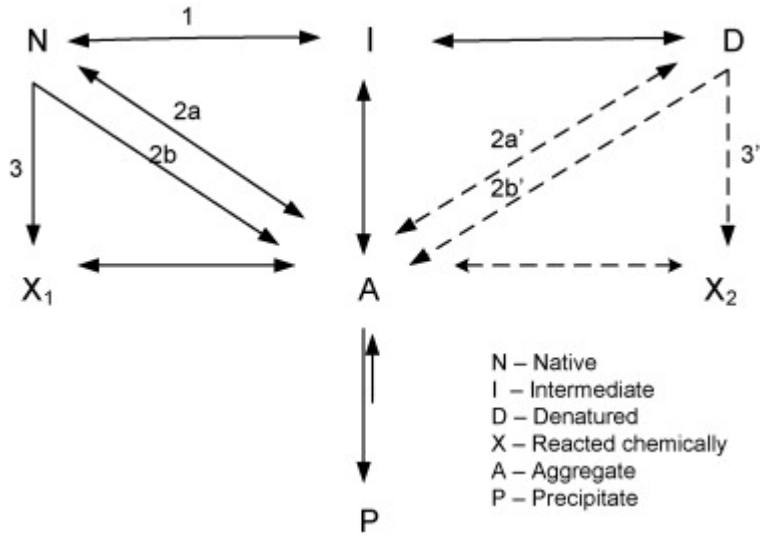


Figure 1-2: Graphic illustration of major protein aggregation pathways (adopted from Wang et al., 2010)

Non-native protein aggregation (hereafter referred to as “aggregation”) describes the assembly from initially native, folded protein aggregates containing non-native intermolecular-sheet structures (Dong et al., 1995). Protein aggregation behaviour, such as onset, aggregation rate, and the final morphology of the aggregated state (i.e. amorphous precipitates or fibrils) has been found to depend strongly on the properties of a protein’s solution environment, such as temperature, pH, salt type, salt concentration, co-solutes, preservatives and surfactants, as well as the relative intrinsic thermodynamic stability of the native state (Chang, 1996).

1.4 Analytical Techniques to Determine Protein Degradation

There are several analytical methods that are widely reported to assess levels of protein aggregation and structural changes. Size exclusion chromatography (SEC) is a well reported technique for detection of aggregation. Also, there are a number of techniques for measurement of sub-visible particles, such as dynamic light scattering (DLS), micro flow imaging (MFI) and resonant mass measurement (RMM). Changes in tertiary structure of the protein may be evaluated using a number of several spectrographic techniques such as circular-dichroism (CD), UV-absorbance, fluorescence and Fourier-transform infrared spectroscopy (FT-IR). Evaluation of thermal events, such as determination of the glass transition and detection of denaturation/unfolding of the protein can be studied using differential scanning calorimetry (DSC) (Houde and Berkowitz, 2014). These techniques are discussed in more detail in **Section 2.3**.

1.5 Freeze/Thaw-Induced Protein Aggregation

Freeze–thaw processes can cause aggregation of proteins due to protein structural perturbations. In turn, aggregates of therapeutic proteins may elicit undesirable immune responses, such as the generation of antidrug antibodies. The mechanisms of freeze/thaw-induced protein aggregation are not well understood, in part, because of the limitations of many commonly used spectroscopic techniques for the analysis of protein structure within frozen samples (Lu et al., 2014).

Freeze–thawing and increased temperature are two relevant stress factors to which therapeutic proteins are exposed during different processing stages including frozen or liquid storage, freeze–drying or shipping. For monoclonal antibodies, heat induced unfolding can be manifested in several transitions corresponding to the unfolding of the Fc and the Fab parts of the immunoglobulin (Fesinmeyer et al., 2009; Vermeer and Norde, 2000). Heat induced denaturation of IgG generally leads to irreversible conformational changes, because of instantaneous aggregation accompanying the unfolding process (Vermeer and Norde, 2000). Partially unfolded intermediates exposing hydrophobic parts, which are often referred to as molten globular intermediates, can serve as nuclei for aggregate formation (Dill and Shortie, 1991; Fesinmeyer et al., 2009).

Freeze–thawing combines several stress factors for a protein, all of which can lead to aggregation (Bhatnagar et al., 2007). During freezing a protein can adsorb to the ice–liquid interface or to the container surface inducing a partial unfolding of the protein and subsequent aggregation (Chang, 1996; Sarciaux et al., 1999; Strambini and Gabellieri, 1996). In addition to formulation and container material related factors, process conditions like freezing and thawing rates play an important role for the stability of a protein upon freeze–thawing (Cao et al., 2003; Kueltzo et al., 2008). These studies referenced focused mainly on the impact of external factors such as

excipients, primary packaging material or freezing rates on the extent of protein aggregation after freeze–thawing, rather than on the structural properties of the formed aggregates.

Freezing-induced denaturation of proteins is a major concern in the development of protein pharmaceuticals. Bulk or final protein products are stored for extended periods in the frozen state, which can protect against undesirable chemical degradation. Freezing also plays a crucial role in the damage incurred to proteins during freeze-drying. Freeze-induced denaturation can be inhibited by including protein-stabilizing solutes in the formulation. Despite the numerous freeze-thawing studies on proteins (Hawe et al., 2009; Kueltzo et al., 2008; Radmanovic et al., 2013; Rayfield et al., 2016), the choice of these solutes and development of stable formulations is still largely empirical because of the lack of a full understanding of the relative importance of the various stresses arising during freezing as well as the mechanisms by which additives protect proteins against these stresses. Routinely recognized freezing-induced stresses include cold temperature, exposure to concentrated solutes due to crystallization of both water and solutes, and the resultant pH changes if buffer salts are involved. Resistance to all of these stresses can be increased if selected solution conditions can increase the thermodynamic stability of the native state of the protein (Chang, 1996). Freezing-induced stress factors are further discussed in the following sub-sections.

1.5.1 Cryo-Concentration

During the process of freezing, water is removed from the amorphous phase as ice formation occurs and is more likely to occur with slower freezing rates. The slower freezing rate results in a smaller number of larger ice crystals that have a lower surface area of ice and thus provide a greater opportunity for the protein molecules to coalesce and interact with each other. This phenomenon which occurs during the freezing is

known as cryo-concentration and can lead to an increase in buffer and protein concentration. Increased protein concentration can result in a higher degree of aggregation due to increased opportunity of molecular collisions between protein molecules (Kueltzo et al., 2008).

In addition to changes in the formulation pH, concentration of the protein and excipients, the freezing step can also lead to the formation of water-ice interfaces. At these interfaces protein adsorption can induce partial protein unfolding and subsequent aggregation. A fast-freezing rate will typically lead to formation of smaller ice crystals and thus, a larger liquid-ice interface. Chang studied the hypothesis that denaturation during freeze-thawing is greater when proteins are frozen with conditions that should generate an increased ice surface area (Chang, 1996). The results of previously reported studies did not unequivocally support the hypothesis that the ice-water interface is the source of this damage because other complex physicochemical changes occurring during the freeze-thawing processes were not fully controlled (e.g. alterations in pH due to selective buffer salt crystallization and lowest temperature of exposure) (Hsu et al., 1995; Nema and Avis, 1993). The results of Chang's study showed that a very slow cooling rate resulted in a much lower ice surface area than that for quench freezing (immersing the sample container in liquid nitrogen). The greater ice surface area generated by quench cooling provided much more stress to the protein than slow cooling, suggesting that denaturation at the surface plays an important role in the aggregation of proteins during freezing (Chang, 1996).

Studies on individual proteins have reported that denaturation during freeze-thawing is greater when proteins are frozen under conditions that should generate a relatively large ice surface area than when conditions leading to less surface area are employed (Chang, 1996; Hsu et al., 1995). One example is a study by Strambini and Gaballieri who found that an increase in ice surface area correlated directly with increased

perturbation of the tertiary structures of azurin, alkaline phosphatase and liver alcohol dehydrogenase in the frozen state, while other physicochemical changes were kept equivalent (Strambini and Gabellieri, 1996).

The concentration profile of solutes entrapped between the ice crystals results from a balance between the ice front velocity versus the rates of diffusive and convective transport of solute away from the interface. Solute exclusion from the nucleating ice domains is influenced by differences in interfacial energy as well as the crystal lattice structure, whereas solute inclusion results when the ice growth rate exceeds the solute mass transfer rate away from the advancing ice front (Miller et al., 2013).

Chang also showed that low concentrations of surfactants (i.e. below the critical micellar concentration), which would not be expected to greatly alter the free energy of protein denaturation, provide a high degree of protein protection during freeze-thawing (Chang, 1996). Surfactants are known to stabilize proteins against surface-induced denaturation, so the results suggested that the ice-water interface can contribute to freeze-induced protein denaturation (Chang, 1996).

1.5.2 Solute Crystallisation

Selective crystallisation of buffer components can occur depending on the cooling rate applied for freezing or the buffering effect of the salts used in the formulation (e.g. crystallisation of disodium phosphate prior to that of monosodium phosphate, which results in a decrease in pH) (Chang, 1996). Each buffer salt has its own critical cooling rate. Crystallisation will only occur when the cooling rate is slower than the critical cooling rate. Therefore, if a protein solution is quench cooled with liquid nitrogen, it is likely that buffer salts will remain amorphous. In contrast, crystallisation and a subsequent change of pH can readily occur during slower cooling (Chang, 1996). This was also observed for other excipients. Izutsu et al. demonstrated that mannitol crystallisation reduced its cryo-protectant effect, resulting in a reduction in activity of

a model enzyme (β-galactosidase), whether it was freeze-dried or freeze-thawed (Izutsu et al., 1993). Sorbitol has also the potential to crystallise in the frozen solution and has been shown to cause increased levels of aggregation in a fusion protein (Kantor et al., 2011).

1.5.3 Low Temperature Destabilisation

It is well documented that proteins unfold with an increase in temperature (i.e. heat denaturation). However, low temperature can initiate cold denaturation of proteins, due to an increased solubility of hydrophobic residues at low temperature, favouring unfolding (Privalov, 1990). Cold denaturation is a thermodynamic consequence of the large heat capacity of unfolding and can be dependent on the pH of the solution, concentration of the protein and presence of additives such as sugars and chaotropic agents (Bhatnagar et al., 2007). Moreover, during freezing a protein can adsorb to the ice–liquid interface or to the container surface inducing a partial unfolding of the protein and subsequent aggregation (Strambini and Gonnelli, 2007).

1.5.4 pH Shifts

Exposure of monoclonal antibodies to an acidic environment can result in conformational changes and aggregation (Jiskoot et al., 1991). As described above, particularly for sodium phosphate buffers, cooling and freezing can result in selective crystallisation of different buffer components, potentially resulting in pH shifts of the frozen solution. The pH shifts have been reported to decrease pH to pH 4.0 for sodium phosphate buffers (Pikal-Cleland et al., 2000; Gómez et al., 2001) and to pH 3.0 for succinate buffers (Lam et al., 1996) .

The degree of reduction in pH of sodium phosphate buffered solutions during freeze-thawing depends on the degree of dibasic salt crystallisation, which in turn is dictated

by processing parameters. As a result of this, it is generally recommended to avoid use of sodium phosphate buffers for bulk drug substance (Wang and Roberts, 2010).

1.5.5 Exposure to Liquid-Air Interface

Agitation can sometimes be utilised to speed up the thawing process, particularly for uncontrolled thawing processes. Mechanical stresses may cause shear or interfacial effects in which the protein adsorbs to the air-water interface, leading to structural alterations which can initiate aggregation. Both stirring and shaking are mechanical stresses that can also cause cavitation, local thermal effects, bubble entrapment, and transportation of the aggregated protein from the air-water or air-container interface into the bulk solution (Telikepalli et al., 2014).

1.5.6 Polar Interactions

A common feature of monoclonal antibodies is that non-polar regions are sequestered into the core of the protein, where they avoid contact with water (Vermeer and Norde, 2000). Privalov showed that the cold denaturation is a general phenomenon caused by the very specific and strongly temperature-dependent interaction of protein nonpolar groups with water (Privalov, 1990). Hydration of these groups is favourable thermodynamically, i.e. the Gibbs energy of hydration is negative and increases in magnitude at a temperature decrease. As a result, the polypeptide chain, tightly packed in a compact native structure, unfolds at a sufficiently low temperature, exposing internal nonpolar groups to water (Privalov, 1990).

Polar interactions between water molecules and the hydrophilic patches of proteins help maintain the native conformation, hence the dehydration of a protein can promote unfolding. Inevitably this leads to increases in aggregation levels due to protein-protein interactions. The mechanism involves a decrease in charge density due to the

transferring of protons to carboxyl groups during dehydration (Rupley and Careri, 1991).

1.6 Freeze/Thaw Studies of Therapeutic Proteins

A major focus of published freeze-thaw studies for therapeutic proteins is the effect of controlled versus uncontrolled systems. Rayfield et al. described an uncontrolled system as one in which a filled drug substance container is placed into a temperature control unit until the material is frozen. Similarly, for uncontrolled thawing, the frozen drug substance container is placed into ambient conditions until fully liquefied (Rayfield et al., 2016). Although, as some proteins may be more susceptible to aggregation from the stresses imposed during phase changes from liquid to solid and back again, a more controlled system to provide for heat transfer from and to the solution may be advantageous to protect the protein from damage. In addition, a controlled system may offer quicker cycle times for freeze and thaw of proteins, allowing shortened overall process time for storage and filling of the formulated protein solutions (Rayfield et al., 2016).

CryoVessel™ (Integrated Biosystems, Inc.) and Celsius® CFT Technology (Sartorius-Stedim Biotech.) are two examples of controlled systems currently commercially available. A large scale cryo-vessel (e.g. CryoFin™) is a portable, jacketed, stainless steel freeze-thaw vessel used for cryopreservation of biopharmaceuticals, vaccines, blood products and gene therapy products, offered in volumes ranging from 20 to 500 L. Volume compartmentalization results in reduction of freezing path lengths, creation of extended heat transfer surfaces to increase heat flux and control of freezing rate. This represents a compact, dimensionally optimized containment design. CryoWedge™ is a scaled down model of the cryo-vessel that can be used to assess the impact of the freeze-thaw cycle on the product quality (Padala et al., 2010). Celsius® CFT is a controlled rate freeze-thaw system offering a full line of disposable single-

use bags (Celsius®-Pak's varying in volume from 30 mL to 16.6 L), control units, freeze-thaw modules, transfer carts, storage modules, and shipping units. Celsius® systems are optimally scalable. The Celsius® S3 Freeze-Thaw Module, the bench-top system, is specifically designed for development and stability studies and allows freeze-thaw runs with as little as 30 mL of product under the same conditions as the production scale system. The FT16 Celsius® system, with a capacity of up to 16 L, offers a pilot-scale alternative and can easily be scaled up to the manufacturing scale FT 100 Celsius® system, with a production capacity of up to 100 L (Padala et al., 2010). The ability to provide a linear scale-down model using the Celsius® S3 system has also been studied by Rayfield et al. and shown to provide a linear scale-down comparison of the manufacturing process where analytical data is comparable between small and large scales (Rayfield et al., 2016).

Another controlled system designed by HOF Sonderanlagenbau GmbH also utilises single-use bags. In contrast, to the Celsius® systems, bags are frozen in a horizontal position with heat-flow being controlled to the faces of the bag rather than to the edges. This utilises a larger surface area for freeze-thaw and thus, potentially quicker process throughput. However, to the best of our knowledge there are no scientific studies reported at this point demonstrating the benefits of this system.

Freezing and thawing processes may also detrimentally affect product quality requiring detailed process understanding and proper process control. Initially, research into freezing–thawing of pharmaceutical products focused on establishing the effect of formulation composition on product quality after freeze–thawing and frozen storage. So far, only a few authors have studied the effect of freezing–thawing process conditions on product quality (Radmanovic et al., 2013; Rayfield et al., 2016).

Quick freezing of enzymes in liquid nitrogen was often recommended in order to preserve the enzymatic activity (Nema and Avis, 1993; Shikama and Yamazaki,

1961), but Eckhardt et al. reported that rapid freezing in liquid nitrogen failed to prevent some proteins from freezing denaturation (Eckhardt et al., 1991). Other studies investigating freezing of protein solutions (Chang, 1996; Jiang and Nail, 1998; Strambini and Gabellieri, 1996) showed that fast freezing produced more damage to proteins and resulted in lower recovery of activity after freezing and thawing. This phenomenon was explained as ice-induced partial unfolding of proteins. However, despite these studies there is a lack of a systematic study of the freezing rate dependence of protein denaturation. Also, there is very little work addressing how damage to proteins can be reduced during freezing and thawing, through the optimization of operation conditions (Cao et al., 2003).

1.6.1 Scalability

Scale-down models are important as they can support process development studies representing the proposed large scale or commercial process. Moreover, it is a regulatory requirement to have a qualified scale-down model. Scale-down models are used to understand the process, while alleviating material requirements as well as the complication and expense of generating the data on a large-scale system. The International Conference on Harmonisation guidance for development and manufacture of drug substances (ICH Q11) states that a scientifically justified model can enable a prediction of quality and can be used to extrapolate operating conditions across multiple scales and equipment (Guideline ICH Q11, 2012).

Freeze-thaw rates can be challenging to duplicate on scaling. Large-scale heat transfer is slower and less efficient. As tank volumes get larger, the surface area to volume ratio decreases rapidly. Therefore, to affect temperature changes as rapidly as at small scale the temperature required at the surface of tanks and heat exchangers must be higher and mixing must be better (Wang and Roberts, 2010). Slow freezing and

thawing increase the exposure of the protein to localised zones of high protein concentrations, high solute concentrations and increased ice-liquid surface exposure.

The important parameters to be considered for the drug substance container are the heat transfer rate and freeze path length. These parameters are difficult to model in an uncontrolled freeze process. The first parameter, heat transfer, can be dependent on environmental factors within the temperature control unit, which in turn is dependent on air flow and unit capacity. The second parameter, freezing path length (the distance from the container surface to the last point to freeze), is often not consistent between scales (Rayfield et al., 2016).

To evaluate small scale models (≤1 L) Rayfield et al. sought a correlation between two factors; surface area to volume ratio (SA:V) and freeze time. A SA:V ratio is related to the freeze path length which impacts the resulting freeze time. Containers with higher SA:V ratio have shorter freeze path lengths and will therefore freeze and thaw faster. To evaluate the impact of SA:V ratio, freezing and thawing was performed on a monoclonal antibody using containers in multiple sizes and both the controlled and uncontrolled rate of freezing and thawing parameters. The findings showed that a scale down model for 30 ml was sufficient to provide a linear comparison to the manufacturing scale process for stable molecules (Rayfield et al., 2016).

A general strategy for scale-down model development is to proportionally scale down the volume-dependent parameters (freeze time, SA:V ratio) while maintaining the volume-independent parameters (heat transfer, fluid temperature, material of construction) at the same set points used in the large-scale (≥ 2 L) process. The scale-down model is considered applicable as long as the freeze profile is comparable with the at scale model for stable molecules (Rayfield et al., 2016).

Rayfield et al. evaluated the impact of the several parameters on the drug substance product quality including freeze/thaw rate, mode of freezing, drug substance container,

drug substance concentration and formulation. This was performed by creating controlled freeze-thaw programs using a Celsius® S3 apparatus. Freezers were used to create uncontrolled freezing rate. Uncontrolled thawing cycles were created by placing frozen containers upright on the bench top at ambient temperatures until temperature at last point to freeze (LPF) reached 20 °C. Further uncontrolled studies were completed, using Celsius S3 programs to mimic an uncontrolled rate large scale-freezing and thawing within a large scale container and also to mimic shipping excursion studies and potential temperature excursions through the glass transition (Tg', typically around -30 °C) that could be experienced during shipping (Rayfield et al., 2016).

Radmanovic et al. investigated a physico-mathematical model to predict product temperature profiles based on the freezing program as input parameter in a commercial freeze–thaw module. Applying this model, the time from first nucleation until the LPF reaching −5 ˚C and the time from −5 ˚C to −30 ˚C at LPF was varied to study the effect on product quality attributes in a full factorial design. Effects of process parameter settings on a typical fully formulated, highly concentrated monoclonal antibody solution as well as a highly concentrated solution formulated with buffer only were investigated. A complex dependency of product quality attributes was observed on both freezing and cooling time and it was found that fully formulated drug product was significantly less susceptible to freeze–thaw stress than a drug substance formulation containing histidine buffer only (Radmanovic et al., 2013).

Studies can also be performed at a very small scale, which allows for faster experimentation but would not be expected to simulate an industrial process. Hawe et al. froze IgG samples at scale of 1.5 ml contained within reaction tubes and identified suitable stress conditions with respect to heating temperature and time, as well as the number of freeze–thawing cycles. The aim was to obtain representative samples for

both types of stress, containing low but measurable levels of aggregates. Characterisation techniques including UV spectroscopy, DLS, light obscuration and HP-SEC revealed that similar types of aggregates were formed when varying the heating time between 1 and 20 minutes and the heating temperature between 70 and 75 °C, or the number of freeze–thawing cycles between one and five. Differences were mainly found in the amount of aggregation. Based on this, heating for 10 minutes at 74 °C and five repetitive freeze–thawing cycles were suggested to create representative samples for further physico-chemical characterisation (Hawe et al., 2009).

An important consideration for any study is the requirement to prove that undergoing freeze/thaw cycling does not impact the stability of the therapeutic protein. Rayfield et al. placed samples on an accelerated stability program at 40 °C for 4 weeks and found no effect on product quality attributes (no increase in particles or change in variants, or oxidation species) relative to control (no freeze/thaw). The freeze/thaw study and the stability data generated suggest that rate of freeze and thaw, container type/size, and mode of freezing did not impact the product quality during the process or stability over time for the monoclonal antibody studied. However, it should be noted that the studied therapeutic molecule was also relatively stable on account of a well-designed molecule sequence supporting its stability (Rayfield et al., 2016).

Although several studies have been performed to evaluate the impact of freezing on protein quality, these studies are limited to small volumes, where the effect of processing parameters such as freezing/thawing rate cannot be correlated to large scale systems. Due to freezing of protein solutions, series of phenomena noted above (pH changes, cryo-concentration, ice–water interface denaturation, etc.) are predominantly dependent on the freezing/thawing rate, freezing temperature, freezing time, and most importantly the overall ‘‘solution working volume’’. Additionally, when the scale is small (small heat and mass transfer dimensions), it is difficult to study the impact of

cryo-concentration, solute redistribution and time in transition phase effects and correlate the observed results to large scale. Therefore, there is a need to perform such experiments at manufacturing scale. Understanding of these effects is essential to better define the process parameters during large scale freezing/thawing and hence, to minimize the impact on protein quality (Kolhe and Badkar, 2011).

1.7 Aims and Objectives

Based on the literature review described above, the overall aim of this thesis was to evaluate the effect of parameters involved in freezing and thawing steps on freezing and thawing time, cryo-concentration, and the aggregation and tertiary structure of a formulated therapeutic protein solution, stored in polycarbonate bottles at a small-scale (lower than commercial volumes). The work was also envisaged to assess the scalability of these experiments to the respective full-scale commercial process.

To achieve these aims, the following specific objectives were established for the project;

- Establish a set of analytical methods to characterise the therapeutic protein focusing particularly on its aggregation and tertiary structure.
- Execute a designed set of experiments to evaluate the key factors; (1) that could cause change in protein structure, (2) that could cause change in aggregate levels in the formulated drug substance and (3) predict the influence of parameters on freezing and thawing times.
- Evaluate the validity of a small-scale model and understand the behaviour of the respective full-scale commercial process.

2.0 EQUIPMENT, MATERIALS AND METHODS

2.1 Equipment

The list of the equipment used for the experimental work is presented in **Table 2-1**.

Table 2-1: List of the equipment used

Equipment Type	Manufacturer	Country
SSM1 Mini orbital shaker	Stuart	United Kingdom
Lexicon II ULT freezer (set to -80 °C)	ESCO	Singapore
Mediline freezer (set to -20 °C)	Leibherr	Germany
OMT lab oven (set to 45 °C)	Sanyo	Japan
Tracksense Pro X Temperature Probes	ELLAB	Denmark
Zetasizer μV	Malvern	United Kingdom
FT-4 Fluoromax fluorescence spectrometer	Horiba Scientific	Japan
Chirascan cicular dichroism spectrometer	Applied Photophysics	UK
Q2000 DSC	TA Instruments	USA
SEC HPLC system	Waters	USA
SevenEasy pH Meter	Metteler Toledo	USA
Haake Mars Rheometer	Thermo Fisher	USA

2.2 Materials

Table 2-2 summarizes all materials and reagents used in this study.

Table 2-2: List of the materials used

Material	Grade	Supplier	Application
Protein Y	N/A	Sanofi	Active pharmaceutical ingredient
Histidine	USP / Ph Eur	Sigma	Dilution buffer preparation
Histidine, mono-hydrochloride, monohydrate	>98 %	Sigma	Dilution buffer preparation
Sucrose	BioUltra (>99.5 %)	Sigma Aldrich	Dilution buffer preparation
Tween 20® (Polysorbate 20)	Molecular Biology	Sigma Aldrich	Dilution buffer preparation
Milli-Q® water	HPLC grade	Millipore	Dilution buffer and HPLC mobile phase preparation
Universal Indicator solution	N/A	Lennox Laboratories	Monitoring pH change
Sodium chloride, 5M solution	>99.5%, Ph Eur	Fisher	HPLC mobile phase
Disodium hydrogen phosphate heptahydrate	>98% ACS reagent	Acros Organic	HPLC mobile phase
Sodium phosphate monobasic monohydrate	>98% ACS reagent	Acros Organic	HPLC mobile phase
Orthophosphoric acid, concentrated	>85%	Fisher	HPLC mobile phase
Sodium hydroxide, 1N solution	N/A	Fisher	HPLC mobile phase
Sulphuric acid, 1M	N/A	Fisher	HPLC mobile phase
Sodium sulphate anhydrous.	N/A	Fisher,	HPLC mobile phase
Acetonitrile, HPLC grade	99.9%, HPLC gradient grade	Fisher	HPLC mobile phase
Protein reference standard	In-house	Sanofi	HPLC analysis
Gel filtration standard (molecular weight std)	N/A	Biorad	HPLC analysis

2.2.1 Drug Substance Technical Overview

The active pharmaceutical ingredient (API) of the product, Protein Y, is a fully human IgG1 monoclonal antibody. An illustration of the Protein Y molecule is shown in the **Figure 2-1**. The antibody, based on the primary sequence (in the absence of N-linked glycosylation), possesses a molecular weight of 145,983.8 Da, taking into account the formation of 16 disulphide bonds and removal of Lys448 from each heavy chain C-terminus (Internal Common Technical Document, Sanofi).

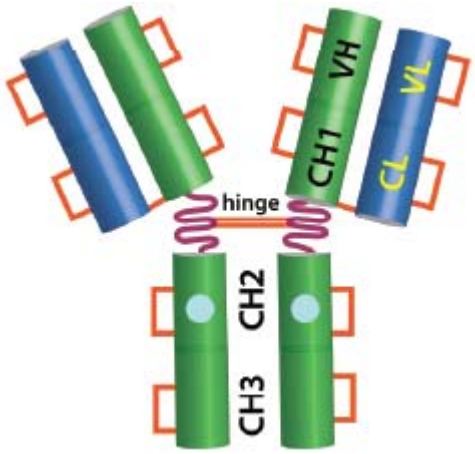


Figure 2-1: Illustration of the molecular structure of Protein Y (Internal Common Technical Document, Sanofi)

2.2.2 Bulk Manufacturing of Protein Y

Protein Y is generated via recombinant DNA technology and expressed in manufacturing using Chinese Hamster Ovary (CHO) cells. The process is initiated at the seed lab where the CHO cells are inoculated into shake flasks and subsequently into a cell bag for expansion of the cultures. The cell numbers are further expanded in bioreactors, prior to harvest of the protein through centrifugation and filtration. The protein is purified via an intensive series of chromatography, viral inactivation and filtration steps. Finally, the bulk is formulated and stored in the frozen state in preparation for filling into syringes.

2.2.3 Formulation of the Product

The composition of the formulated drug substance (FDS) is listed in **Table 2-3**.

Table 2-3: Nominal composition of Protein Y solution for injection

Component	Function/ Characteristic	Reference to Quality Standard
Protein Y	active ingredient	In-house specification
Histidine [a, b]	buffering agent	USP, Ph. Eur., JP
Histidine, Mono-hydrochloride, monohydrate [b, c]	buffering agent	Ph. Eur., JP
Sucrose	tonicity and stabilizing agent	NF, Ph. Eur., JP
Polysorbate 20	stabilizing agent	NF, Ph. Eur., JPE
Water for injection	solvent	USP, Ph. Eur.

[a] Named L-histidine in JP.
[b] The amounts of L-histidine mono-hydrochloride monohydrate and L-histidine in the concentrated excipient buffer containing 10mM histidine are 1.027 mg/mL and 0.791 mg/mL, respectively. It is expected that the histidine ratio will be similar in the Protein Y drug product. However, given the contribution of the two histidines from the diafiltration buffer, the impact of the Donnan effect and the contribution from the sucrose adjustment buffer and dilution buffer, actual amounts of L-histidine monohydrochloride monohydrate and L-histidine in the DP cannot be calculated.
[c] Named L-histidine hydrochloride hydrate in JP.
JP = Japanese Pharmacopeia; JPE = Japanese Pharmaceutical Excipients; NF = National Formulary; Ph. Eur. = European Pharmacopeia; USP = United States Pharmacopeia.

2.3 Methods

2.3.1 Formulation Characterisation Studies

Prior to evaluation of the impact of processing parameters, initial characterisation experiments were performed to understand the bulk FDS in the context of freezing and thawing. In particular, the critical temperatures at which the formulation undergoes changes (glass transition, Tg' and collapse temperature, Tc) were determined. In addition, changes in pH of the buffer solution during freeze-thaw experiments was also assessed.

2.3.1.1 Differential Scanning Calorimetry (DSC)

Both formulated drug substance (FDS) and the dilution buffer solution (without Protein Y) were analysed by modulated DSC, each in three replicate runs. DSC analysis were performed by cooling the samples to -70 °C and re-heating to +30 °C at a ramp rate of 2 °C/min. The modulation period was 100 seconds with temperature amplitude of ±1 °C. TA Instruments Hermetic Tzero pans and lids were used for all experiments. Data was processed by using the Universal Analysis Software (version 4.5A). Tg' values were measured as midpoint temperature of the thermal event observed in the reversing heat flow thermogram.

2.3.1.2 Freeze Drying Microscopy (FDM)

In order to determine Tc, three FDM runs were performed (runs I-III). All samples were cooled at a freezing rate of 10 °C/min to either -60 °C (run I) or -30 °C (runs II and III), followed by the holding time of 10 minutes (runs I and II) or 30 minutes (run III) to achieve isothermal equilibration. Then, a vacuum of approximately 6000 Pa was applied to initiate sublimation and maintained through the temperature ramp of 1 °C/min until the full collapse of the material was reached, with pictures captured every 5 seconds.

2.3.1.3 Evaluation of pH Change in Dilution Buffer

Universal Indicator solution was added to samples of the dilution buffer in four plastic tubes. The dilution buffer and indicator solutions were placed in storage at -80 °C, -20 °C, +5 °C (refrigerator) and at a controlled room temperature for 2 days. The samples were then visually inspected and compared. In addition, the pH of the non-frozen refrigerated and the room temperature solutions was measured using a pH meter.

2.3.2 Protein Y Characterisation Studies

A number of analytical characterisation methods were established and optimised to confirm their suitability to assess changes in protein aggregation and its tertiary structure.

2.3.2.1 Differential Scanning Calorimetry (DSC)

The suitability of the DSC technique was assessed for the three sets of samples: (1) dilution buffer, (2) FDS diluted to 15 mg/ml (FDS-15) and (3) FDS with high protein concentration of 150 mg/ml (FDS-150). Initially, a sample volume of 20 µl and a 5 minute equilibration at 25 °C was performed for all samples, followed by heating step to 100 °C with a ramp rate of 2 °C/min. The method was further optimized by varying the sample volume (10 µl and 20 µl), the starting equilibration temperature (25 °C and 40 °C) and the end temperature (96 °C and 100 °C), as well as the ramp rate (0.5, 1, 2 and 10 °C/min). TA Instruments Hermetic Tzero pans and lids were used for all experiments. Data was processed by using the Universal Analysis Software (version 4.5A).

2.3.2.2 Size Exclusion Chromatography (SEC)

The SEC-HPLC method was used to separate and detect high and low molecular weight species, which are CQAs for Protein Y. The method employed was similar to a previously reported method (Bond et al., 2010), and was validated and is in routine use for QC release testing in Sanofi. Therefore, no method development was required for FDS used in our study. The method parameters are proprietary to Sanofi.

2.3.2.3 Dynamic Light Scattering (DLS)

An initial DLS analysis was performed to see if freezing and thawing of Protein Y effected protein aggregation. Samples of Protein Y FDS in 1.5 ml Eppendorf tubes were placed in a freezer at -80 °C for 24 hours, thawed at 40 °C for 20 minutes and then this process repeated twice (i.e. three freeze-thaw cycles). This sample was then diluted, and a final concentration range from 0 mg/ml (i.e. dilution buffer solution) to 150 mg/ml (FDS) was analysed using a default DLS method and a sample viscosity of 0.88 mPaS. Equivalent dilutions were prepared for a control sample of Protein Y, which had not been frozen. The effect of Protein Y FDS concentration on the product viscosity was performed at 25 °C using the Haake MARS rheometer. It was determined that viscosity was constant at 1.4 mPaS between 0 mg/ml (dilution buffer only) and 15 mg/ml but increased above this concentration. Therefore, further DLS analysis were performed using a sample viscosity of 1.4 mPaS and protein concentration of 15 mg/ml. To determine if the DLS method can detect changes in protein aggregation, Protein Y samples were aged in Eppendorf tubes for 15 minutes at 40 °C and 80 °C. The samples were then diluted to 15 mg /ml (1:10 dilution) and analysed by DLS, both unfiltered and filtered through a 0.45 μm filter to assess any effect of filtration. A summary of the DLS method parameters used for analysis is presented in **Table 2-4**.

Table 2-4: **DLS method parameters**

Parameter	Setting
Sample concentration	15 mg/ml
Sample viscosity	1.4 mPaS
Sample volume	1.0 ml
Cuvette	Low volume disposable cuvette
Pre-filtration	0.45 μm
Reporting data	Z-Average and PdI Report average of 3 repeats
Equilibration temperature	25 °C
Equilibration time	120 seconds

2.3.2.4 Circular Dichroism Spectroscopy (CD)/UV-Absorbance

CD method development was performed at concentration ranges of 0.15 – 1.5 mg/ml using a 1 cm path length quartz cuvette, a step value of 0.3 nm and time of 2 seconds per point. UV absorbance was recorded in addition to CD to investigate total protein content and tertiary structure through second derivative analysis. A concentration of 0.75 mg/ml was selected to optimum UV absorbance values, however the CD spectra generated were not clear. Therefore, the time per point was increased to 5 seconds and the step value increased to 1 nm, which resulted in generation of a clearer spectrum. In order to determine if the developed method could detect changes in the tertiary structure of Protein Y, the method was run with a temperature ramp, and spectra recorded at 20, 40, 60 and 80 °C.

Based on the ability of near-UV CD scans to detect unfolding of Protein Y, the parameters listed in **Table 2-5** were selected as optimal for the method.

Table 2-5: Near-UV/CD parameters

Parameter	Setting
Sample Concentration	0.75 mg/ml
Scan range	315 – 250 nm
Number of replicates	3
Step	1 nm
Time per point	5 seconds

2.3.2.5 Fluorescence Spectroscopy

Intrinsic fluorescence spectroscopy was employed for analysis of the FDS containing Protein Y at protein concentration of 150 mg/ml (undiluted) and subsequent dilutions to 0.15 mg/ml, with excitation at 295 nm. The excitation was then adjusted to 280 nm in order to maximise the intensity for tryptophan residues. Furthermore, optimum slit widths were investigated to determine the best setting that provides a corrected intensity ratio of less than 2 x 10^6 units. A temperature ramp was also performed, samples were heated using a water bath at 20 °C, 40 °C, 60 °C, 80 °C and analysed after cooling back to 20 °C. Optimized method parameters are detailed in **Table 2-6**.

Table 2-6: Fluorescence method parameters

Parameter	Setting
Sample concentration	0.75 mg/ml
Sample volume	1 ml
Cuvette	1 ml Low volume quartz cuvette
Excitation	280 nm
Excitation slit	1.5 nm
Emission scan range	295 – 450 nm
Emission slit	1.5 nm
Reporting data	Intensity, λ_{max}

2.3.3 Freeze-Thaw Studies

2.3.3.1 Experimental Design of Experiments (DoE)

Following the initial formulation characterization studies and optimization of the analytical characterization methods, a designed set of experiments (DoE) was performed to provide an assessment of different freeze/thaw process parameters related to the current uncontrolled freeze/thaw steps in the manufacturing process that were thought to have the potential to affect the properties of Protein Y. The following five parameters were selected and input into the design:

- Freezing temperature; the temperature inside the freezer used to freeze the FDS
- Freezing equilibration; the temperature inside the freezer prior to removal from the freezer for thawing
- Freeze co-load; a categorical factor used to mimic the FDS being loaded on its own or with other bottles. If co-loaded, the surrounding bottles were filled with water (**Figure 2-2**).
- Thaw co-load; a categorical factor used to mimic the FDS being thawed on its own or with other bottles. If co-loaded, the surrounding bottles were filled with water (**Figure 2-2**).
- Thaw agitation speed.

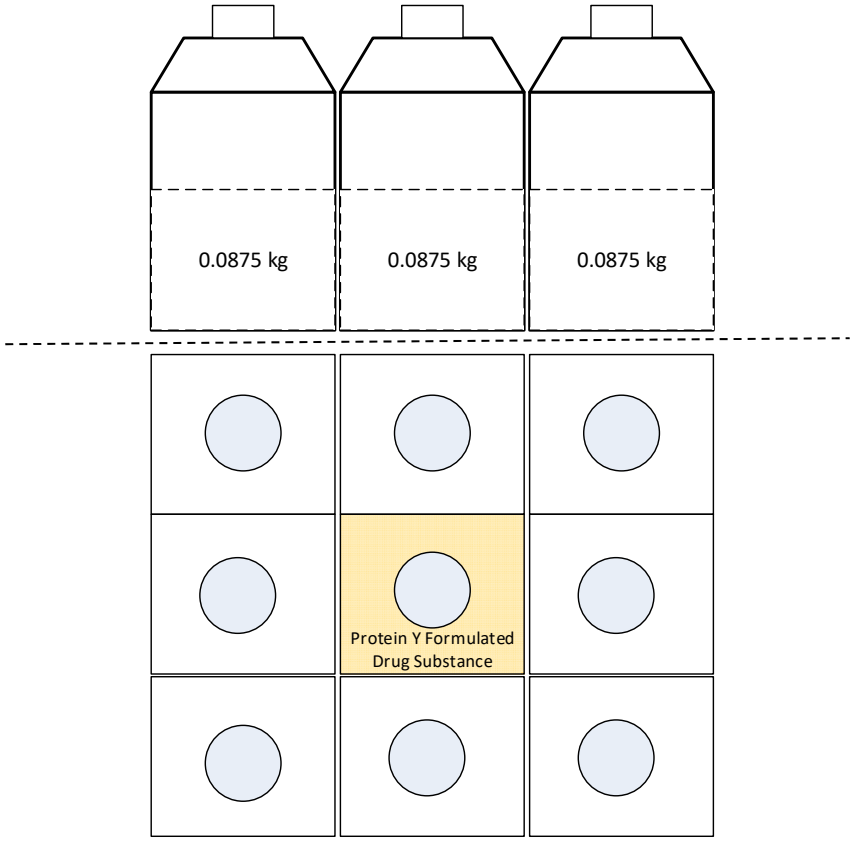


Figure 2-2: Container layout for Protein Y freeze and thaw DoE. Top and cross-section view

As this was an initial screening DoE, a reduced 2-level factorial design, with no blocks or centre points was selected in order to provide an appropriate level of runs for execution, which would allow for single factors having a significant effect to be identified. This design resulted in eight runs evaluating the five factors chosen, as presented in **Table 2-7** and **Table 2-8**.

Table 2-7: DoE design for freeze-thaw studies

Factor	Name	Units	Type	Low Actual	High Actual	Low Coded	High Coded
A	Freezing temperature	°C	Numeric	-80	-20	-1	1
B	Freezing equilibration	°C	Numeric	-80	-20	-1	1
C	Freeze co-load	n/a	Categoric	Yes	No	n/a	
D	Thaw co-load	n/a	Categoric	Yes	No	n/a	
E	Thaw agitation speed	rpm	Numeric	0	69	-1	1

The DoE design, with the experimental plan listed in **Table 2-9** was scheduled and freeze-thaw cycles executed over the course of approximately 6-weeks, with subsequent 4-week stability profile following the respective runs. Each run consisted of one 125 ml bottle containing 87.5 g of FDS.

Table 2-8: Experimental plan

Run Order	Freezing Temperature (°C)	Freezing Equilibration (°C)	Freezing Co-load	Thawing Co-load	Agitation Speed (m/s)
1	-20	-20	No	No	0.054
2	-80	-20	No	Yes	0
3	-80	-20	Yes	Yes	0.054
4	-20	-20	Yes	No	0
5	-80	-80	Yes	No	0.054
6	-20	-80	No	Yes	0.054
7	-20	-80	Yes	Yes	0
8	-80	-80	No	No	0

Design Expert (V7.02) software was used to perform statistical analysis of the DoE results. The responses listed in **Table 2-9** were evaluated following each run at time zero and after 1, 2 and 4-weeks storage at 45 °C by monitoring the temperature and time. Responses related to protein structure were measured by wide range of analytical techniques (i.e. UV absorbance, fluorescence spectroscopy, DSC, DLS, SEC-HPLC). The DSC was performed at the first and last time-point. In addition to statistical responses in the DoE, qualitative assessments were made by comparison of near-UV CD, $1^{st}/2^{nd}$ derivative of UV absorbance and intrinsic fluorescence spectra responses from the DoE runs compared to the control sample (i.e. initially thawed bulk FDS).

Table 2-9: DoE process responses

Response	Product /process attribute	Parameter monitored/analyzed
Freezing process performance	Pre-cooling rate (pre-plateau)	Temperature over time
	Freezing time (freezing plateau)	Time
	Post-cooling rate (post-plateau)	Temperature over time
	Overall freezing time (to freezer temperature)	Time
Thawing process performance	Initial thaw rate (pre-plateau)	Temperature over time
	Thawing time (thawing plateau)	Time
	Thaw rate (post-plateau)	Temperature over time
	Overall thawing time (to freezer temperature)	Time
Protein Y stability	Cryo-concentration	% RSD of UV absorbance at 280 nm (A280)
	Protein Y tertiary structure	Arbitrary peak height ratios attributed to aromatic amino acid residues in second derivative of UV absorbance spectra
		Emission intensity and wavelength maxima (λ_{max}) of intrinsic fluorescence spectra
	Protein Y thermal stability	Unfolding temperature onset and mid-point by DSC
	Protein Y aggregation	Z-average and PDI by DLS
		High molecular weight / low molecular weight species by SEC HPLC

2.3.3.2 Thawing of Bulk FDS

One 5 L bottle of FDS was removed from frozen storage and thawed by placing the bottle on the rotary shaker at room temperature until a liquid layer was visible (approx. 6 hours). The FDS was then agitated at 69 rpm until thawing was complete (approximately 19 hours). Sample aliquots for analysis were taken as per the experimental plan. Approximately 87.5 g of FDS was dispensed into each 125 ml bottle required for experimentation on the day of initiating the respective freeze/thaw experiments. The thawed FDS in the bulk 5 L bottle was stored at 2 – 8 °C during execution of the series of experiments.

2.3.3.3 Freeze/Thawing Experimental Procedure

Temperature was monitored using the ELLAB probes, which were inserted into the 125 ml bottles in two locations: inside the bottle with tip of probe suspended near to the centre (Probe 1), and on inside wall of the bottle with tip of probe ending at the base of the bottle (Probe 2). PTFE tape was used as required to ensure probes remain in place (**Figure 2-3**).

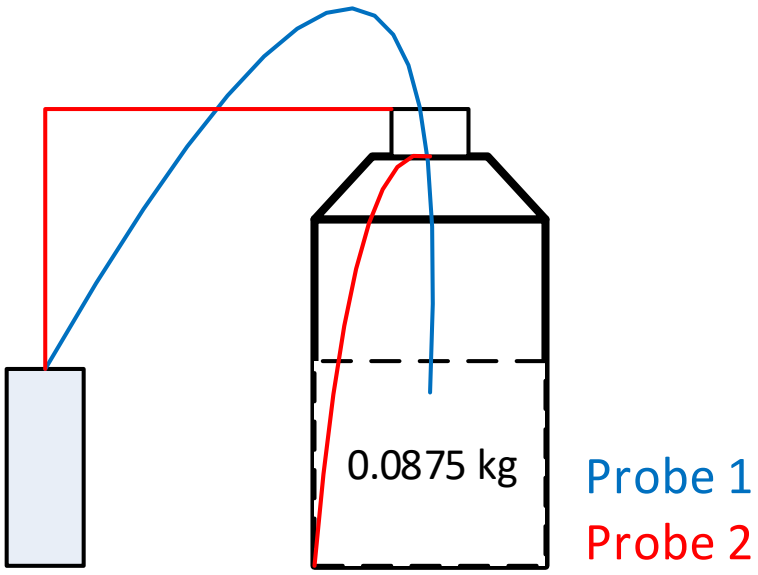


Figure 2-3: Illustration of FDS bottle and ELLAB probe set up

The bottles were placed into the respective freezer as per the DoE plan outlined in **Table 2-8** and stored for approximately 24 hours to ensure the bottle has equilibrated at the freezer temperature. The bottles were then moved to a different freezer if the experimental plan required and kept in the equilibration freezer for a further 24 hours. Following the bottles removal from the freezer, they were placed onto the rotary shaker table, if agitation was required. The agitation speed was set, if required per the experimental plan and the bottles were left to thaw. The time of the thawing process completion was noted. The ELLAB temperature probes were then removed from the bottle and the cap replaced to a cap without holes for probes. Samples were taken from the top, middle and bottom of the bottle to assess protein concentration levels at time zero (T0). The cap was secured and then the bottle inverted three times to homogenise the solution. Additional T0 samples were taken for analysis in centrifuge tubes according to the pre-determined sampling plan. These samples were stored at 2 – 8 °C prior to analysis. The thawed 125 ml bottle was then placed into an oven, set to 45 °C for 4-weeks, with samples taken after 1, 2 and 4-weeks.

3.0 RESULTS

3.1 Formulation Characterisation

A range of analytical techniques were established to investigate their ability to determine Protein Y characteristics and physical instability.

3.1.1 Modulated Differential Scanning Calorimetry (DSC)

Figure 3-1 displays representative DSC thermograms for Protein Y FDS and the dilution buffer, with attempted determination of glass transition temperature. A subtle inflexion can be observed in the dilution buffer solution at approximately -30 °C, which is not as prominent in the FDS, therefore it was not thought to be the glass transition point for Protein Y. This thermal event corresponds with the glass transition temperature of sucrose (Wang, 2000), which is the major excipient in the formulation and therefore it would be more detectable in the absence of Protein Y. Thermograms for the FDS did not exhibit any thermal events prior to the major endotherm that occurs with the melt indicating that the glass transition temperature occurs within this thermal event. An inflexion point within the melt endotherm was determined using the TA universal analysis revealing a possible glass transition around -6 to -10 °C. However, due to its very subtle effect in comparison with the heat flow associated with the melt of the FDS, a confirmation of the glass transition temperature was required by employing a second characterisation technique, freeze-drying microscopy.

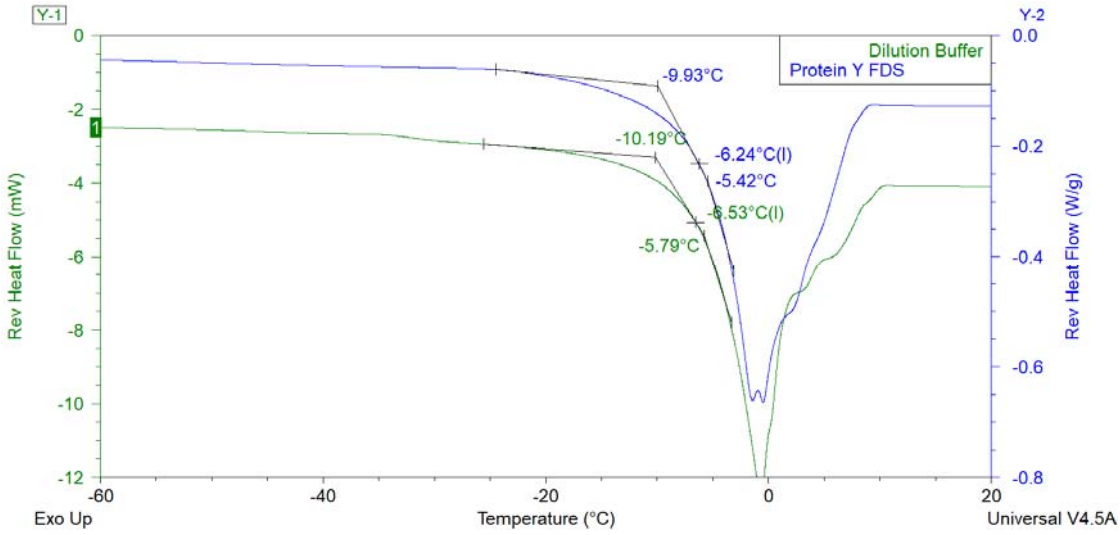


Figure 3-1: Representative DSC thermograms for Protein Y FDS and dilution buffer

3.1.2 Freeze Drying Microscopy (FDM)

No major collapse was observed in any of the FDM runs until approximately -12 °C, with further progression of withdrawal of the ice boundary until melt started to be observed at around -4 °C (**Figure 3-2**). These observations support the findings from the DSC thermograms that the glass transition midpoint occurs at approximately -8 °C.

Based on the characterisation of the FDS and its thermodynamic behaviour, a storage temperature of -20 °C or lower would appear appropriate to ensure the stability of the protein. #

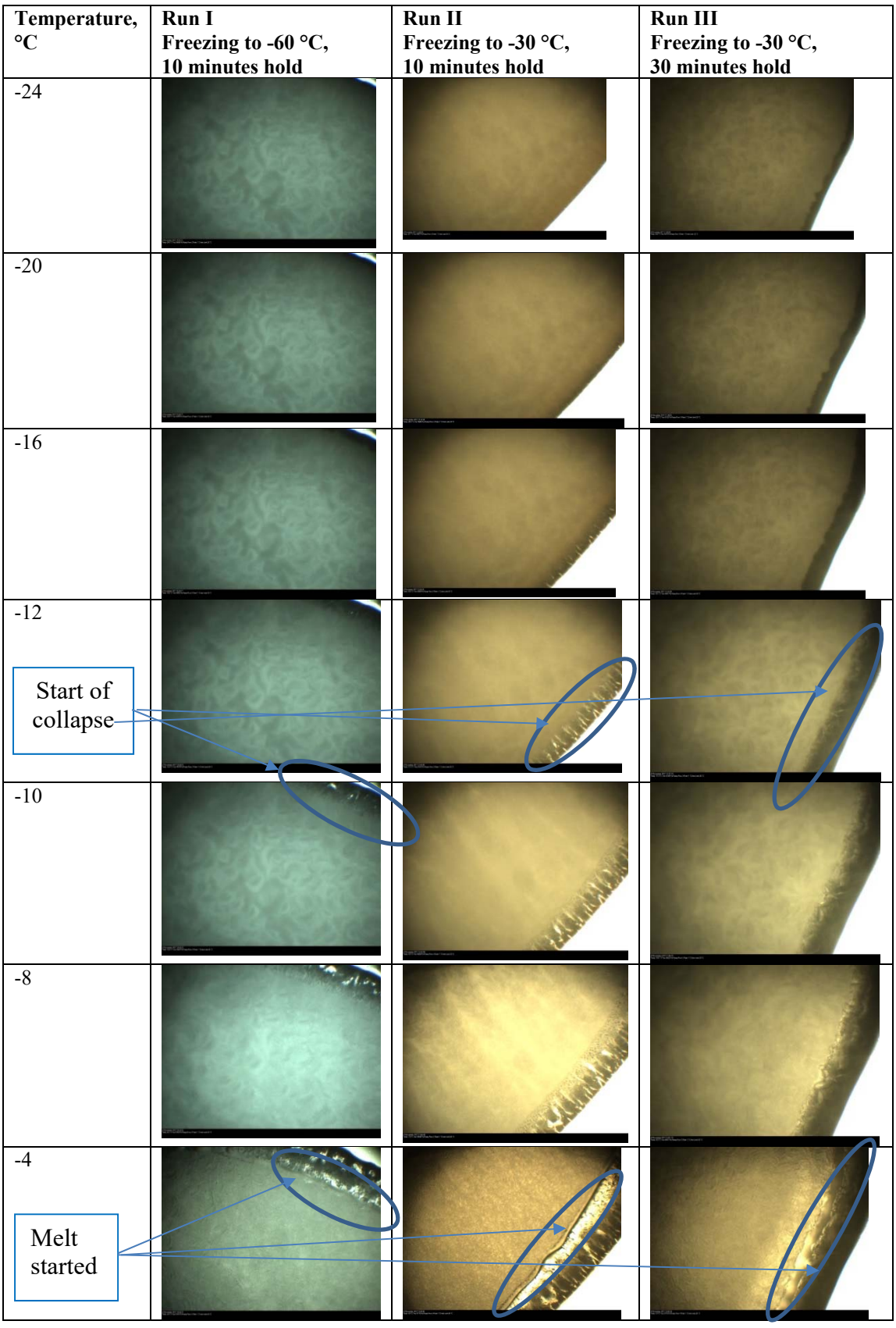


Figure 3-2: Images of Protein Y FDS at -16 to -4 °C for three FDM runs

3.1.3 Evaluation of pH Change in Dilution Buffer upon Freezing

Protein Y FDS is specified to have a pH of 5.7 – 6.3 at 2 – 8 °C. Universal Indicator solution was added to samples of the dilution buffer and placed in storage at -80 °C, -20 °C, +5 °C (refrigerator) and at a controlled room temperature for 2 days. Despite the frosted appearance of the frozen samples, there was no visibly determinable change in the colour of the samples. All samples exhibited an orange colour, indicating the pH of approximately 6 for the dilution buffer solution and its effectiveness at minimising pH shifts during freezing of the FDS (**Figure 3-3**). In addition, the pH of the non-frozen solutions was measured and found to have a pH of 6.1 and 5.9 for the refrigerated and the room temperature samples, respectively. For the purpose of a visual comparison, the pH of the room temperature sample was increased using 0.1 M NaOH and measured with a pH meter to calibrate the colour change observed. At pH 6.4, the solution was observed to start turning from orange to green and at pH 6.8 the solution colour had turned green, as shown in **Figure 3-3**.

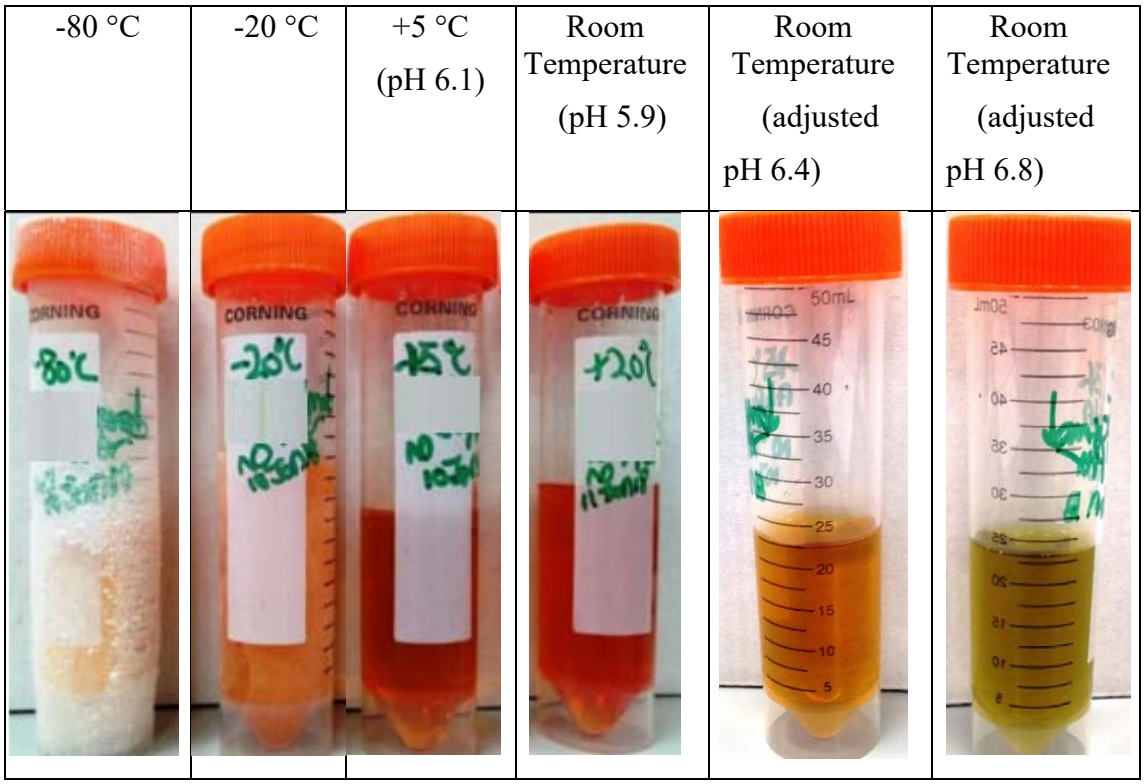


Figure 3-3: Visual assessment of pH change for dilution buffer solution following storage at four different storage conditions for 2 days

3.2 Protein Y Characterisation Studies

3.2.1 Differential Scanning Calorimetry (DSC)

The suitability of the DSC technique to detect protein unfolding temperature was assessed for FDS samples diluted to 15 mg/ml (FDS-15) and FDS samples with high protein concentration of 150 mg/ml (FDS-150). Samples of dilution buffer were also assessed as a negative control. Representative thermograms have been plotted in **Figure 3-4**.

In order to optimise the DSC method, the following changes were made:

- The sample volume was reduced from 20 µl to 10 µl to minimise the risk of the sample pan bursting open at higher temperatures
- The equilibration and ramp start temperature was changed from 25 °C to 40 °C to minimise the run time
- The end temperature was reduced from 100 °C to 96 °C also to minimise the risk of the pan bursting

No endothermic peak was observed in the dilution buffer. The thermograms for the FDS-15 sample did exhibit a small endotherm at the same temperature as for the FDS-150 thermogram but was significantly less defined. Therefore, FDS with a protein concentration of 150 mg/ml was deemed suitable to be used for DSC analysis of protein unfolding temperature.

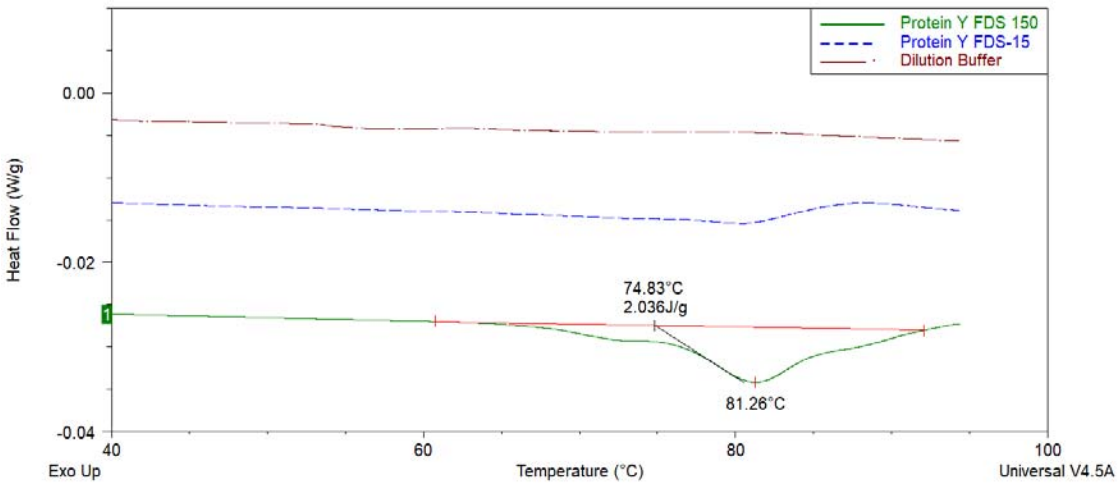


Figure 3-4: DSC thermograms of dilution buffer, Protein Y FDS-15 and Protein Y FDS-150. Temperature ramp 2 °C/ minute and 20 µl sample size.

Increasing the ramp rate from 2 °C/min to 10 °C/min was then investigated to see if this would increase the intensity of the endotherm occurring at around 80 °C for the 150 mg/ml samples (FDS-150). Representative thermograms are displayed in **Figure 3-5**. Also, to investigate if improved resolution of the thermal event could be obtained by using a ramp rate slower than 2 °C/min, thermograms were obtained with a slower ramp rate of 0.5 °C/min and 1 °C/min, with representative thermograms also displayed in **Figure 3-5** for comparative purposes. The higher ramp rate 10 °C/min resulted in a less stable baseline, making it harder to integrate the enthalpy involved with the endothermic peak, although determination of the mid-point temperature was still precise with the onset and midpoint shifting upwards by approximately 3 °C. Temperature ramps slower than 2 °C/min resulted in the diminution in onset and mid-point of the endotherm, with decrease in ramp rate but no significant improvement in repeatability of the enthalpy determination was observed.

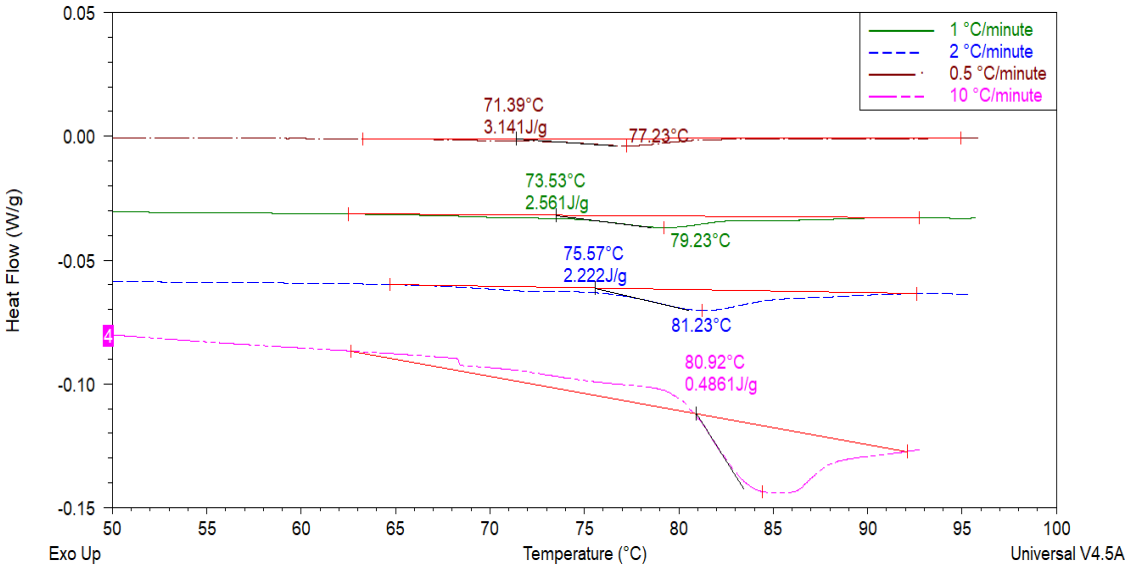


Figure 3-5: DSC thermograms of Protein Y FDS-150. Temperature ramp 0.5, 1, 2 and 10 °C / minute and 10 µl sample size.

Our finding showed that the optimised DSC standard ramp method was able to qualitatively identify an endotherm around 80 °C, at ramp rates from 0.5 – 10 °C/min, with the optimum ramp rate appearing to be at 2 °C/min.

3.2.2 Dynamic Light Scattering (DLS)

An initial DLS analysis was performed to see if freezing and thawing of Protein Y altered its size. The Z-average for the size distributions ranged from 10 to 22 nm (**Figure 3-6**). Corresponding polydispersity (PdI) values ranged from 0.16 to 0.76, with lower concentrations having a higher PdI value. The high variation in PdI was due to use of a default viscosity value of 0.88 mPaS, instead of the actual viscosity value for the respective concentration. There was no significant difference observed between Z-average for control or freeze-thaw samples.

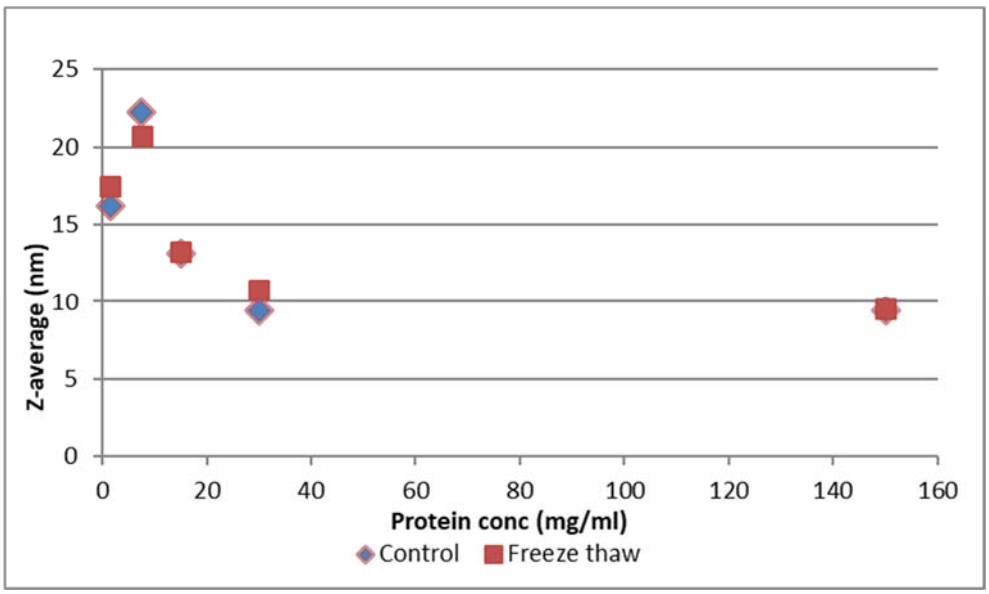


Figure 3-6: Concentration effect on Z-average of Protein Y for samples before and after a freeze-thaw cycle (default viscosity of 0.88 mPaS)

Figure 3-7 shows the viscosity data referred to in **Section 2.3.2.3**, where the viscosity increases at concentrations above 15 mg /ml. Based on this data an optimum protein concentration of 15 mg/ml was selected for the DLS method and viscosity value used in DLS analysis changed to 1.4 mPaS.

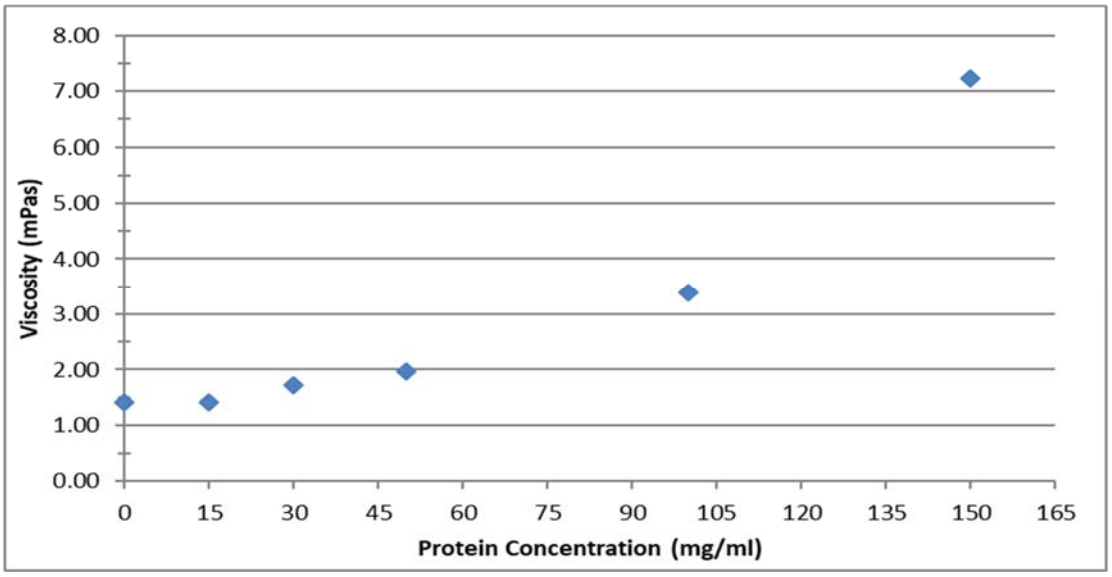


Figure 3-7: Viscosity of Protein Y solution at different concentrations and 25 °C

The initial DLS displayed in **Figure 3-6** was reprocessed based on the viscosities determined at the respective concentrations **(Figure 3-7)**. This lowered the Z-average values to a range between 1 to 14 nm and more importantly showed a divergence in the Z-average values for the freeze-thaw samples and the control at the respective concentration (**Figure 3-8).** This finding further confirmed 15 mg/ml as a suitable protein concentration for DLS analysis.

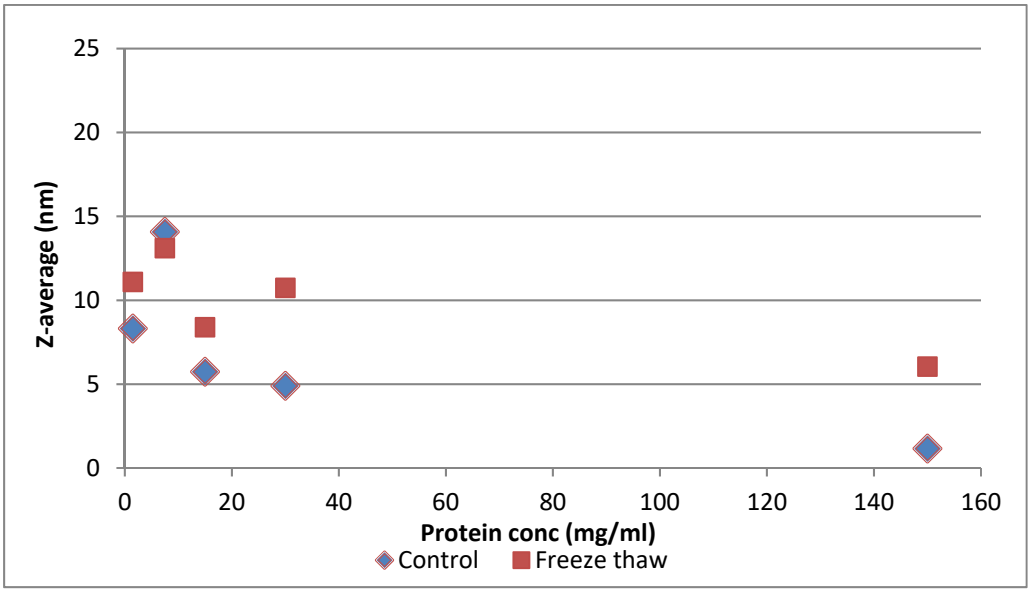


Figure 3-8: Concentration effect on Z-average of Protein Y for samples before and after a freeze-thaw cycle (Corrected viscosity for each concentration)

In order to determine if the DLS method can detect changes in protein aggregation, Protein Y samples were aged and analysed by DLS both unfiltered and filtered to assess any effect of filtration. No significant change was observed in Z-average the control and the 40 °C sample. However, Z-average of the 80 °C aged sample was significantly increased (**Figure 3-9**). In addition, a more gradual increase in PdI was observed as shown in **Figure 3-10**. There was no significant difference in PdI between filtered and unfiltered samples for the control and 80 °C aged sample, however a significant effect of filtration was observed for 40 °C aged sample. A second peak at a

mean size of 1112.8 nm and a mean intensity of 7.9% was observed only for unfiltered sample at 40 °C.

Based on the large size and low intensity of this peak, it is thought that filtration is still appropriate, to remove potential noise from extraneous particles.

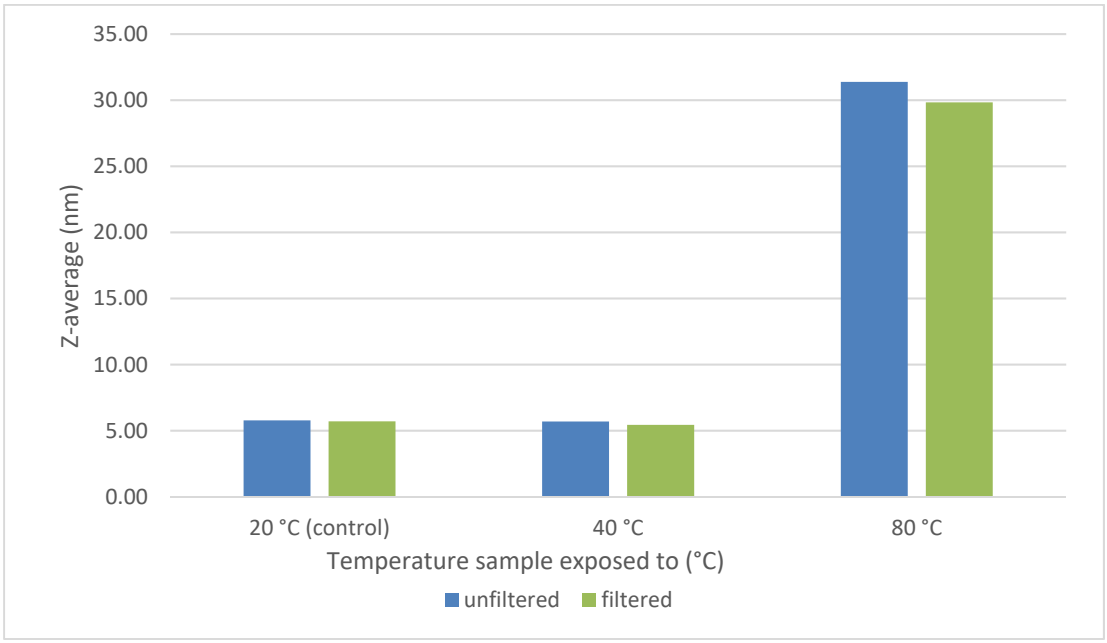


Figure 3-9: Protein Y DLS Z-average at a range of temperatures before and after filtration

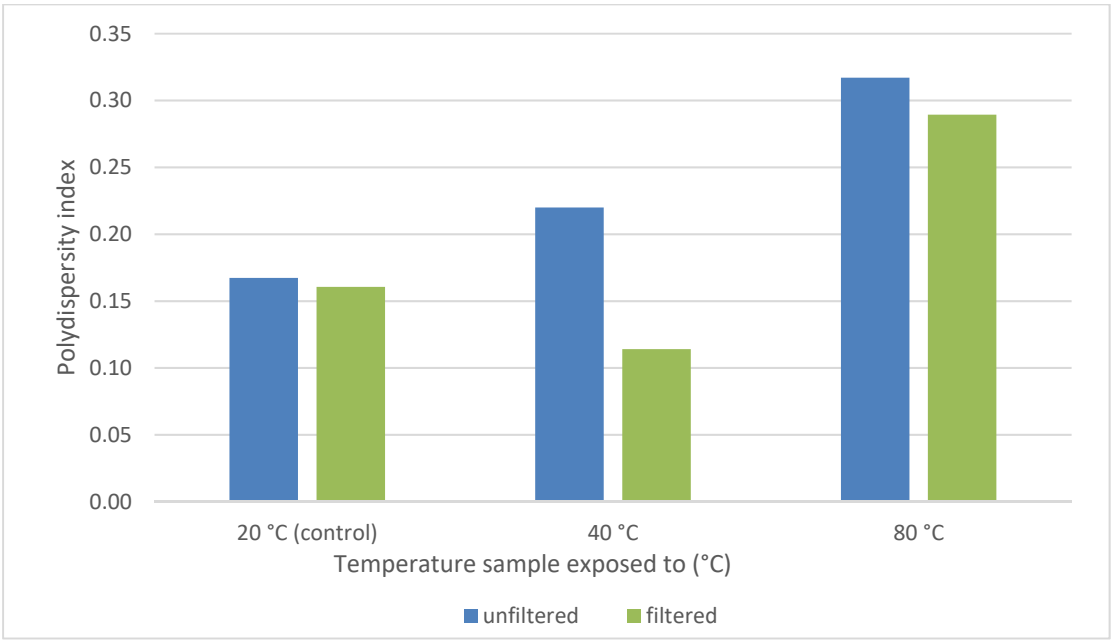


Figure 3-10: Protein Y DLS PDI at a range of temperatures before and after filtration

Use of DLS was proven as a suitable method to determine changes in aggregation of the Protein Y in the nano-/sub-micron ranges (1 – 1000 nm).

3.2.3 Circular Dichroism Spectroscopy (CD)/UV-Absorbance

In general, peak wavelength increases as the polarity of the microenvironment decreases. Due to the presence of L-histidine in the dilution buffer solution used in the Protein Y formulation, the FDS is very polar and excipient interference is expected in the far-UV region (250 – 190 nm). Therefore, focus was maintained on development of a characterisation method in the near-UV region (315 – 250 nm).

The optimum concentration for measurement was found to be 0.75 mg/ml, which gave a UV absorbance of <1.5 absorbance units at 280 nm. However, the CD spectra were very noisy and therefore further optimisation of the step and time per point values was performed with optimum values being obtained at 1.0 nm and 5 seconds as shown in **Figure 3-11** and **Figure 3-12,** respectively.

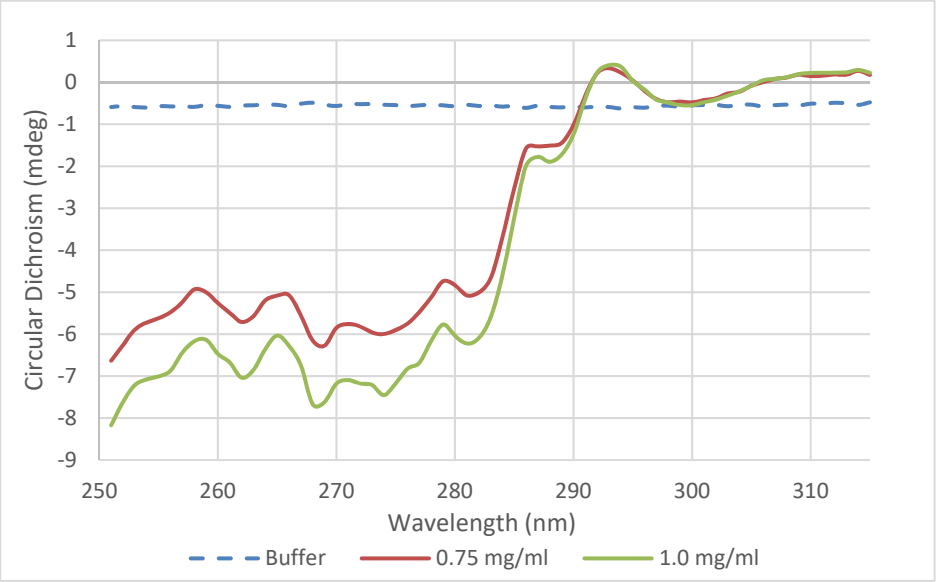


Figure 3-11: **CD spectra for 0.75 and 1.0 mg/ml Protein Y; 1 nm step / 5 seconds per time point**

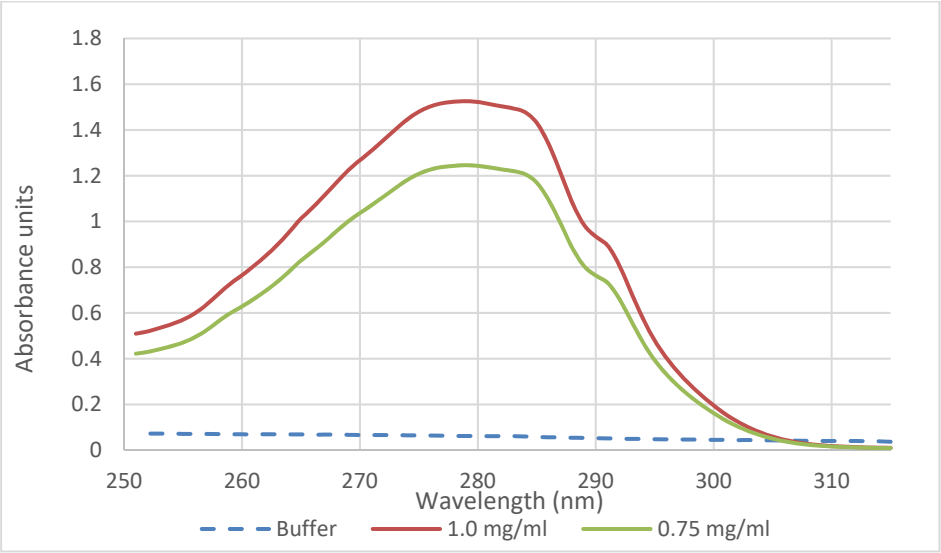


Figure 3-12: **UV absorbance spectra for 0.75 and 1.0 mg/ml Protein Y; 1 nm step /5 seconds per time point**

To see if the developed method could detect changes in the tertiary structure of Protein Y, the method was run with a temperature ramp, with spectra recorded at 20, 40, 60 and 80 °C, as displayed in **Figure 3-13**. No significant change was observed from 20 °C to 60 °C. However, there was a dramatic change noted in the CD spectra at 80 °C with most of the spectral peaks having flattened. The change in CD spectra at 80 °C corresponds with thermal events observed with DSC, indicating unfolding of the protein at 75 - 80 °C.

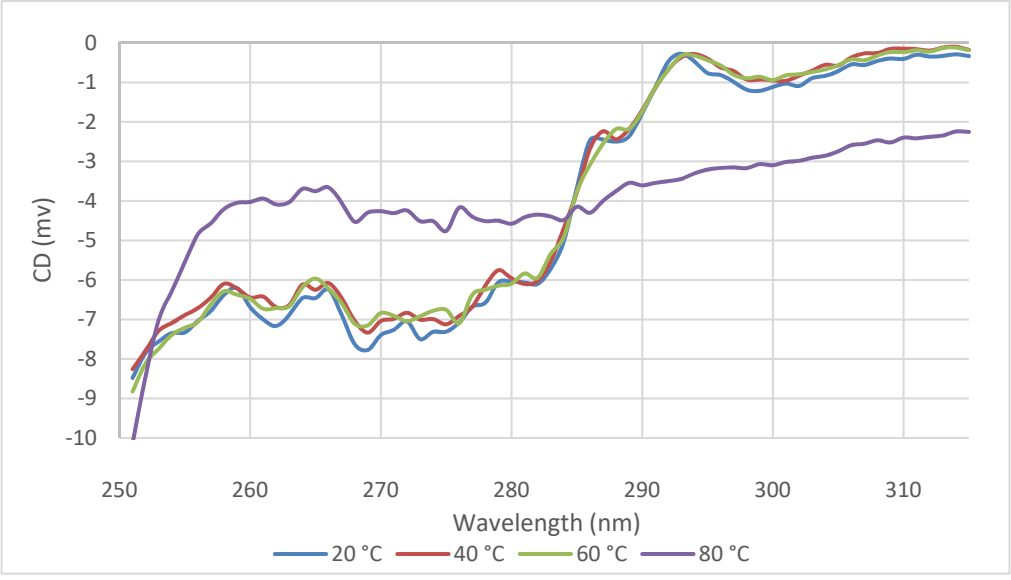


Figure 3-13: **Protein Y CD spectra with change of temperature**

3.2.4 Fluorescence Spectroscopy

Intrinsic fluorescence spectroscopy was employed to study FDS containing Protein Y at a range of protein concentration (150 mg/ml – undiluted, and subsequently dilutions down to 0.15 mg/ml), with excitation at 295 nm. The optimum concentration, giving a corrected intensity ratio of around 2,000,000 units was obtained at 1 mg/ml. The excitation was adjusted to 280 nm in order to maximise the intensity for tryptophan residues.

Optimum slit widths were investigated to determine the best setting that provided a corrected intensity ratio of less than 2,000,000 units, as shown in **Figure 3-14**. An optimum corrected intensity ration was determined by setting both excitation and emission slit widths to 1.5 nm.

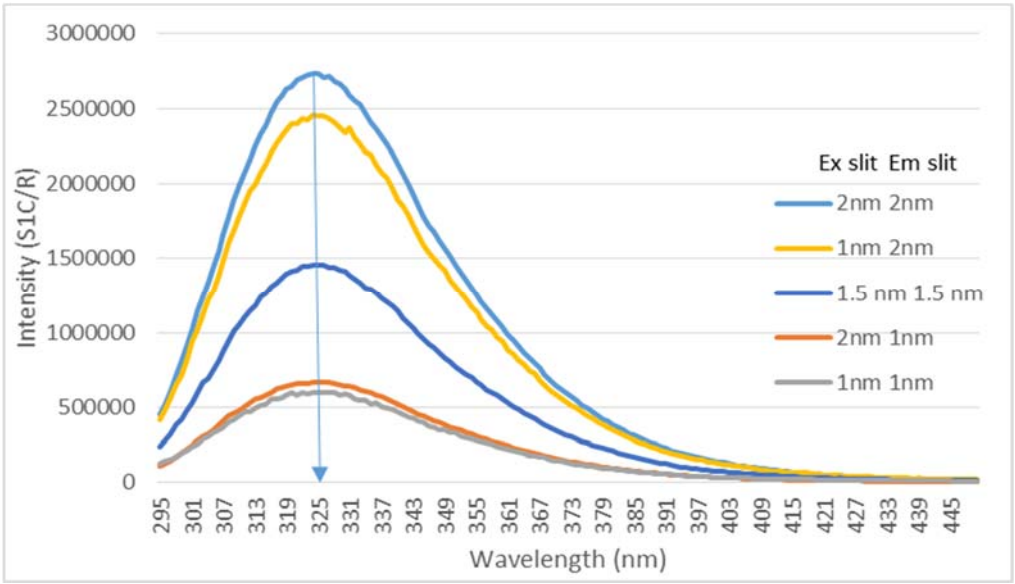


Figure 3-14: Intrinsic fluorescence spectra of Protein Y at 0.75 mg/ml measured at a range of slit settings and excitation wavelength at 280 nm

The temperature ramp exhibited decrease in corrected intensity ratio with increase in temperature but with no change in λ_{max} until the sample spectra at 80 °C, which demonstrated an increased shift in the lambda max from 324 nm to 333 nm. When the heated sample was cooled back to 20 °C, the corrected intensity ratio had increased

significantly beyond what it originally was at 20 °C but the λ_{max} remained at 333 nm (**Figure 3-15**).

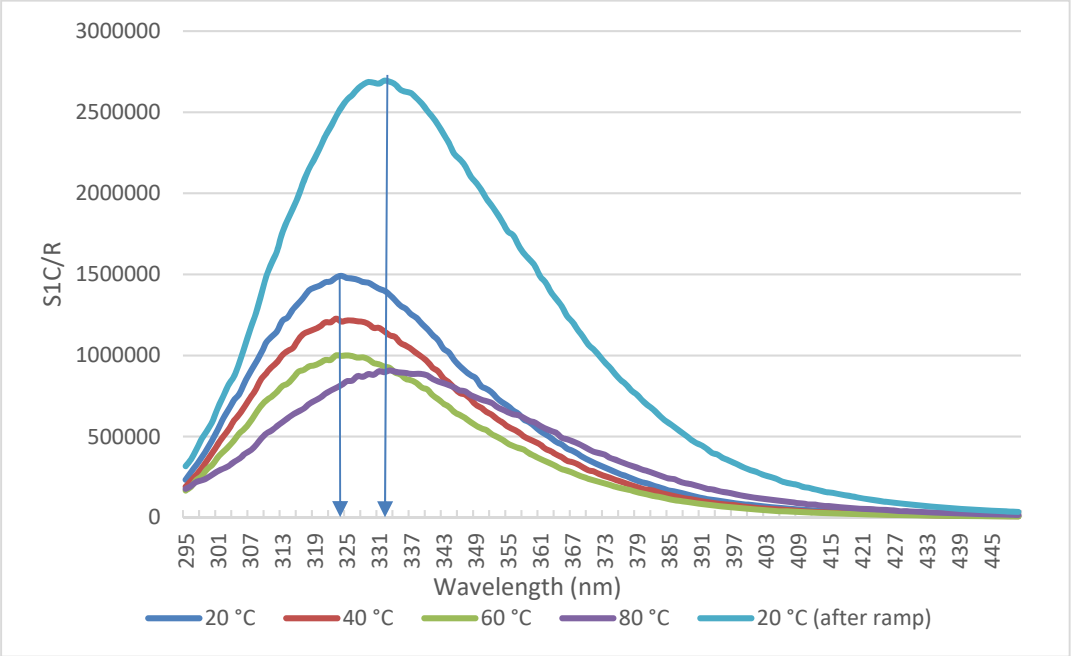


Figure 3-15: **Protein Y fluorescence spectra at temperatures from 20 – 80 °C and a sample heated to 80 °C and cooled to 20 °C**

Intrinsic fluorescence appeared to be capable detecting changes in the structure of Protein Y.

3.3 Freeze-Thaw Studies

Based on initial knowledge gathered from characterisation of the formulation and the selection of analytical methods that can detect perturbations in the structure and aggregation of Protein Y, a DoE study was conceived to achieve the aim of evaluating potential parameters that could cause change in structure or aggregate levels in the formulated drug substance.

As outlined in the **Section 2.3.3**, the DoE design generated a plan of eight runs, with the sequence listed in **Table 2-8**. The results of the DoE study are summarized and presented into the following sections:

- The effect of critical parameters on the freezing and thawing temperature profiles
- The effect of freeze/thawing process on Protein Y stability, immediately after thaw (time zero, T0)
- The effect of freeze/thawing process on Protein Y stability over 4 weeks at accelerated storage at 45 °C.

The techniques described in **Sections 2.3.1 and 2.3.2** were used to generate responses in order to establish predictive models for the attributes analysed. The following criteria were set to determine whether the respective response can be used to predict and optimize the process for the responses evaluated:

- The P-Value must be <0.05 for the model to be significant
- 2-level interactions between factors were only included if they improved model significance. Also, non-significant variables were included in the model if required to support hierarchy
- Predicated R-squared (R^2) is a measure of the amount of variation in new data explained by the model, the more terms (or predictors) in the model, the higher the predicted R^2. Adjusted R^2 is the fit adjusted for the number of parameters in the model relative to the number of points in the design. It will only increase in value if the newly added predictor enhances the model. To ensure the predicted R^2 has good descriptive power it must be within 0.2 of the adjusted R^2
- Adequate precision is a ratio of the predicted result relative to the average predicted error value for the model. Adequate precision should be greater than 4 for use in determination of model discrimination

- In some cases, data transformation was required, based on the data as indicated by a Box-Cox evaluation within the DoE software. For example, to process negative values for freezing temperature rates or for time-based responses, where the data can only increase. If data transformation was required, the transformation method, lambda (power value) and constant (k) are included in the respective significant parameter effect table.

If the above criteria were satisfied for a respective response, a model R^2 and significant parameter effect table has been included summarising the overall fit (R^2) and significant factors in the model. Single level factors with significant effect in a model are indicated by black '+' or '-' symbols in the respective model summary tables. For visualisation purposes, a relative indication of the parameter contribution is indicated by blue shading related to the F-value for the respective significant parameter, with darker blue showing a bigger effect (**Table 3-1**). In some cases, single factors are included in the model to support model hierarchy, although the single level factors may not be significant. These have been indicated in the model summary tables in bracketed red '+' or '-' symbols. If the factor was not selected in the model, this has been indicated with a '0'.

Table 3-1: Shading key for significant parameter F-value in model summary tables

Significant model parameter F-value	Shading in significant parameter table
0 - 20	
20 - 50	
50- 100	
100 - 200	
>200	

3.3.1 Temperature Profile Results

Temperature data was gathered using ELLAB double Smartflex probes as per the experimental design, with the one probe located at the bottom inside edge of the bottle ('bottom') and the other probe located towards the top and centre of the FDS ('top'). To provide an initial understanding of freeze-thaw process times, an average freeze and thaw rate was determined for each run simply based on the time taken for the difference in temperature the FDS experienced during freeze and thaw respectively to reach set-points. These values are shown in **Table 3-2**. The temperature data has been broken down into the freeze and thaw steps and further discussed in **Sections 3.3.1.1** and **3.3.1.2**.

Table 3-2: Key temperature and time data from freeze-thaw runs

Run	Temperature of FDS when placed into freezer (°C)	Time from freezer entry to set point (hh:mm)	Overall freezing rate (°C / minute)	Temperature of FDS when removed for thawing (°C)	Time from freezer removal to 15 °C (hh:mm)	Overall thaw rate (°C / minute)
1	11.37	04:30	-0.12	-23.25	02:59	0.21
2	10.09	03:00	-0.47	-26.41	13:52	0.05
3	20.02	06:27	-0.24	-23.95	08:50	0.07
4	14.05	13:32	-0.04	-23.14	03:54	0.16
5	11.22	06:59	-0.21	-80.65	03:56	0.41
6	11.22	04:37	-0.11	-80.05	10:40	0.15
7	10.25	13:58	-0.04	-75.89	13:53	0.11
8	11.50	02:03	-0.70	-78.82	03:47	0.41

The overall freezing rate was determined by the time taken for the top probe in the bottle to reach the respective freezer set point, as this was deemed to be the last point to freeze. Although a -80 °C freezer was used in the DoE, two of the four runs where

FDS was initially frozen using this freezer did not reach the freezer set-point (run 2; -75.0 °C and run 3; -73.9 °C). Therefore, a value of -75 °C was used for the purposes of determining overall freezing rate and post-cooling rates to be consistent across all runs.

The overall thawing rate was determined by the time taken for the top probe in the bottle to go from temperature at time of removal from the freezer to reach 15 °C, as this was shown to be the last point to thaw. This temperature was chosen as it was a minimum temperature that was recorded for all runs after thaw. The overall freeze and thaw rates across all three phases for each run are shown in **Figure 3-16.**

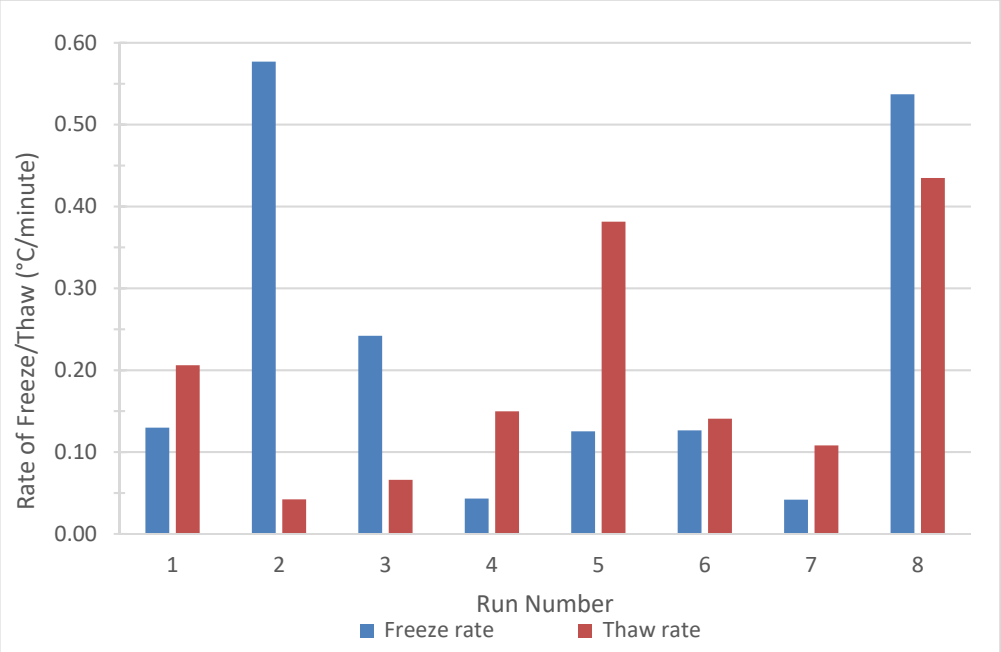


Figure 3-16: Freeze/thaw rates by run

3.3.1.1 Freezing

The full freezing profiles determined by the temperature probes at the top and bottom of each container for freeze are illustrated in **Figure 3-17** and **Figure 3-18**, respectively. The area highlighted in **Figure 3-18A** is displayed in **Figure 3-18B**, indicating exothermic changes in temperature observed by the bottom probe.

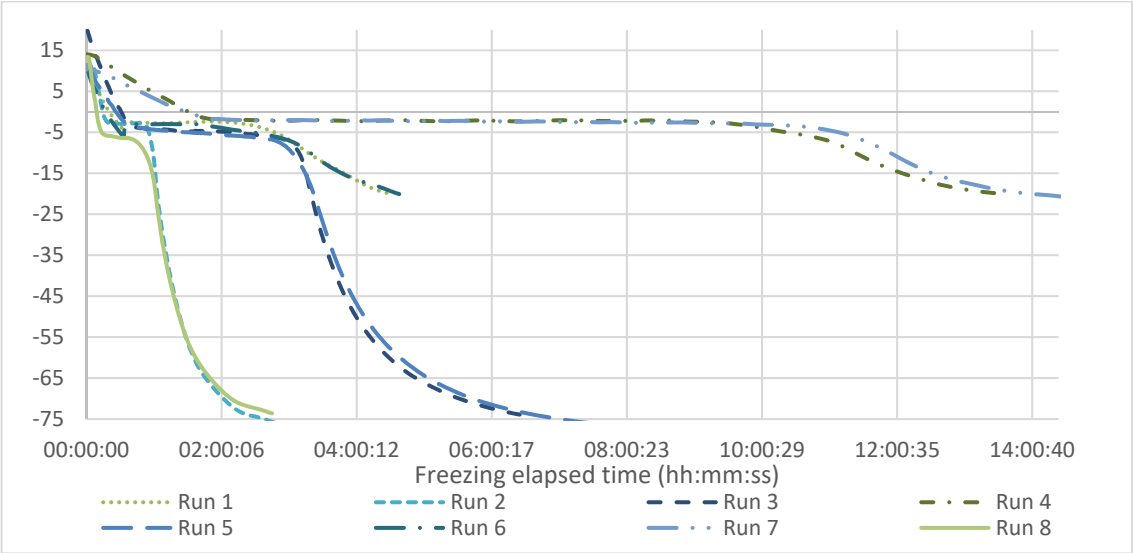
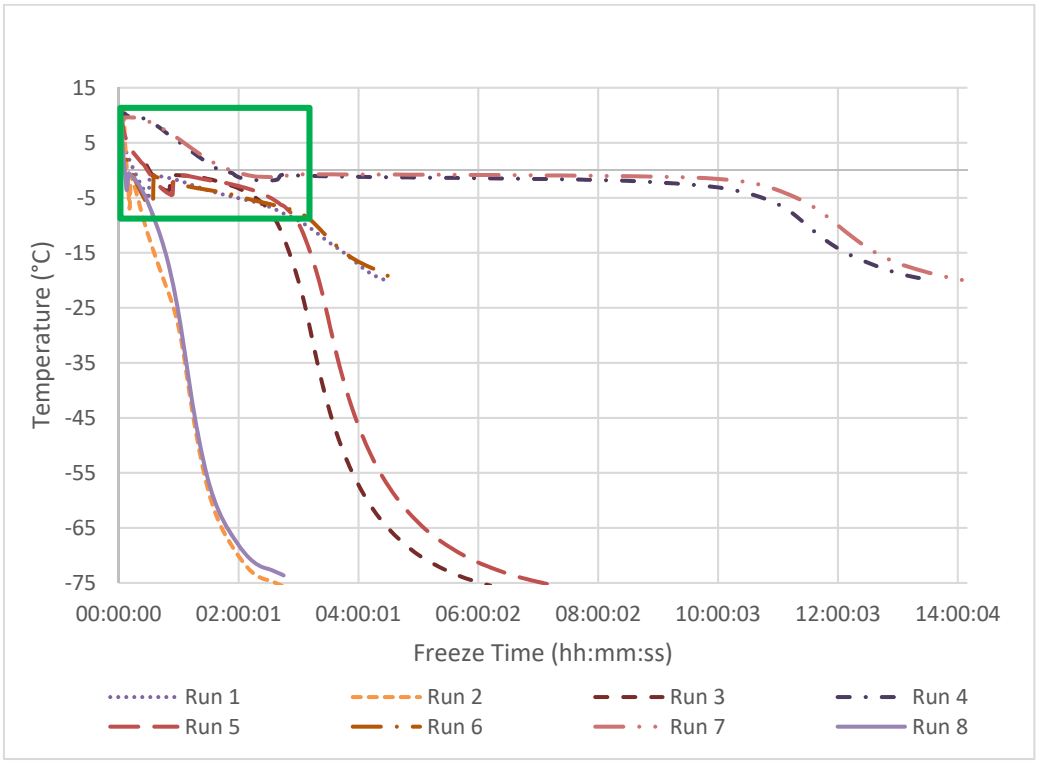


Figure 3-17: Freezing profile of FDS measured by the top probe for each DoE run

A



B

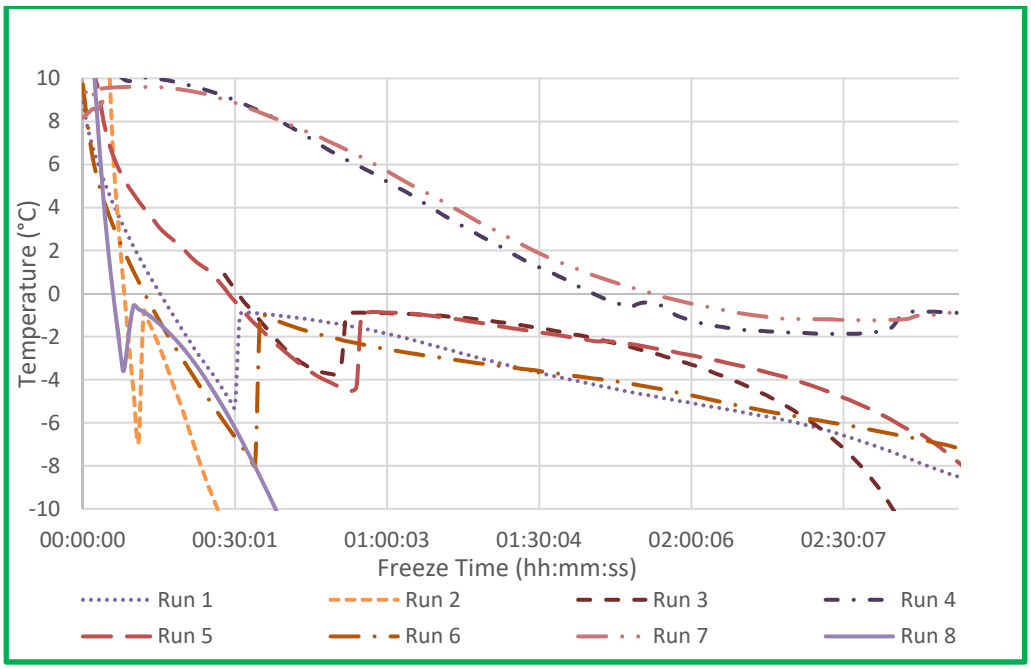


Figure 3-18: Freezing profile of FDS. A: Measured by the bottom probe for each DoE run, and B: Displaying insert area highlighted in A showing nucleation exotherms

It is interesting to note the temperature at the bottom of the bottle does exhibit a rise in temperature (exotherm) as shown in **Figure 3-18B**, which is indicative of ice nucleation.

Surrounding the FDS bottle with co-loaded bottles (runs 3, 4, 5 and 7) was shown to have a significant effect on the time to reach freezer set point. The extended time was due to a plateau occurring at temperatures between -1 to -8 °C and is considered as the 'actual' freezing time, as the plateau is the result of the time it takes for the latent heat of fusion to be removed, as water is converted into ice (Padala et al., 2010). As expected, freezing temperature also had a significant effect on the freezing behaviour. Bottles frozen in a -80 °C freezer (runs 2, 3, 5 and 8) had a shorter time to reach the final temperature, hence a faster freeze rate.

Expanding on this approach, the freezing profiles were broken down into three different phases: pre-cooling, freezing and sub-cooling (López-Leiva and Hallström, 2003; Radmanovic et al., 2013). The freezing phase was defined as having initiated

when a rate of change in temperature of greater than -0.10 °C/min was observed for three consecutive minutes or, in the event that there were less than three readings, then the freezing time was taken as 1 or 2 minutes, as applicable. The freezing phase was defined as having been completed when the temperature change returned to being lower than -0.10 °C/min. This freezing period resulted in a 'plateau' in temperature. Values for pre-cooling rate, freezing time and sub-cooling rate are shown in **Table 3-3**.

Table 3-3: Freezing phase times and rates

Run	Time from freezer entry to plateau (pre-cooling) (hh:mm)	Pre-cooling rate (°C / minute)	Freezing time (plateau) (hh:mm)	Time to go from plateau to freeze set point (sub-cooling) (hh:mm)	Sub-cooling rate (freeze rate from plateau to set point) (°C / minute)
1	00:35	-0.39	02:12	01:42	-0.17
2	00:17	-1.06	00:01	02:41	-0.42
3	00:51	-0.47	02:09	03:26	-0.34
4	01:42	-0.16	09:23	02:26	-0.12
5	00:41	-0.37	02:08	04:09	-0.29
6	00:36	-0.40	02:26	01:34	-0.18
7	01:32	-0.13	09:54	02:32	-0.12
8	00:09	-2.15	00:01	01:52	-0.60

The duration of the freezing plateau was capable of being described by a statistically significant model (P-value 0.0001), with the model heavily influenced by the significant parameters of presence of co-load bottles surrounding the FDS bottle as well as the freezer temperature.

The pre-cooling and sub-cooling rates of change in temperature were also described by statistically significant models (P-values of 0.0005 and 0.0001 respectively), with both

freezer temperature and freeze co-load being significant factors for both responses. As expected, freeze equilibration, thaw co-load and agitation speed did not have any significant contribution to the models for freezing rates and times and were not selected in the models. A summary of significant parameters for all freezing parameters is shown in **Table 3-3**. It should be noted that, as the change in temperature for a freezing process decreases, a negative rate occurs which required data transformation to allow analysis in the DoE. This has been described in **Table 3-4**, where applicable.

Table 3-4: Combined model R^2 and significant parameter effect for freezing times and rates

	Model R^2	**Freezing temperature**	**Freeze co-load**	**Freezing equilibration**	**Thaw co-load**	**Agitation speed**
Pre-cooling rate (power, lambda: 1.95, k: 1.0593)	0.9505	+	-	**0**	**0**	**0**
Freezing time (plateau)	0.9949	+	-	**0**	**0**	**0**
Post-cool rate after plateau (lambda: 1, k: 0.763342)	0.9690	+	-	**0**	**0**	**0**
Overall time to get to set point (inverse square root, lambda: -0.5)	0.9374	-	+	**0**	**0**	**0**

+ positive interaction; - negative interaction

Interestingly, the onset of the ice nucleation event shown in **Figure 3.18**, displays an exponential relationship with the pre-cooling rate, which has been shown in **Figure 3-19**. A faster cooling rate resulted in an earlier onset of the exotherm. However, there is no clear relationship for the magnitude (change in temperature) to cooling rate.

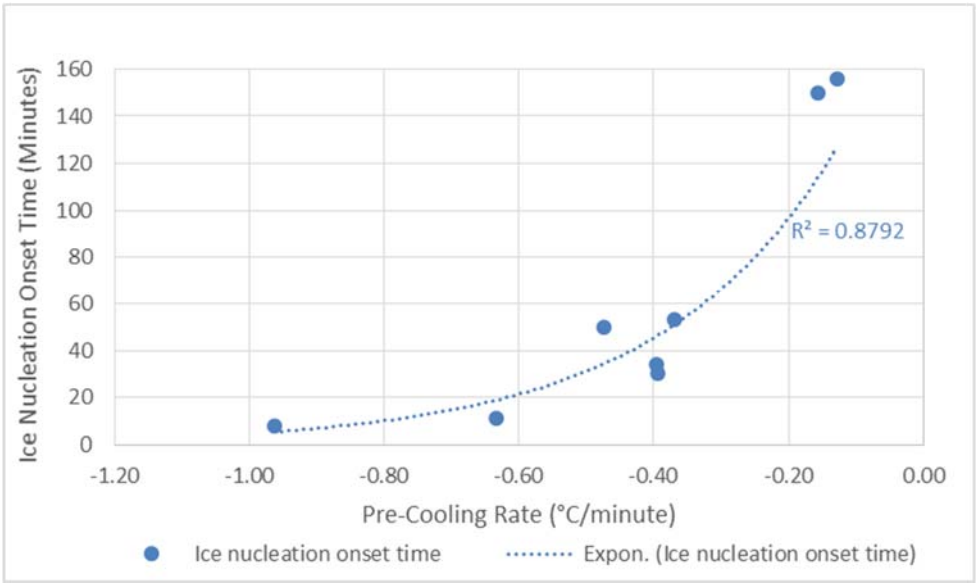


Figure 3-19: Relationship between ice nucleation onset time and pre-cooling rate

3.3.1.2 Thawing

The full thawing profiles determined by the temperature probe at the top and bottom of each container are illustrated in **Figure 3-20** and **Figure 3-21**, respectively.

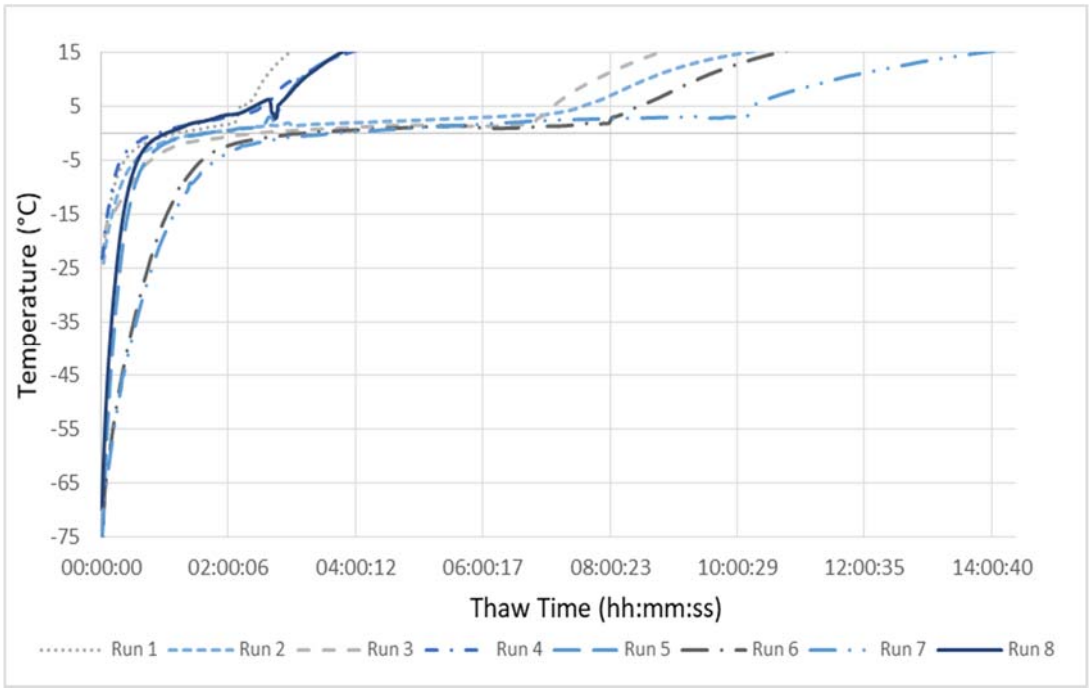


Figure 3-20: **Thawing temperature profile of FDS measured by the top probe for each DoE run**

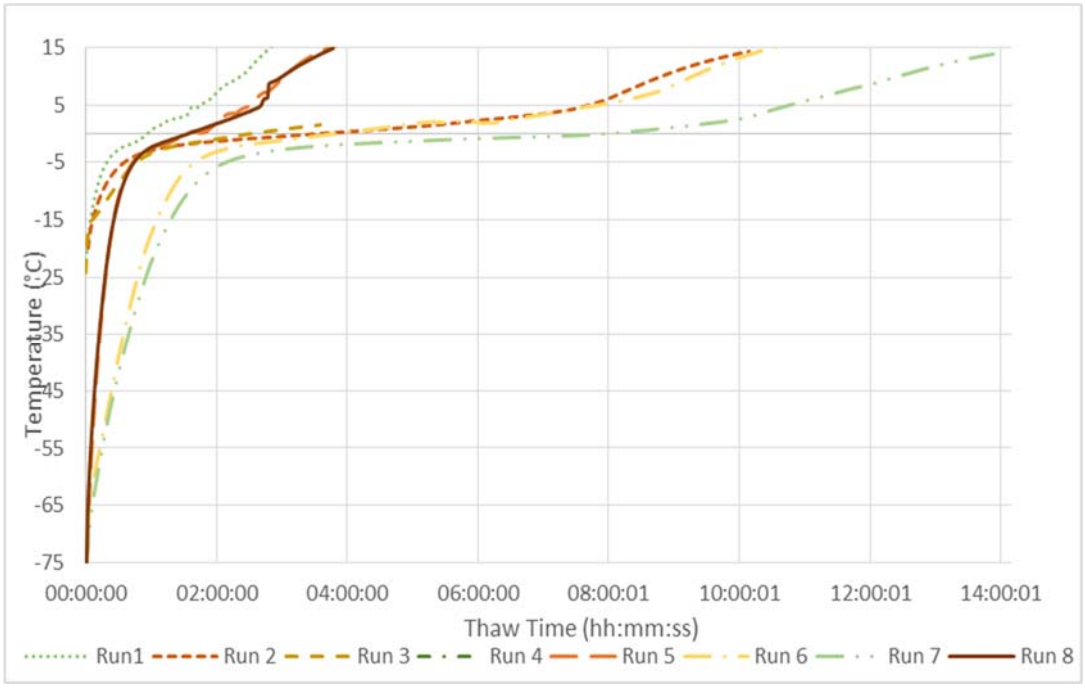


Figure 3-21: Thawing temperature profile of FDS measured by the bottom probe for each DoE run

Surrounding the FDS bottle with co-loaded bottles was shown to have a significant effect on overall thaw time, resulting in a plateau in temperature between 0 to 3 °C, where the ice melt occurs. The time to thaw was also affected by whether agitation was used or not, with agitation resulting in reducing a thawing time by 1 and up to 4 hours for single and co-loaded bottles, respectively.

Similar to freezing parameters, the thawing step was broken down into three sub-phases: pre-thawing, thawing (temperature plateau) and post-thaw and the values are presented in **Table 3-5.** For the purposes of analysis, the plateau was defined as when the rate of increase in temperature was less than 0.10 °C/ minute.

Table 3-5: Thawing phase times and rates

Run	Time from freezer removal to thaw plateau (hh:mm)	Pre-thaw rate (°C / minute)	Thaw plateau time (hh:mm)	Time from thaw plateau to 15 °C (hh:mm)	Post-thaw rate (°C / minute)
1	00:38	0.62	01:33	00:47	0.31
2	04:36	0.10	06:40	02:35	0.08
3	01:09	0.36	05:45	01:55	0.12
4	00:42	0.61	01:49	01:22	0.15
5	01:06	1.22	01:33	01:16	0.20
6	01:53	0.72	06:21	02:25	0.10
7	02:00	0.64	08:11	03:42	0.06
8	01:01	1.33	01:18	01:27	0.15

Thaw plateau time was found to be heavily influenced by the presence of co-load bottles (runs 3, 4, 6 and 7) surrounding the FDS bottle during thawing (P-value of 0.0001). Statistically significant models were generated to describe both pre-thaw and post-thaw phases (P-values of 0.0005 for initial thaw rate and 0.0027 for thaw rate, post-plateau). Freezing equilibration temperature and thaw co-load were both significant factors within the model for pre-thaw rate. Thaw co-load and agitation speed were both significant factors for the post-thaw rate. A statistically significant model was also generated for prediction of overall thaw time (P-value 0.0017) with thaw co-loading and agitation speed selected as significant parameters. Freezing equilibration temperature was selected as a non-significant factor in the overall thaw time to support model hierarchy. As expected, freezing temperature and freeze co-load did not have any significant contribution to the model for thawing rates and times and were not selected in the models. A summary of significant parameters for all freezing parameters is shown in **Table 3-6**.

Table 3-6: Combined model R^2 and significant parameter effect for thawing responses

	Model R^2	Freezing temperature	Freeze co-load	Freezing equilibration	Thaw co-load	Agitation speed
Pre-thaw rate	0.9512	**0**	**0**	-	+	**0**
Thaw plateau time	0.9412	**0**	**0**	**0**	-	**0**
Post-thaw rate plateau (inverse square root, lambda: -0.5)	0.9057	**0**	**0**	**0**	-	-
Overall time to thaw (square root, lambda: 0.5)	0.9993	**0**	**0**	**(-)**	-	-

+ positive interaction; - negative interaction; (-): non-significant negative interaction

3.3.2 DoE Results – Post Thaw

3.3.2.1 Cryo-Concentration

3.3.2.1.1 UV Absorbance

Samples were taken from the top, middle and bottom of the FDS immediately after completion thawing, taking care not to disturb the solution during sampling. Each sample was diluted to 0.75 mg/ml and UV absorbance spectra were generated.

An assessment of the variation in protein concentration was made by comparing UV absorbance at the scan maxima of 280 nm (A280). Run 8 had the lowest variation in A280 values, with Run 4 exhibiting the highest variation. The A280 from top, middle and bottom of each run are displayed in **Figure 3-22**.

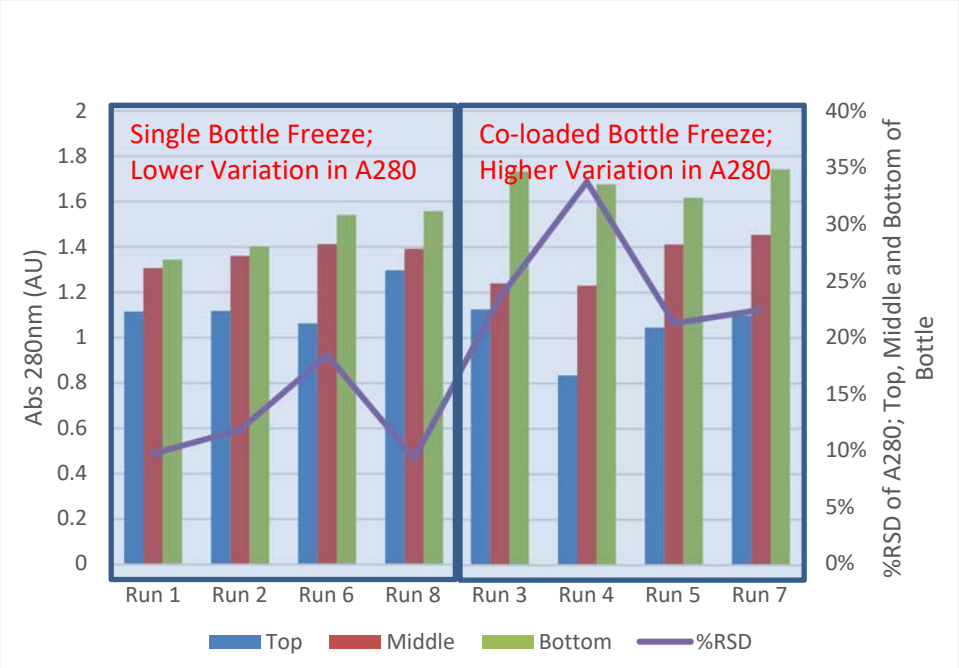


Figure 3-22: Assessment of Protein Y cryo-concentration by UV absorbance and %RSD at 280nm vs sample locations in bottle

Cryo-concentration was assessed by analysing the variability in UV absorbance at 280 nm (A280) from samples taken from top, middle and bottom of the FDS, immediately post-thaw. A statistically significant model was generated (P-value 0.0109), with freezing co-loading as a significant factor; where the FDS bottle is surrounded by co-loaded bottles a higher variation in A280 values from top to bottom of the FDS was observed (**Table 3-7**). As presence of co-loaded bottles also significantly affects all phases of freezing, it is thought that a slower freezing rate results in a higher protein concentration at the bottom of the bottle and therefore higher variability.

Table 3-7: Combined model R^2 and significant parameter effect for variation in A280 across top, middle and bottom of FDS

	Model R^2	Freezing temperature	Freeze co-load	Freezing equilibration	Thaw co-load	Agitation speed
A280 –variation (%RSD) post-thaw	0.6876	**0**	**-**	**0**	**0**	**0**

- negative interaction

3.3.2.2 Protein Unfolding

3.3.2.2.1 Differential Scanning Calorimetry (DSC)

Protein unfolding was assessed using DSC method developed (**Section 3.2.1**) and the results for unfolding onset and mid-point temperature are shown for each run in **Table 3-8**.

Table 3-8: DSC unfolding onset and midpoint temperatures for Protein Y post-thaw (± standard deviation)

	Mean Unfolding Onset Temperature (°C)	Mean Unfolding Mid-Point Temperature (°C)
Bulk control	75.2 (±0.12)	81.1 (±0.05)
Run 1	75.2 (±0.11)	81.1 (±0.05)
Run 2	75.2 (±0.28)	81.1 (±0.14)
Run 3	75.3 (±0.06)	81.2 (±0.12)
Run 4	75.5 (±0.24)	81.2 (±0.08)
Run 5	74.9 (±0.11)	81.2 (±0.00)
Run 6	75.0 (±0.11)	81.2 (±0.05)
Run 7	75.2 (±0.09)	81.3 (±0.09)
Run 8	74.8 (±0.41)	81.3 (±0.09)

There was only slight change noted in the onset or mid-point of the unfolding temperature for Protein Y across all runs. The DoE was able to generate a statistically significant predictive model for unfolding onset temperature (P-value 0.0089), which exhibited greater variation than mid-point temperature. Freezer temperature, freezing

co-load and freezer equilibration temperature were all statistically significant factors within the model for unfolding on-set temperature (**Table 3-9**).

Table 3-9: Combined model R^2 and significant parameter effect for unfolding onset temperature by DSC

	Model R2	Freezing temperature	Freeze co-load	Freezing equilibration	Thaw co-load	Agitation speed
DSC unfolding onset	0.9303	+	-	+	**0**	**0**

+ positive interaction; - negative interaction

3.3.2.3 Protein Tertiary Structure

3.3.2.3.1 Circular Dichroism (Near-UV)

Circular dichroism spectra were generated in triplicate and averaged for each sample as per the parameters developed for the method (3.2.3). The average spectra obtained for each sample from each run is shown in **Figure 3-23**.

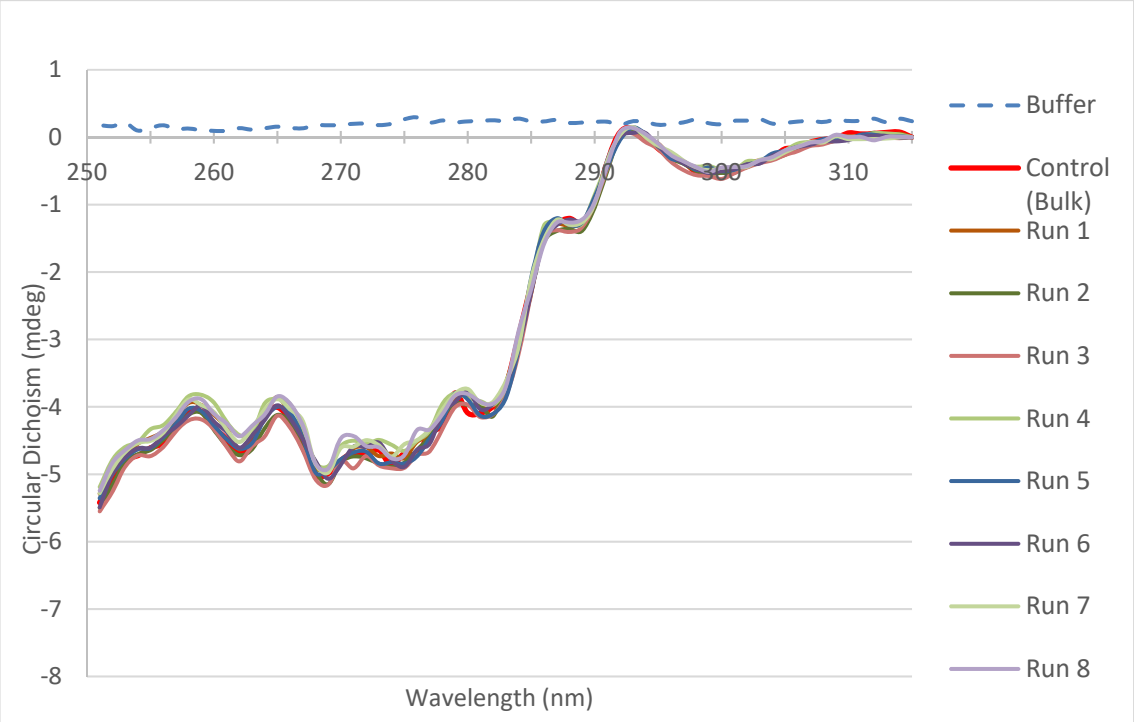


Figure 3-23: Averaged circular dichroism spectra normalised against respective A280 and then aligned based off CD value at 315 nm

The spectra were examined qualitatively and were not analysed as a response in the DoE. The shape of the spectra for all runs appear consistent, with the greatest area of variation appears to be between 270 nm and 280 nm, which is an area of the spectra attributed to tyrosine residues (Kelly et al., 2005).

3.3.2.3.2 UV Absorbance

UV absorbance spectra were also measured. The average spectra obtained for each sample is shown in **Figure 3-24**.

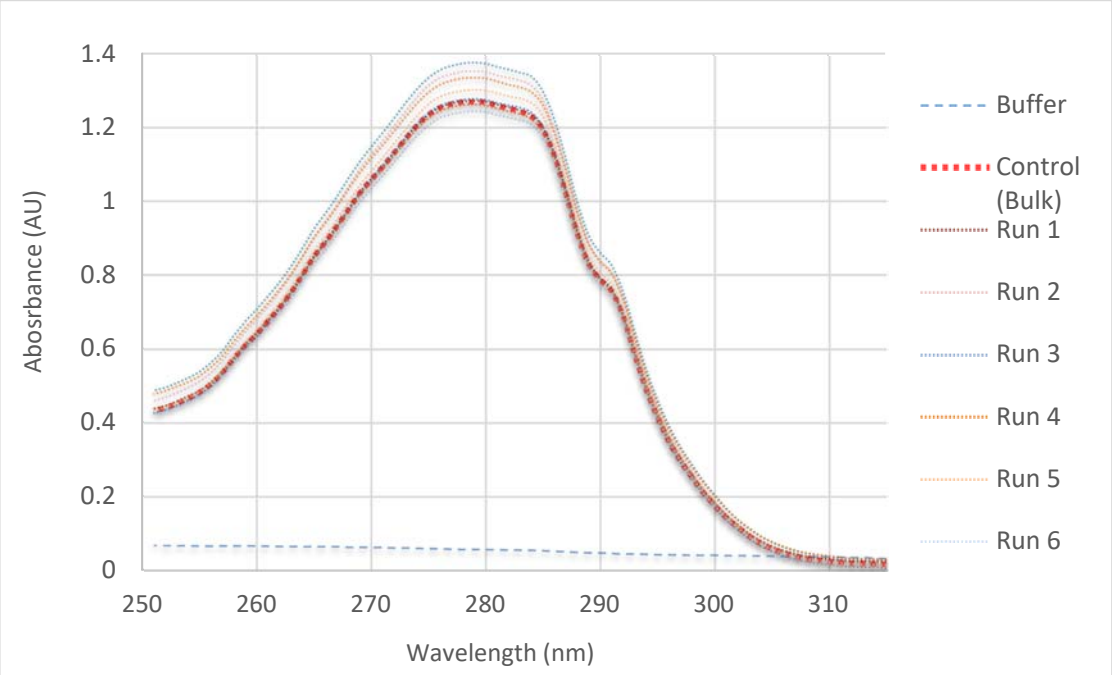


Figure 3-24: UV absorbance spectra of Protein Y FDS following freeze/thaw for each DoE run of DoE

The 1st and 2nd derivatives of the near-UV absorbance spectra were generated using Origin software and are displayed in **Figure 3-25** and **Figure 3-26** below.

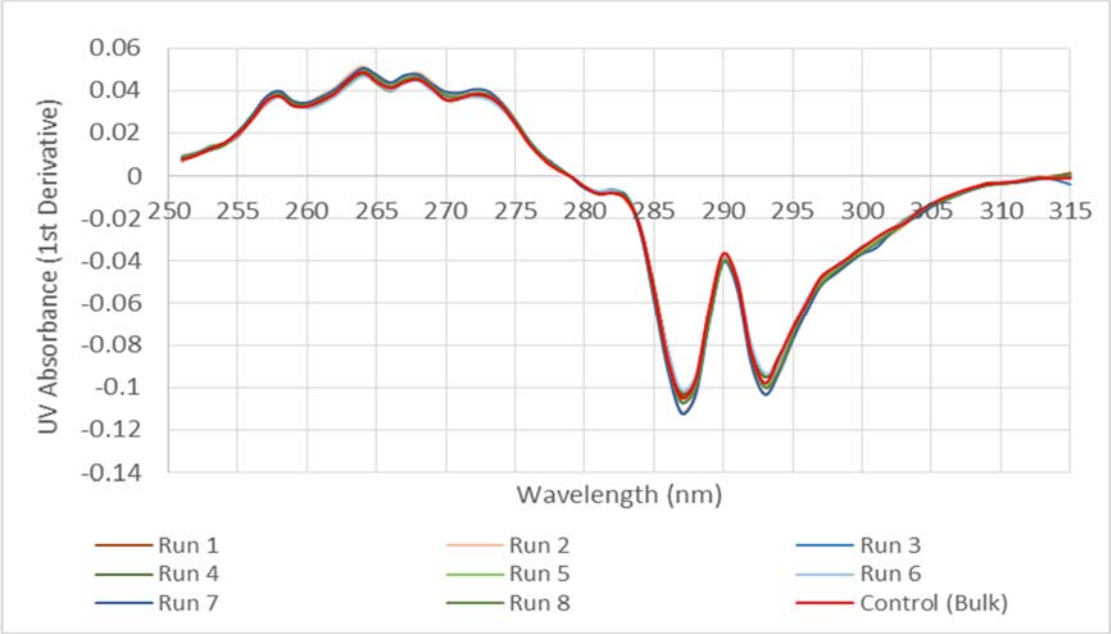


Figure 3-25: First derivative UV absorbance spectra of Protein Y FDS following freeze/thaw for each DoE run

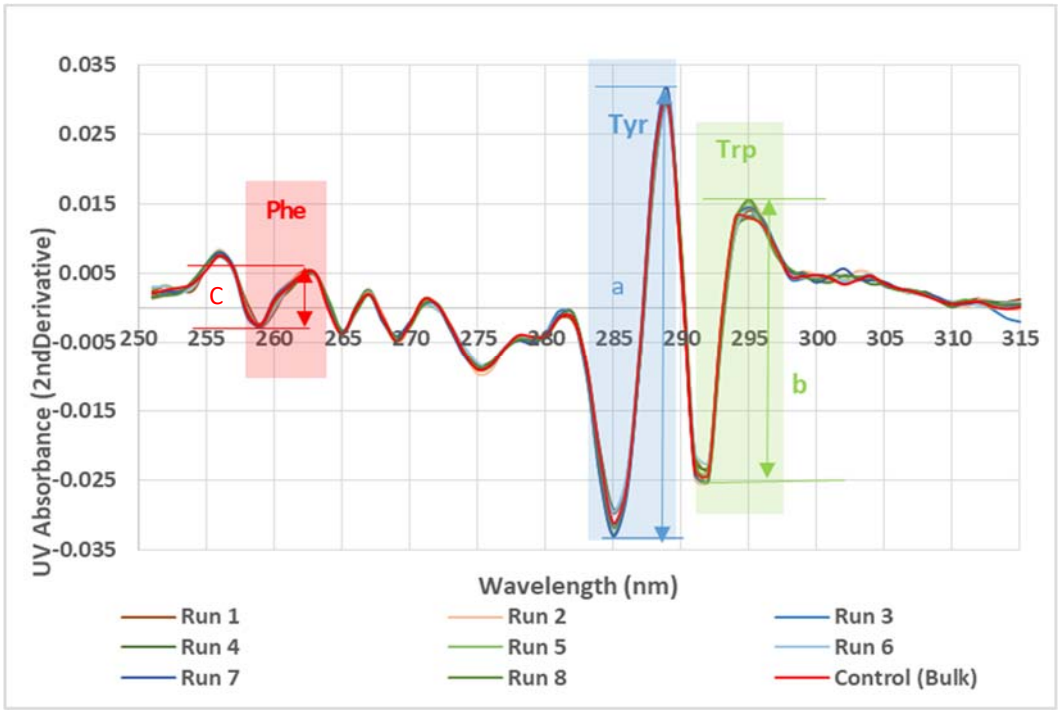


Figure 3-26: Second derivative UV absorbance spectra of Protein Y FDS following freeze/thaw for each DoE run. Peaks associated with tyrosine (Tyr), tryptophan (Trp) and phenylalanine (Phe) are identified

In order to analyse the effect of freeze and thaw parameters on the tertiary structure, peak height difference of the second derivative UV spectra, corresponding to an arbitrary distance from peak to trough can be measured for the three aromatic amino

acid residues; tryptophan (Trp), tyrosine (Tyr) and phenylalanine (Phe). Ratios of these distances were generated to assess any changes in the microenvironment of Protein Y (Katayama et al., 2005), as illustrated in **Figure 3-26**.

Statistically significant models were generated for Tyr/Trp and Tyr/Phe ratios (P-values of 0.0081 and 0.0083 respectively), with significant factors as indicated in **Table 3-10**. The data indicates that there are subtle changes in the microenvironment, with co-loading of bottles at freezing being a significant factor in the peak ratio of tyrosine to tryptophan. As reported in **Section 3.3.1.1**, a slower freezing rate will occur with co-loaded bottles. The consequence of a slower freezing rate could result in the exposure of tyrosine residues in the core of the protein to become more exposed relative to tryptophan and therefore increasing the peak ratio for these two aromatic amino acid residues. A slow thaw rate as described by co-loaded bottles could also induce the same effect. The model of tyrosine to phenylalanine peak ratio contained significant factors for freezing temperature and thaw co-load, as negative interactions, indicating that slower freeze and thaw rates will expose tyrosine residues within the hydrophobic core of the protein.

Table 3-10: Combined model R^2 and significant parameter effect for aromatic amino acid residue peak distances as generated by 2° UV spectra

	Model R^2	**Freezing temperature**	**Freeze co-load**	**Freezing equilibration**	**Thaw co-load**	**Agitation speed**
UV second derivative Tyr/Trp ratio post-thaw	0.9335	**0**	**-**	**(-)**	**(-)**	**0**
UV second derivative Tyr/Phe ratio post-thaw	0.8529	**-**	**0**	**0**	**-**	**0**

- negative interaction (-): non-significant negative interaction

3.3.2.3.3 Intrinsic Fluorescence

Spectra of intrinsic fluorescence were generated using the Fluoromax FT-4 spectrometer in triplicate. The averaged spectra are shown in **Figure 3-27**.

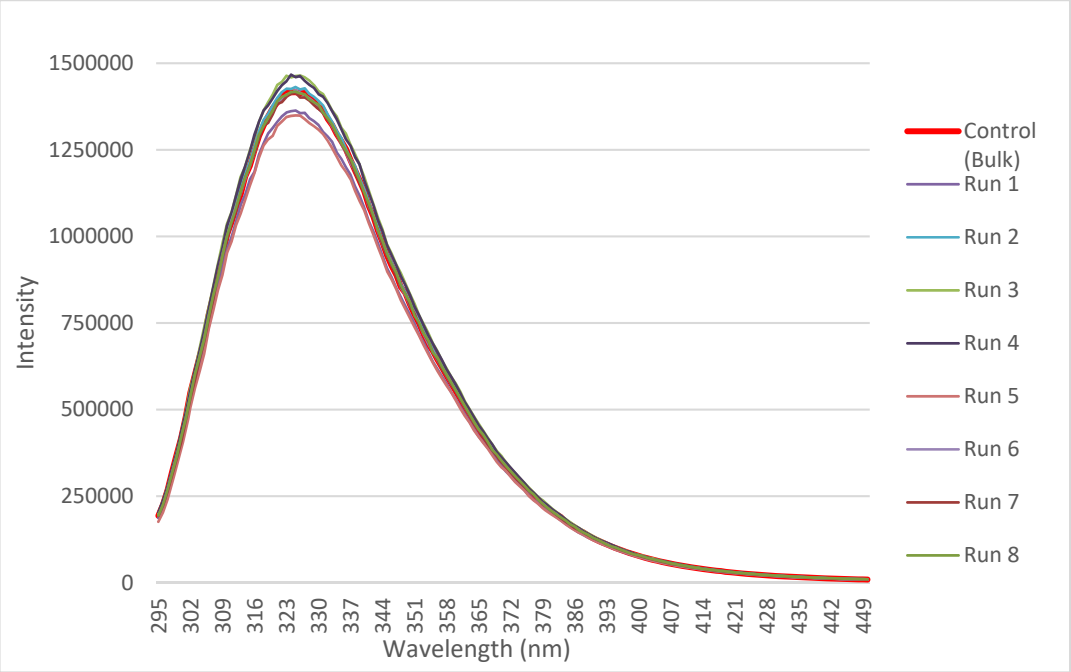


Figure 3-27: **Intrinsic fluorescence spectra of Protein Y FDS following freeze/thaw for each DoE run.**

The fluorescence spectra were analysed for shifts in the wavelength at which maximum intensity occurred (λ_{max}) and changes in the maximum intensity recorded. There was negligible change in the λ_{max} indicating no evidence of unfolding of the protein, as shown in **Figure 3-28**.

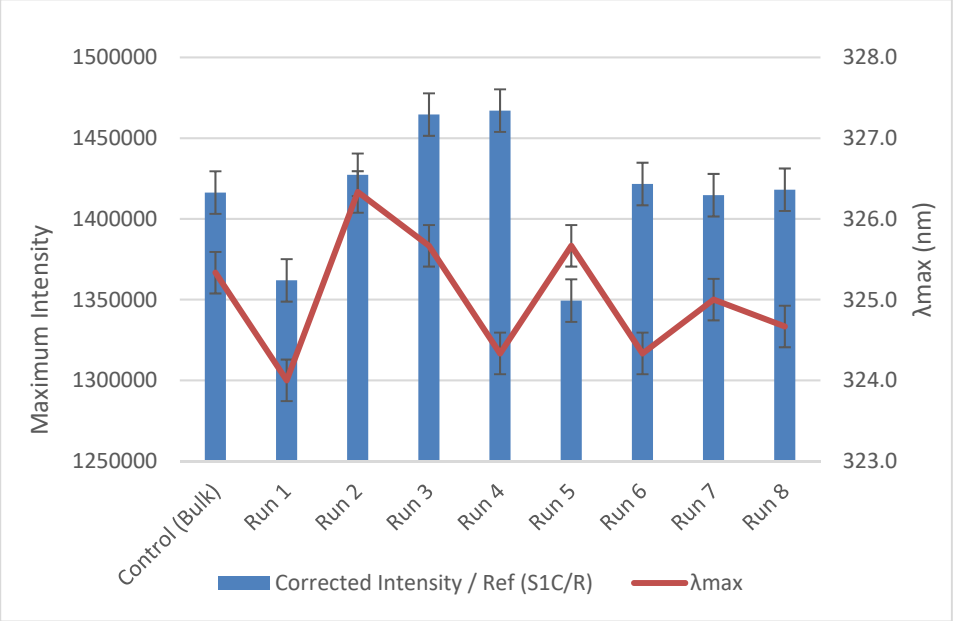


Figure 3-28: **Protein Y maximum fluorescence intensity and corresponding λ_{max} of Protein Y FDS following freeze/thaw for each DoE run.**

A statistically significant model was generated to describe prediction of intensity for the intrinsic fluorescence method post-thaw (P-value: 0.0018), as summarised in **Table 3-11**. Freeze co-load, freezing equilibration temperature, thaw co-load were all significant factors for intensity, whilst freezing temperature did not contribute to the response variation and was not included in the model. The model for λ_{max} was weaker and although a model could be generated with a P-value of <0.05, the predictive power as indicated by proximity of predicted R^2 to adjusted R^2 was not sufficient to allow for use.

Table 3-11: Combined Model R^2 and parameter effect for intrinsic fluorescence maximum intensity and λ_{max}

	Model R^2	**Freezing temperature**	**Freeze co-load**	**Freezing equilibration**	**Thaw co-load**	**Agitation speed**
Corrected intensity ratio post-thaw	0.9993	**0**	-	+	-	-

+: positive interaction -: negative interaction

3.3.2.4 Protein Aggregation

3.3.2.4.1 DLS

The Z-average and PdI of Protein Y FDS was determined by DLS. The average results for Z-average and PdI of each freeze-thaw run are shown in **Figure 3-29**.

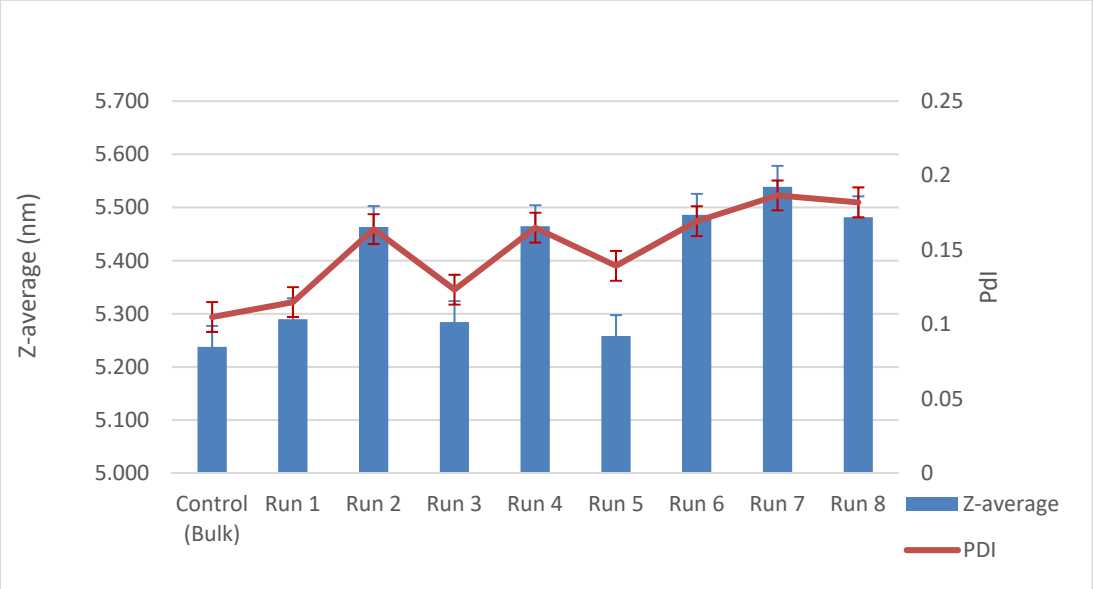


Figure 3-29: **Z-Average and PdI of Protein Y FDS following freeze/thaw for each DoE run.**

There was only slight variation noted in the Z-average and PdI determined by DLS for Protein Y, post-thaw between runs. The DoE was able to generate a statistically significant model for PdI (P-value of 0.0054), despite the Run 6 PdI result appearing to be an outlier from the predicted PdI value. Agitation speed and freezing equilibration were selected as statistically significant factors, with a negative interaction, i.e. a higher freezing equilibration temperature and an increased rotational speed for agitation, resulted in lower PdI values, post-thaw (**Table 3-11**). Freezing equilibration temperature was included as an experimental factor with the intent of studying the effect of change in temperature whilst maintaining the FDS in the frozen state. However, from analysis of thawing rates, freezing equilibration temperature is also a significant factor in the initial thawing rate as it is the starting temperature for the thawing step. Therefore, it appears the variation in the population of species

detected by the DLS method from post-thaw samples is linked more to thawing than to freezing.

Table 3-12: Combined model R^2 and significant parameter effect for DLS Z-average and PDI

	Model R^2	Freezing temperature	Freeze co-load	Freezing equilibration	Thaw co-load	Agitation speed
DLS PdI post-thaw	0.8764	**0**	**0**	**-**	**0**	**-**

- negative interaction

3.3.2.4.2 SEC-HPLC

HPLC data for purity, high molecular weight (%HMW) and low molecular weight (%LMW) species are illustrated in **Figure 3-30**.

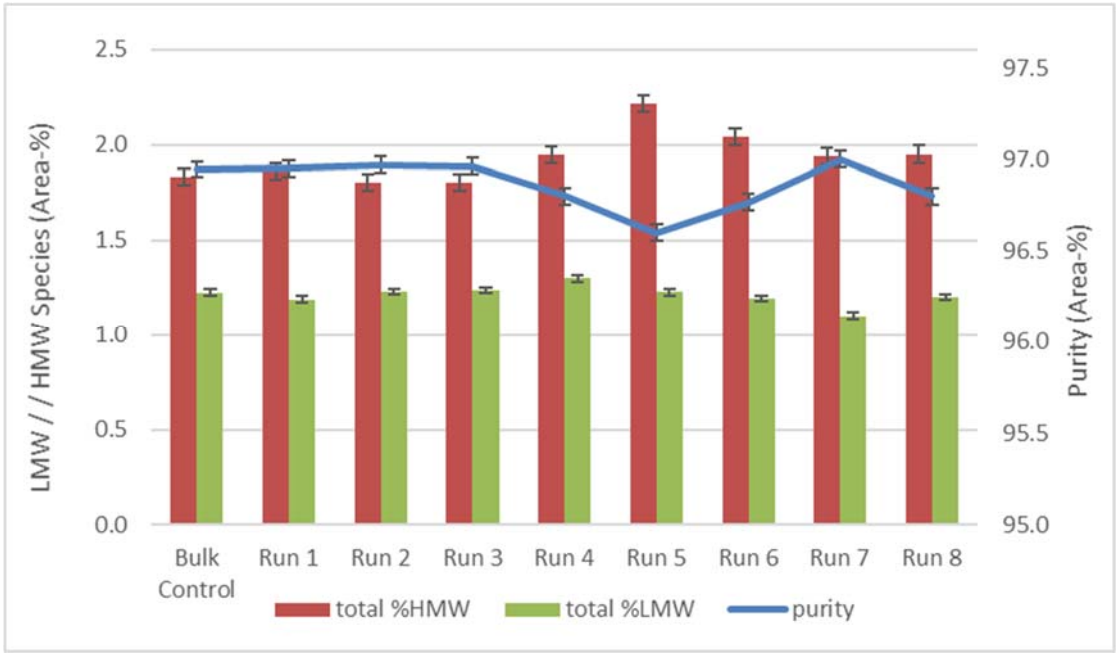


Figure 3-30: **Purity, %LMW and %HMW of Protein Y FDS by SEC-HPLC following freeze/thaw for each run of DoE.**

SEC monomer purity for Protein Y in post-thaw samples varied from 96.6 – 97.0%, this variation was primarily driven by variation in percentage of HMW species, which

ranged from 1.8 – 2.2%. The percentage of LMW species was less variable, with values ranging from 1.1 – 1.3%.

Overall, SEC-HPLC data indicated less variability than DLS, with no statistically significant model being generated that satisfied the criteria outlined in the **Section 3.3**. The model for %HMW was statistically significant indicating freezing equilibration temperature as a significant factor, however the P-value was only slightly <0.05 (0.042) and predicted R^2 was not in agreement with adjusted R^2 (0.431 versus 0.813).

3.3.3 Stability Studies

3.3.3.1 Protein Unfolding

3.3.3.1.1 Differential Scanning Calorimetry (DSC)

Samples for each run stored at 45 °C were analysed by DSC after 4 weeks. The results for unfolding onset and mid-point temperature are shown for time zero (T0) and week four (T4) samples of each run in **Table 3-13.** No significant change was observed in unfolding onset or mid-point, indicating that variation in freeze and thaw process parameters studied do not have an impact on the accelerated stability of the protein. DoE analysis was not performed as only two time points were available and change was not significantly different.

Table 3-13: DSC unfolding onset and midpoint temperatures of Protein Y FDS following freeze/thaw for each DoE run at T0 and T4 weeks storage at 45 °C (± standard deviation, s.d.)

	Average Unfolding Onset Temperature (°C) (± s.d.)		Average Unfolding Mid-Point Temperature (°C) (± s.d.)	
Weeks at 45°C	**T0**	**T4**	**T0**	**T4**
Bulk control	75.2 (±0.12)	75.2 (±0.14)	81.1 (±0.05)	81.1 (±0.06)
Run 1	75.2 (±0.11)	75.2 (±0.17)	81.1 (±0.05)	81.3 (±0.14)
Run 2	75.2 (±0.28)	75.1 (±0.21)	81.1 (±0.14)	81.2 (±0.07)
Run 3	75.3 (±0.06)	75.2 (±0.05)	81.2 (±0.12)	81.2 (±0.16)
Run 4	75.5 (±0.24)	75.1 (±0.01)	81.2 (±0.08)	81.2 (±0.14)
Run 5	74.9 (±0.11)	75.2 (±0.18)	81.2 (±0.00)	81.2 (±0.09)
Run 6	75.0 (±0.11)	74.9 (±0.06)	81.2 (±0.05)	81.2 (±0.09)
Run 7	75.2 (±0.09)	75.3 (±0.33)	81.3 (±0.09)	81.4 (±0.22)
Run 8	74.8 (±0.41)	75.3 (±0.34)	81.3 (±0.09)	81.4(±0.12)

3.3.3.2 Protein Tertiary Structure

3.3.3.2.1 Circular Dichroism (Near-UV)

Circular dichroism spectra were generated in triplicate and averaged for each sample/ time point as per the parameters described earlier. Due to the large number of spectra generated, only the averaged spectra obtained for each time point of the bulk control and run 5 are shown in **Figure 3-31** and **3-32**, respectively.

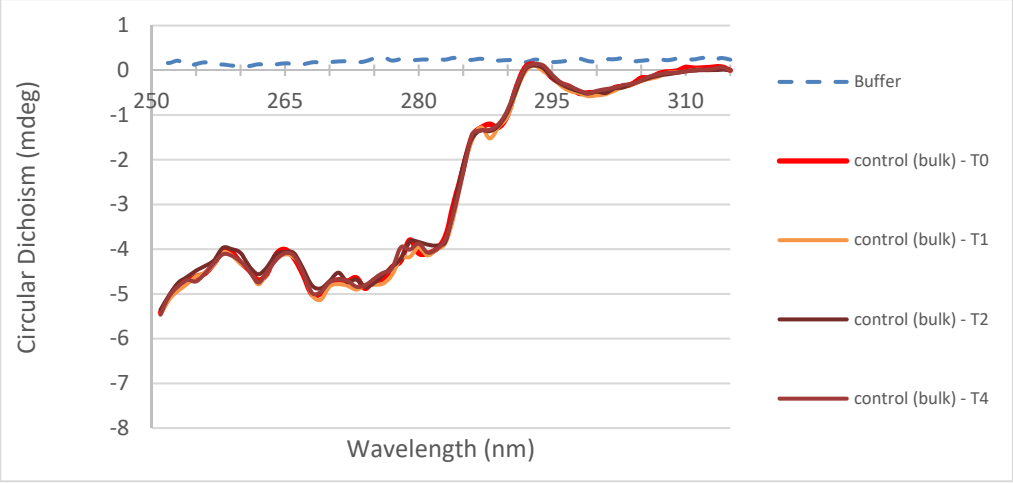


Figure 3-31: **Protein Y normalised and aligned CD spectra (near-UV) of bulk control across 4-weeks storage period at 45 °C**

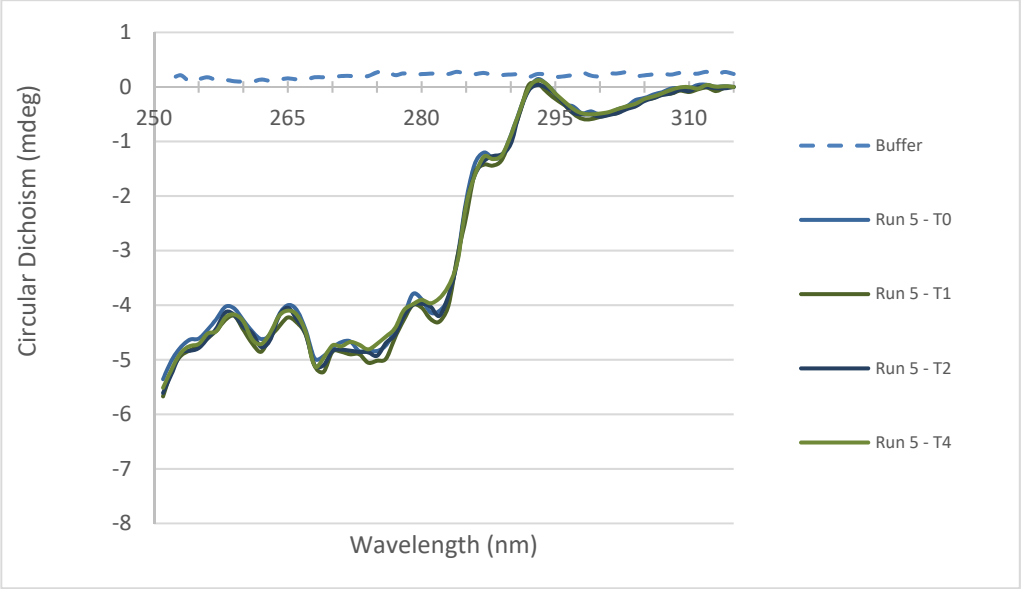


Figure 3-32: Protein Y normalised and aligned CD spectra (near-UV); stability DoE Run 5 post thaw across 4-weeks storage period at 45 °C

The spectra were examined qualitatively to assess any change over 4-week storage period at 45 °C and were not analysed as a response in the DoE. There appeared to be minimal change in the spectra across each time point. Similar to the spectra post-thaw, there were some fluctuations noted between 270 nm and 285 nm, which are regions associated with tryptophan and tyrosine residues (Kelly et al., 2005).

3.3.3.2.2 UV Absorbance

UV absorbance spectra were equivalent to those generated post-thaw (**Section 3.3.2.3.2**). The 1st and 2nd derivatives of the near-UV absorbance spectra were generated using Origin software. Representative spectra for the 2nd derivative of the bulk control and run 3 are displayed in **Figure 3-33** and **Figure 3-34**, respectively.

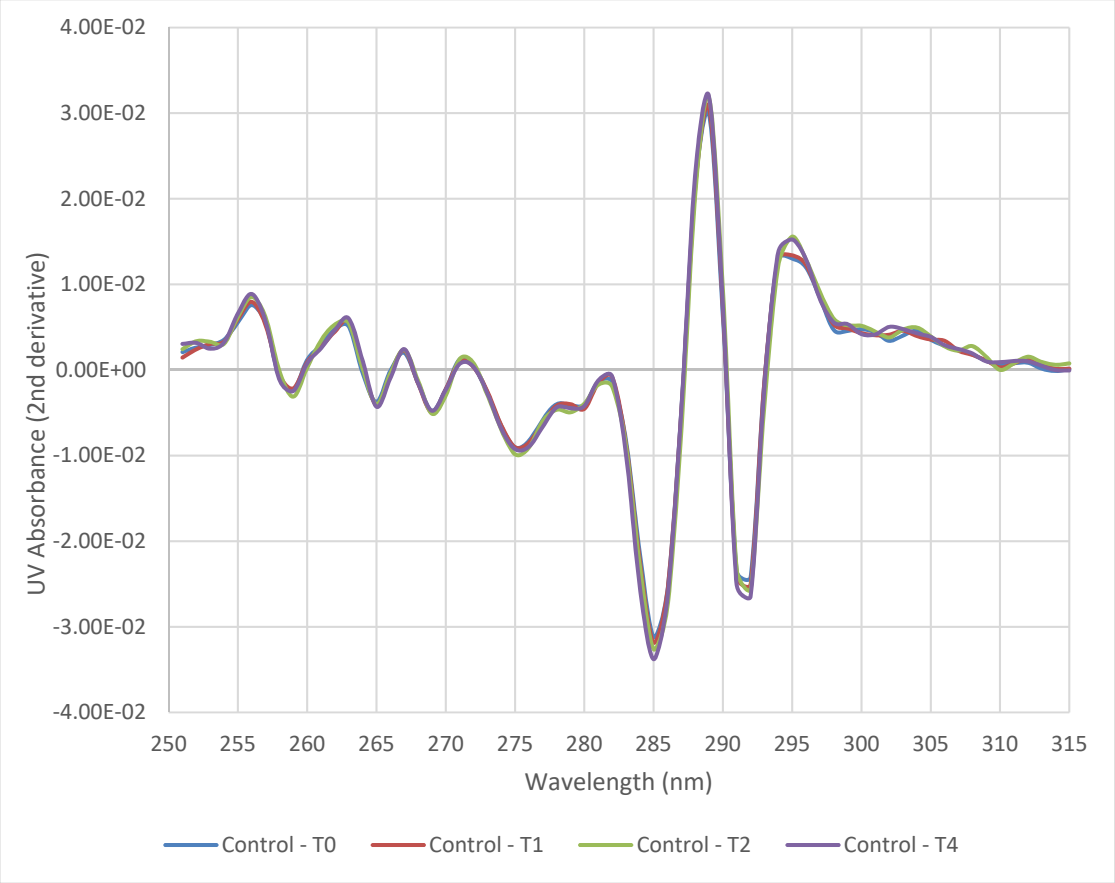


Figure 3-33: **Second derivative of Protein Y UV spectra of bulk control across 4-weeks storage period at 45 °C**

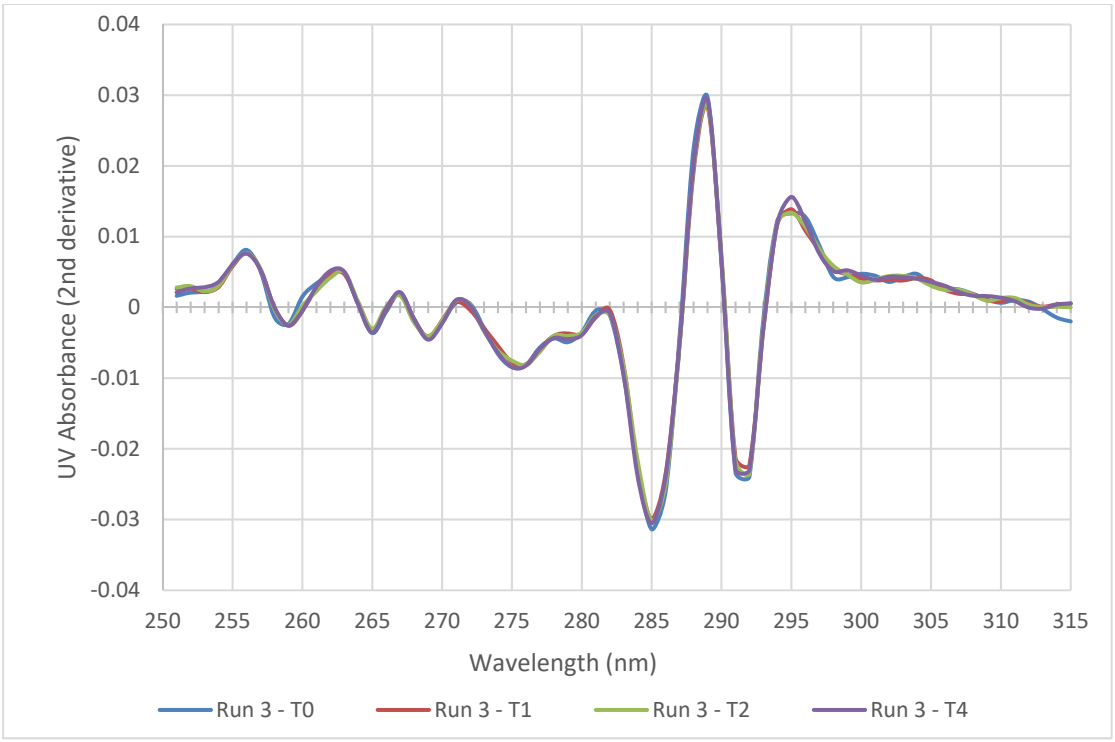


Figure 3-34: **Second Derivative of Protein Y UV spectra of DoE run 3 post-thaw across 4-weeks storage at 45 °C**

The rate of change in the ratio of peak heights for Tyr to Trp, Trp to Phe and Tyr to Phe over 4-weeks were all capable of being described by statistically significant models, with P-values of 0.0003, 0.0015 and 0.0067 respectively (**Table 3-14**). The model for change of tyrosine to tryptophan peak ratio's contained freeze co-load, freezing equilibration temperature, thaw-co-load and agitation speed as significant factors. The model for change in the ratio of peak heights for tryptophan to phenylalanine contained freeze co-load, thaw-co-load and agitation speed as significant factors. The change in the ratio of peak heights for tyrosine to phenylalanine was also able to be described with a model containing freeze co-load, thaw-co-load and agitation speed as significant factors. Interestingly, freezing temperature was found not to be a significant factor in any of the three models for rate of change in amino acid peak ratios.

Table 3-14: Combined Model R^2 and parameter effect for change in aromatic amino acid residue peak height ratios as generated by 2° UV spectra

	Model R^2	**Freezing temperature**	**Freeze co-load**	**Freezing equilibration**	**Thaw co-load**	**Agitation speed**
UV 2nd derivative Tyr/Trp ratio slope (power K=0.02474 and lambda of 1.6)	0.9978	**0**	+	-	+	-
UV 2nd derivative Trp/Phe ratio slope	0.9805	**0**	-	**0**	+	+
UV 2nd derivative Tyr/Phe ratio slope	0.9875	**0**	**0**	-	+	+

+ positive interaction; - negative interaction

3.3.3.2.3 Intrinsic Fluorescence

Intrinsic fluorescence spectra were generated in triplicate for samples on storage. Representative averaged spectra are shown in **Figure 3-35** and **Figure 3-36** for the control and run 6, respectively.

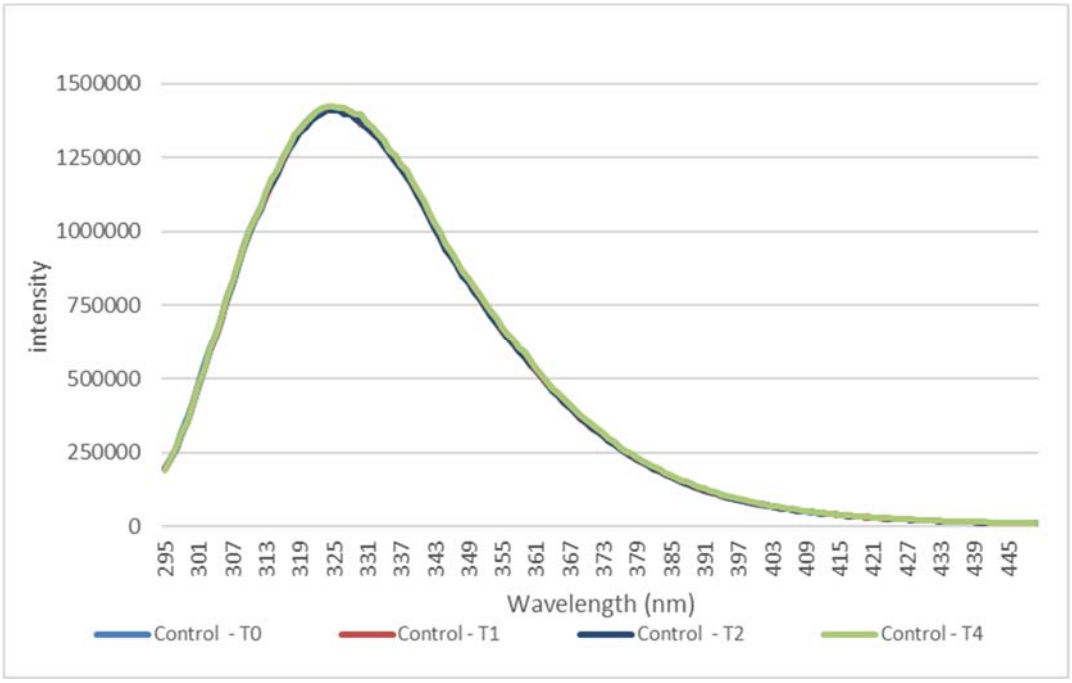


Figure 3-35: **Intrinsic fluorescence spectra of Protein Y UV spectra of bulk control across 4-weeks storage period at 45 °C**

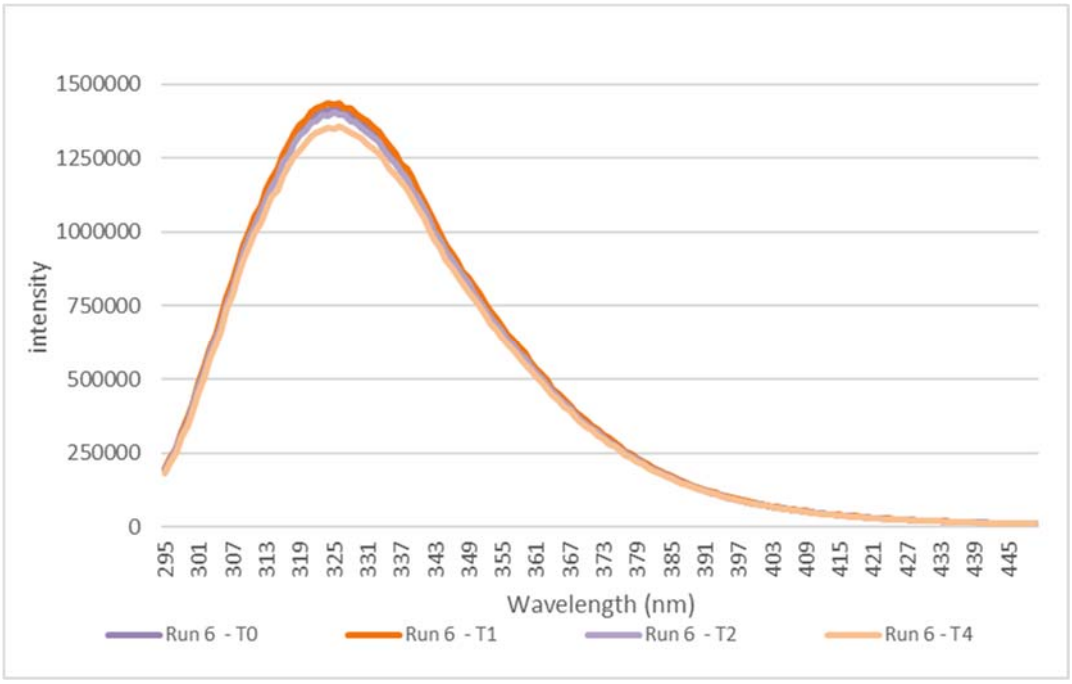


Figure 3-36: **Intrinsic fluorescence spectra of Protein Y for DoE run 6 across 4-weeks storage period at 45 °C**

The fluorescence spectra were then analysed for shifts in the wavelength at which maximum intensity occurred (λ_{max}) and also changes in the maximum intensity recorded. This is illustrated in **Figure 3-37** and **Figure 3-38**, respectively. There was negligible change in the λ_{max} indicating that no unfolding of the protein was detected. A certain variation in intensity was observed for each run across all time points, but no consistent trend was noted by visual analysis of the data.

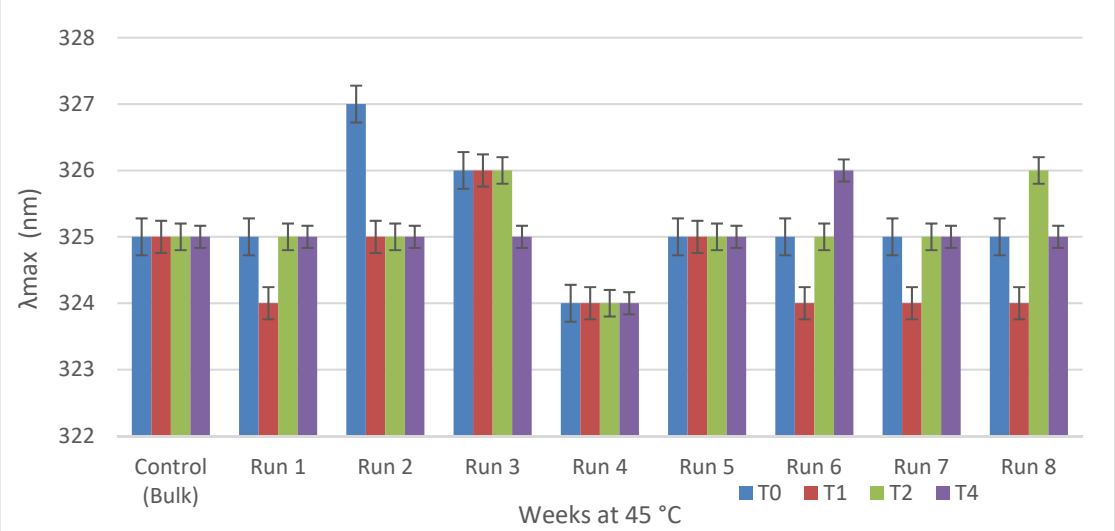


Figure 3-37: Intrinsic fluorescence λ_{max} by run over 4-weeks storage at 45 °C

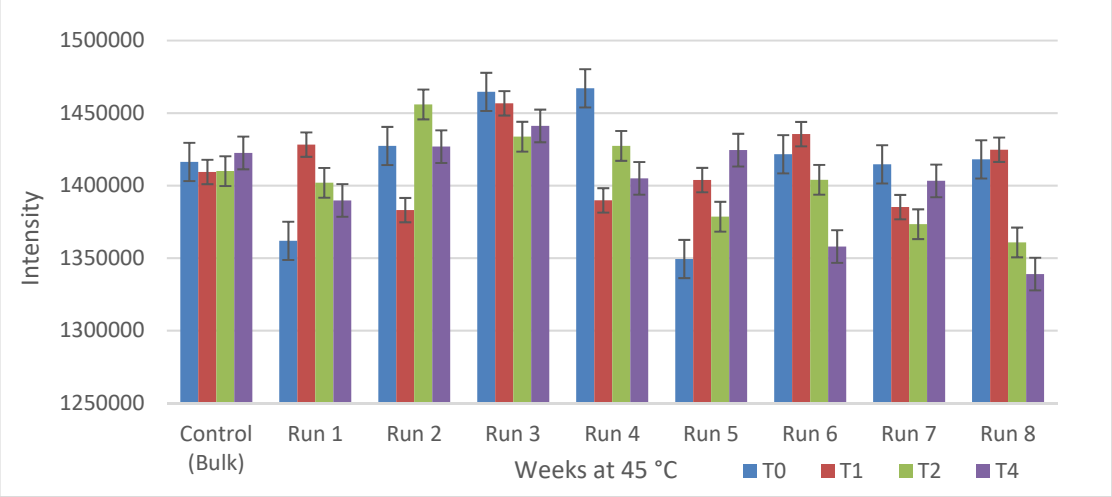


Figure 3-38: **Maximum fluorescence intensity by run over 4-weeks storage at 45 °C**

For the freeze thaw studies described, there was no significant change observed in λ_{max} but there was variation observed in maximum intensity across all runs and time points. The DoE was able to attribute the variation in intensity to some of the experimental variables for the T0 result but not for the change of intensity over storage time, although the level of variation in intensity at each time point was of a similar order of magnitude.

The fluorescence method developed used an excitation wavelength of 280 nm in order to generate a maximum intensity response. However, generation of fluorescence spectra with excitation of Protein Y at 295 nm would enable a more targeted examination of tryptophan residues, as the fluorescence contribution of tyrosine residues is diminished at this excitation wavelength per (Hui, Xue, Xuesong, and Yan, 2015).

The DoE generated statistically significant models for both change in λ_{max} and in maximum intensity over the 4-week storage period at 45 °C. The model for change in λ_{max} had an F-value of 8.2 and a p-value of 0.027, with freezing temperature and freezing co-load both selected as significant factors. The model for rate of change in intensity was weaker, with an F-value of 7.4 and a p-value of 0.042. However, the predictive power of the models for both change in λ_{max} and intensity was not satisfactory with predicted R^2 and not in agreement with adjusted R^2 (0.400 versus 0.672 and 0.388 versus 0.7324 respectively).

3.3.3.3 Protein Aggregation

3.3.3.3.1 DLS

The Z-average and PdI of Protein Y FDS was determined by DLS for samples stored at 45 °C as per the experimental plan. The average results for the 45 °C stability profile of each freeze-thaw run are shown in **Figure 3-39** and **Figure 3-40**.

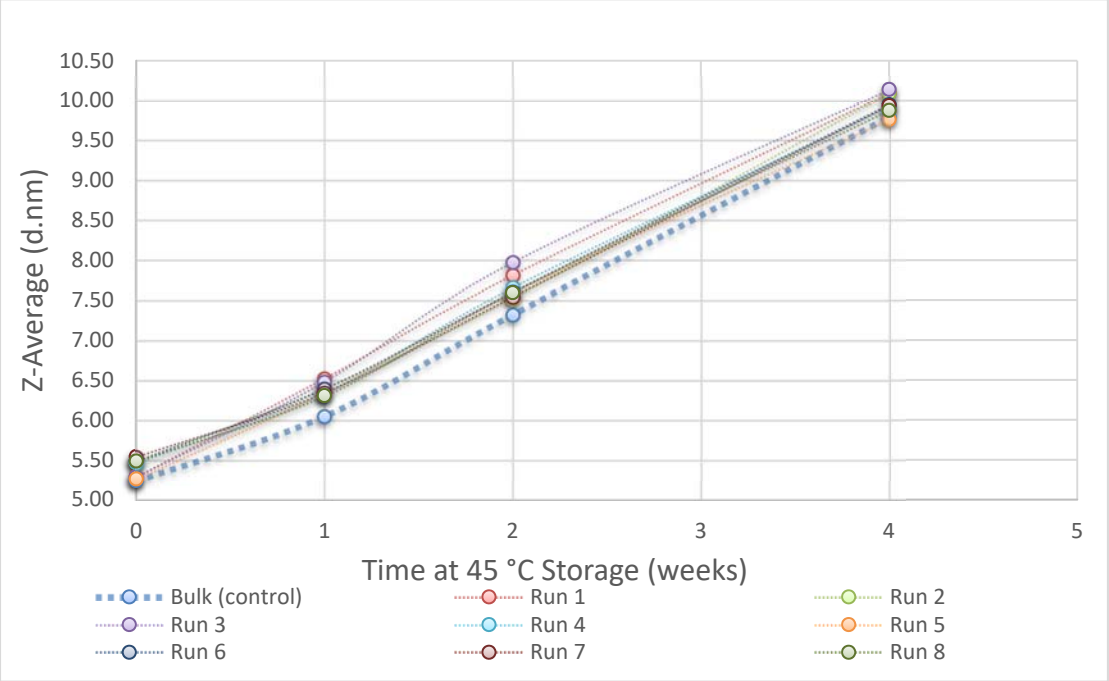


Figure 3-39: **Protein Y DLS Z-average by run over 4-weeks storage at 45 °C**

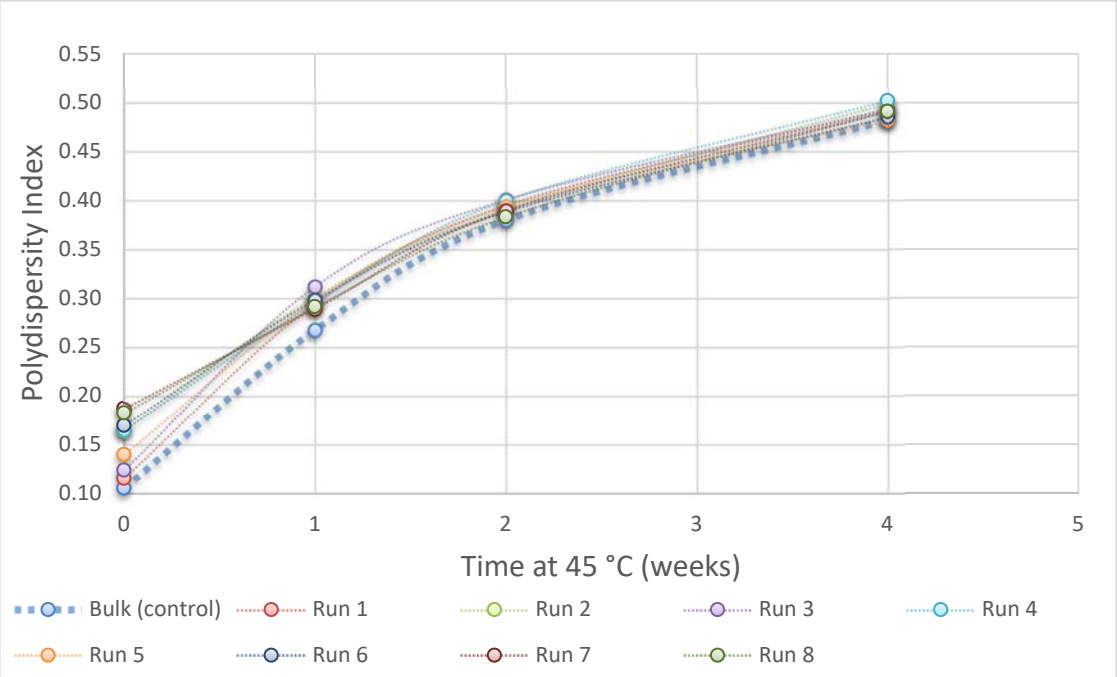


Figure 3-40: **Protein Y DLS PdI by run over 4-weeks storage at 45 °C**

The DoE was able to generate statistically significant models for rate of change of Z-average and PdI (per week at 45 °C). Statistically significant models were capable of being generated for both rate of change (slope) for Z-average (F-value of 16.0 and P-value of 0.011) and PdI (F-value of 16.7 and P-value of 0.006) and are summarised in

Table 3-15. Freezing equilibration temperature and thaw agitation speed were found to be significant factors with a positive interaction for both change in PdI and in Z-average, i.e. a higher value for freezer equilibration temperature and agitation rate result in higher rates of change in PdI and Z-average.

It is interesting to note that the same factors that were significant for DLS Z-average and PdI from post-thaw samples are significant for assessment of the rate of change observed per week at 45 °C accelerated stability, although the interactions have changed from negative to positive. It is thought this can be explained by the increase in Z-average and PdI for 45 °C not being truly linear. As can be seen in **Figure 3-39** and **Figure 3-40**, the variability in Z-average and PdI at T0 reduces at subsequent time points. This may indicate that in order to assess the potential longer-term changes using accelerated temperatures at 45 °C that it would be more appropriate to analyse more points at between time zero and 2-weeks. After the 2-week time point the thermodynamic effect of the storage temperature has a greater effect than differences attributed to freezing and thawing parameters.

Table 3-15: Combined model R^2 and significant parameter effect for rate of change for Protein Y Z-average and PdI by DLS over 4-weeks storage at 45 °C

	Model R2	Freezing temperature	Freeze co-load	Freezing equilibration	Thaw co-load	Agitation speed
DLS PdI rate of change (slope)	0.8696	0	0	+	0	+
DLS Z-average rate of change (slope)	0.9231	0	0	+	0	+

+ positive interaction

3.3.3.3.2 SEC-HPLC

HPLC data for purity, high molecular weight (%HMW) and low molecular weight (%LMW) species are illustrated in **Figure 3-41**, **Figure 3-42** and **Figure 3-43**,

respectively, for all runs up to week 2 or 3, and for a subset of samples (bulk control run and runs 1- 4) up to the 4-week time point at 45 °C. Trend lines generated for runs 1-4 indicates that the rate of change in purity, %HMW and %LMW would appear to be equivalent across samples for all runs.

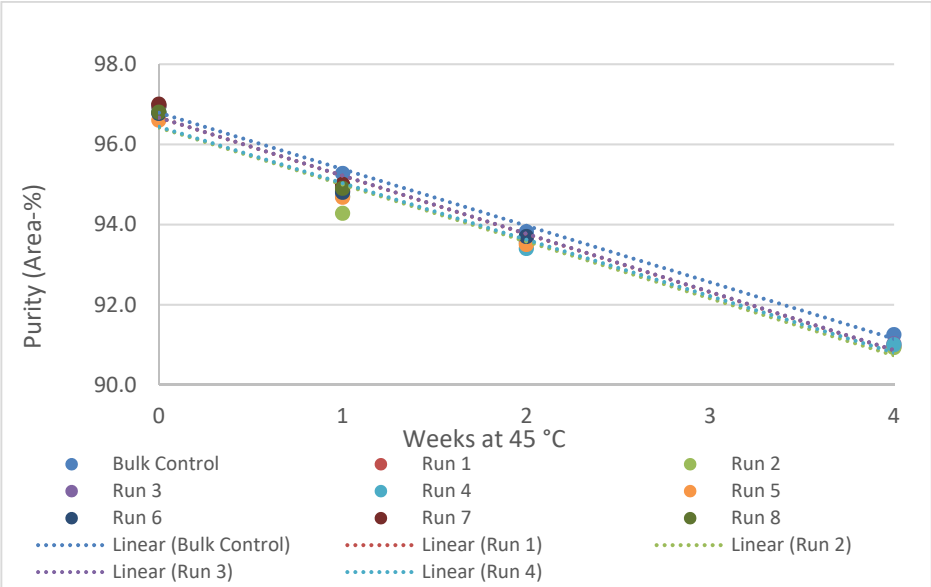


Figure 3-41: **Protein Y SEC-HPLC % purity by run across 4-weeks storage at 45 °C (with trend line for bulk control and runs 1-4)**

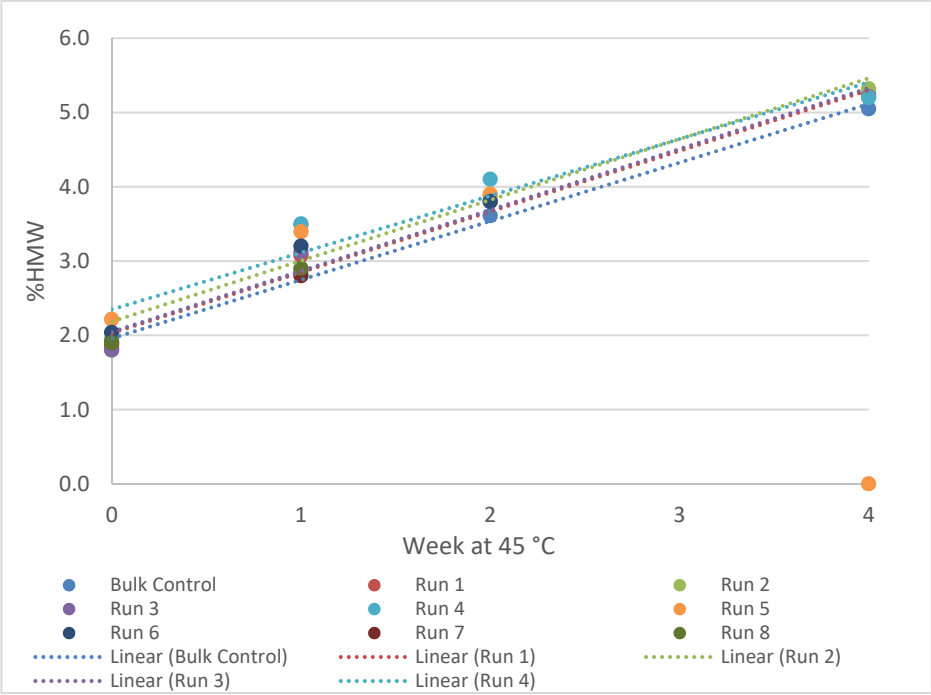


Figure 3-42: **Protein Y SEC-HPLC % HMW by run across 4-weeks storage at 45 °C (with trend line for bulk control and runs 1-4)**

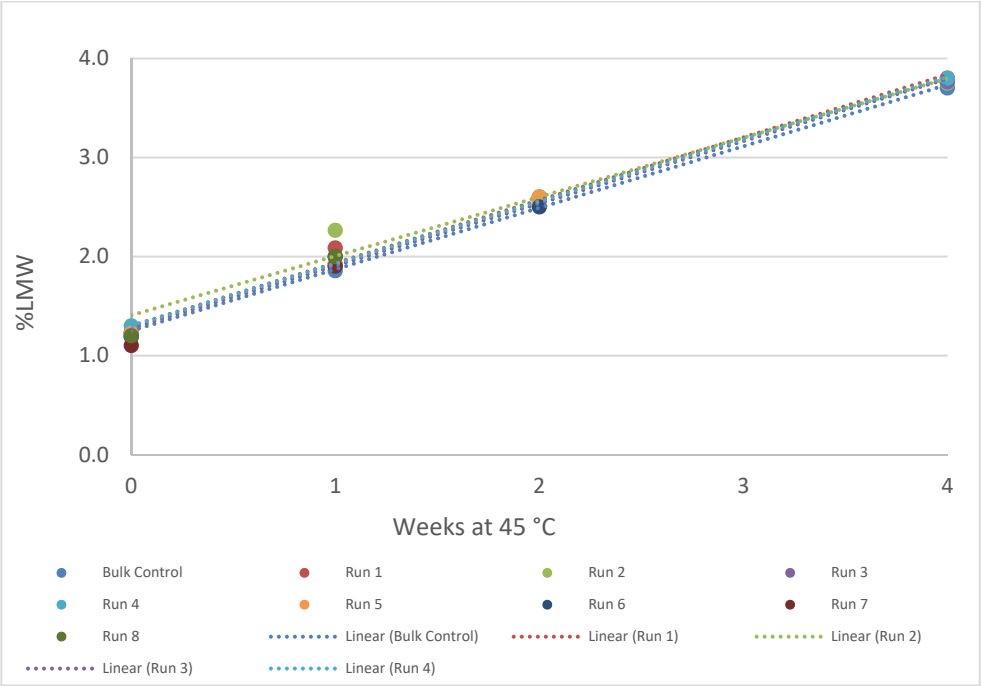


Figure 3-43: Protein Y SEC-HPLC % LMW by run across 4-weeks storage at 45 °C (with trend line for bulk control and runs 1-4)

3.4 Scalability of the Data

To establish a relationship between behaviour in the small-scale model employed in this study (87.5 g in 0.125 L container) and the larger production scale volume (3,500 g in 5 L container), a correlation was sought between 2 factors, surface area to volume (SA:V) ratio and freeze time. The SA:V ratio is a related parameter to the freeze path length which impacts the resulting freeze time. Containers with higher SA:V ratio have shorter freeze path lengths and will therefore freeze and thaw faster (Rayfield et al., 2016). A dimensional comparison of the commercial freeze/thaw process for Protein Y versus lab scale employed in this study was made (**Table 3.16**).

Table 3-16: Dimensional comparison of commercial versus small scale models

Attribute	Commercial Scale	Lab Scale (DoE)
Bottle nominal capacity (L)	5	0.125
Height (mm)	299	104.6
Width (mm)	163	49
Length (mm)	163	49
Load in bottle (kg)	3.50	0.0875
Estimated volume in bottle (based on density of 1.083 g/ml at 20 °C, L)	3.23	0.0813
Estimated % fill of bottles	65%	65%
Surface area of base (W x L/1000000, m^2)	0.027	0.0024
Estimated height of fill in bottle (liquid state, mm)	121.6	33.8
Estimated surface area of bottle(s) in contact with heat /cold source (m^2)	0.106	0.009
Surface area to volume ratio (m^2/L)	**0.033**	**0.111**

As the SA:V ratio reduces, it would be expected that the freeze and thaw time would increase. There is no results available on the commercial scale freezing process, however thawing at ambient temperature at commercial scale typically takes approximately 24 hours to complete. Observations from the small-scale experiments relative to the full-scale commercial process showed a significant reduction in thaw time, which can be attributed to the smaller SA:V ratio. The SA:V ratio of the individual small-scale bottle of formulation studied was 3.36 times larger than the ratio for the commercial process. The SA:V ratio can be used as a scaling factor to predict freeze and thaw cycle times for commercial scale. The empirical models for prediction of time for overall freezing and thawing steps (inclusive of all three respective sub-phases) are shown in **Table 3-17**.

Table 3-17: Empirical models for overall freeze and thaw times with predicated R^2 and P-value for models

Process step	Co-load / Single Bottle	Equation	Predicated R^2 for model	P-value
Freeze	Co-load	$\sqrt{time\ to\ freeze} = 29.861 + (0.080 * A)$	0.8398	0.001
	Single	$\sqrt{time\ to\ freeze} = 18.580 + (0.080 * A)$		
Thaw	Co-load	$\sqrt{time\ to\ thaw} = 29.224 + (0.007 * B) - (129.290 * C) - (0.848 * B * C)$	0.9891	0.002
	Single	$\sqrt{time\ to\ thaw} = 15.214 + (0.007 * B) - (54.269 * C) - (0.848 * B * C)$		

A: Freezer temperature; B: Freezing equilibration temperature; C: Agitation speed

Figure 3.44 highlights the interactive effect of the co-load (factor 'C') with freezing temperature (factor 'A') on the overall time to freeze.

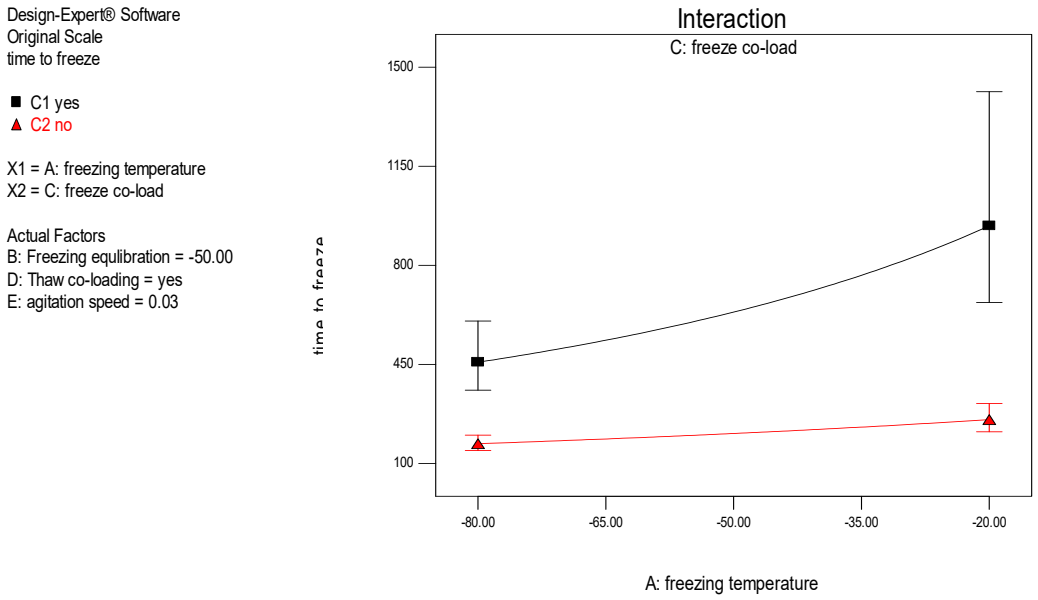


Figure 3-44: Effect of freezing temperature (Factor A, X-axis) for prediction of overall time to freeze (Y-axis); presence of co-loaded bottles (C1: black squares) versus individual bottle (C2: red triangles)

Figure 3.45 highlights the interactive effect of the co-load (factor 'D') with agitation speed (factor 'E') on the time to thaw. From the error bars in these figures, it can be seen that the time is much harder to predict when co-loaded bottles surround the FDS bottle in the centre, with freezing time being harder to predict than thaw time.

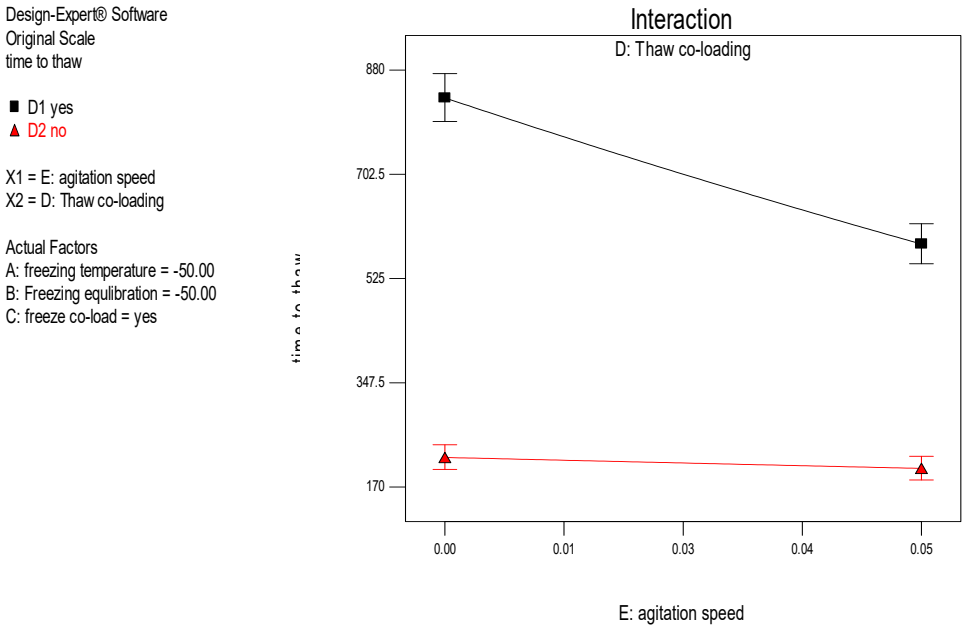


Figure 3-45: Effect of agitation speed (Factor E, X axis) and co-loading (Factor D) for predicated overall time to thaw (Y axis); co-loaded bottles (D1: black squares) versus individual bottle (D2: red triangles)

The predicted freeze and thaw times based on the models determined for the DoE are shown in **Table 3-18**. The values that have been typically observed at commercial scale were determined using the scaling factor to calculate overall times for freeze and thaw. However, the range of predicted values, based on the 95% confidence interval for the respective models in **Table 3-17** also demonstrates the inherent variability in uncontrolled freeze and thaw processes. This variability relates to the factors selected for the models and make an accurate prediction challenging. Due to the absence of accurate data for the commercial freezing and thawing times and the factors, such as co-load and ambient temperature influencing these times, it is difficult to determine if

these predicted times are accurate. However, the variation in predicted times, are heavily influenced by co-load and therefore it would be expected to observe variation for freezing and thawing times, at the commercial scale. This variation may be amplified at commercial scale based on the smaller SA:V ratio and the distribution of the individual containers.

Table 3-18: Predicted freeze and thaw times for lab and commercial scale using scaling factor of 3.36 for surface area to volume (SA:V) ratio

Run	Observed freeze time, hours	Observed thaw time, hours	Predicted freeze time 125ml bottle, hours	Predicted thaw time 125 ml bottle, hours	Predicted commercial scale freeze time based on scaling factor, hours (95% confidence interval range)	Predicted commercial scale thaw time based on scaling factor, hours (95% confidence interval range)
1	5	3	5	3	16 (5 – 24)	10 (7-11)
2	3	14	3	14	9 (4 - 14)	47 (43 – 51)
3	6	9	10	9	32 (22 – 42)	31 (27 – 33)
4	14	4	13	4	45 (33 – 58)	13 (11 – 15)
5	7	4	10	4	32 (22 – 42)	13 (11 – 15)
6	5	11	5	11	16 (10 – 24)	37 (32 – 39)
7	14	14	13	14	45 (33 – 58)	46 (42 – 50)
8	2	4	3	4	9 (4 – 14)	12 (10 – 14)

4.0 DISCUSSION

This research project was conceived to perform a high-level experimental assessment of the freeze and thaw process for Protein Y FDS in polycarbonate bottles at a reduced scale in order to evaluate the factors related to freeze thaw times that could cause a change in (1) protein structure and (2) aggregate levels in the formulated drug substance. A designed set of experiments (DoE) were executed to estimate the key process parameters via the development of empirical polynomial models, which were used to predict the influence parameters on freezing and thawing times and protein stability. The validity of the models developed at small-scale was also evaluated to understand the behaviour of the respective full-scale commercial process.

4.1 Analytical Methods

Prior to execution of the DoE a set of analytical methods were established to characterise structural changes in the therapeutic protein, focusing particularly on its aggregation and tertiary structure. Following evaluation, a range of techniques, CD (Near-UV), fluorescence spectroscopy, DSC and DLS were used to characterise Protein Y FDS and detect changes in aggregation and tertiary structure of the protein. In terms of aggregation, DLS showed better sensitivity to detect changes than SEC-HPLC but higher variability was observed. Second derivative UV absorption spectra showed particularly good discriminative power, relative to the CD spectra and to intrinsic fluorescence spectra to determine changes in the tertiary structure of Protein Y. Fluorescence method development with Protein Y FDS has shown that thermally induced unfolding of the molecule induces an upward shift the wavelength of maximum intensity (λ_{max}), indicative of exposure of tryptophan and possibly tyrosine residues within Protein Y. Based on the relative emission spectra for the three aromatic amino acid residues (i.e. tryptophan, tyrosine and phenylalanine), it would be thought that the major contributor would be tryptophan (Hui et al., 2015). However,

there is proportionally a larger number of tyrosine residues situated in the hydrophobic core of the protein.

4.2 Freeze-Thaw DoE

4.2.1 Influence of process parameters on freeze/thaw profiles and Protein Y cryo-concentration

For all DoE runs, freezing profiles followed a similar profile as those reported in the literature, with Protein Y undergoing distinct phases during the freezing process (López-Leiva and Hallström, 2003). The approach taken by Radmanovic et al. involved the three phases overlapping (Radmanovic et al., 2013), however in the experiments described, the phases were divided based on inflexions in rate of temperature change. A rate of decrease greater than -0.10 °C/min was used as the value to define the freezing time for ice-formation. When the rate of decrease in temperature slowed to a value greater than -0.10 °C a 'plateau' in temperature occurs, whilst ice is formed through the solution. The time taken for freezing plateau completion varied across all eight experiments from 1 minute to greater than 9 hours. This time was heavily influenced by whether the FDS was co-loaded with other bottles and also freezing temperature. Co-loading of bottles was found to be a significant factor, resulting in increases to the freeze and thaw time. Therefore, co-loading of bottles can be considered as effectively increasing the path length, elongating the time for the ice front to reach the centre of the FDS bottle.

The ice nucleation shown in **Figure 3-18**, indicates an exponential relationship between time to onset of ice nucleation and the pre-cooling rate, which has been shown in **Figure 3-19**. As described by Singh and Nema, faster onset of nucleation should lead to faster ice formation throughout the solution and result in a larger surface area of ice (Singh and Nema, 2010). A slower onset therefore results in more

gradual ice formation through the bottle and provides the potential for cryo-concentration to occur.

Cryo-concentration was assessed by analysing the variability in UV absorbance at 280 nm (A280) from samples taken from top, middle and bottom of the FDS, immediately post-thaw. A statistically significant model was generated, with freezing co-load as a significant factor. When the FDS bottle was surrounded by co-loaded bottles, a higher variation in A280 values from top to bottom of the FDS was observed. Also, the presence of co-loaded bottles was shown to significantly affect all phases of freezing. It is thought that a slower freezing rate results in a higher protein concentration at the bottom of the bottle and therefore higher concentration variability. Fewer/larger ice-crystals formed can force the proximity of protein molecules closer to each other. Based on the relative lighter density of ice to liquid water, and convective currents within the bottle due to the increasing temperature differential between the edge and the centre of the bottle, the ice crystals will coalesce towards the top of the solution which results in reduced protein concentration at the top of the bottle and increasing at the bottom (Singh and Nema, 2010).

Similar to freezing parameters, the thawing step was broken down into three sub-phases: pre-thawing, thawing (temperature plateau) and post-thaw. The thaw plateau was found to be heavily influenced by the presence of co-load bottles surrounding the FDS bottle during thawing. Freezing equilibration temperature and thaw co-load were both significant factors within the model for pre-thaw rate, with a lower freezing equilibration temperature and no co-loaded bottles resulting in a faster increase in temperature. Thaw co-load and agitation speed were significant factors for the post-thaw rate and the overall thaw time, with faster agitation and single bottles also resulting in a faster temperature increase.

4.2.2 Protein Y structural changes during freeze/thaw processes

Structural changes in Protein Y were observed during the freeze-thaw experiments. These changes may be a consequence of a more concentrated solution and/or changes in the microenvironment of the protein, related to slower freeze and thaw rates (Singh and Nema, 2010).

There was subtle variation noted in the onset or mid-point of the unfolding temperature for Protein Y as determined by DSC. The DoE was able to generate a predictive model for unfolding onset, which demonstrated more variability than the mid-point temperature. Freezer temperature, freezing co-load and freezer equilibration temperature were all statistically significant factors within the model for unfolding on-set temperature, with higher freezing and equilibration temperatures and co-loaded bottles resulting in an increased on-set temperature of Protein Y unfolding. The DSC thermograms exhibited an initial endothermic event with an onset at around 65 °C. In a study by Shah et al. investigating the photo-stability of a monoclonal antibody, DSC profiles showed two unfolding events. By comparing with the published DSC thermograms of similar IgG1 mAbs, the first peak in the DSC thermogram that occurs at lower temperature (with a Tm of ~71 °C) was attributed to the unfolding of the C_H2 domain and the second larger peak occurring at higher temperatures (with a Tm of ~82.5 °C) was attributed to the unfolding of Fab and C_H3 domains (Shah et al., 2018). It is thought that variation in freeze and thaw parameters are having a similar effect occurred with the Protein Y melting behaviour observed in this study. A similar finding has been reported by Shah et al., although the initial endothermic event for Protein Y is more of an inflexion without a clear peak. However, due to the proximity of the initial endothermic event to the main peak with a midpoint at 81 °C, variability in the onset of the main peak is being affected by the initial thermal event, thus making on-set of the main peak harder to detect.

Structural changes in Protein Y were observed by spectroscopy following the freeze-thaw experiments, both in terms of fluorescence emission intensity and also in terms of tyrosine to tryptophan and tyrosine to phenylalanine second derivative UV peak height ratios. Statistically significant models were generated for the arbitrary peak height ratios for tyrosine to tryptophan and tyrosine to phenylalanine ratios in second derivative UV absorbance spectra. The data indicates that there are subtle changes in the microenvironment, with co-loading of bottles at freezing being a significant factor in the peak ratio of tyrosine to tryptophan. Co-loading of bottles in close proximity to each other will result in slower freeze rates. It is thought the increase in tyrosine to tryptophan peak height ratios are induced by these slower freeze rates, thus indicating the exposure of these aromatic amino acid residues normally in the hydrophobic core of Protein Y to the aqueous environment (Katayama et al., 2005).

Intensity, as determined by intrinsic fluorescence was shown to be a highly sensitive technique with a high amount of variation between samples from different freeze/thaw regimes. A statistically significant model was able to predict variation in intensity post-thaw. Freeze co-load, freezing equilibration temperature, thaw co-load and agitation speed were all significant factors for intensity. The model for fluorescence intensity is more complex than second derivative UV but also shows that co-loaded bottles during freezing, which shown to result in slower freezing rates results in a higher intensity. The model also demonstrates the effect of thawing parameters on intensity. A higher freezing equilibration temperature, co-loaded bottles and no agitation are all linked to slower thawing rates and also result in an increase in fluorescence intensity. The limitation for the fluorescence method is that with excitation at 280 nm it is not specific for tryptophan or tyrosine (Hui et al., 2015), so it is unknown which of these aromatic residues are causing the change in intensity.

4.2.3 Protein Y aggregation during freeze/thaw processes

The variability of Protein Y particle size was observed during the freeze-thaw experiments via the PdI measurements obtained by DLS. The DoE generated a significant model for PdI with agitation speed and freezing equilibration emerging as statistically significant factors. Negative interactions were determined, i.e. a higher freezing equilibration temperature and an increased rotational speed for agitation resulted in lower PdI values, post-thaw. It appears the variation in the population of species detected by DLS in post-thaw samples was linked more to thawing parameters than freezing, as freezing equilibration is more related to the point of starting the thaw step than the freezing step itself. The SEC-HPLC data did not fit to a significant model with acceptable predictability.

4.2.4 Protein Y structural changes during post-thaw stability study

Changes in the structure of Protein Y were assessed during storage at 45°C post-thaw. No significant change was observed in unfolding onset or mid-point for samples analysed at 4 weeks compared to the post-thaw (T0) value. DSC results did not indicate that variation in freeze and thaw process parameters impacted the accelerated structural stability of the protein. However, evaluating the change in 2° UV-absorbance peak height ratios over 4 weeks resulted in statistically significant models for tyrosine to tryptophan, tryptophan to phenylalanine and tyrosine to phenylalanine peaks.

No significant models were generated to describe changes in intrinsic fluorescence intensity or λ_{max} over 4 week's storage at 45 °C. Also, significant models were generated to describe changes in Protein Y tertiary structure using 2° UV-absorbance peak height ratios for post thaw samples. This suggests that the intrinsic fluorescence method can detect 'flex' in the tertiary structure of Protein Y post thaw, but the discriminatory power diminished with longer term storage of the samples. Analysis of

2° UV-absorbance peak height ratios proved to be a useful technique for detecting structural changes in Protein Y post-thaw and upon storage.

4.2.5 Protein Y aggregation during post-thaw stability study

Changes in Protein Y size was assessed during storage of samples of 45°C post-thaw. Freezing equilibration temperature and thaw agitation speed were found to be significant factors with a positive interaction for both the change in DLS Z-average and PdI values over four weeks at 45 °C. This was inverse to the relationship for Z-average and PdI model for post-thaw samples. Z-average and PdI value measured for stability at 45 °C all increased over 4 weeks storage, as would be expected. The rate of increase in these attributes between 1 and 2 weeks was most pronounced for the runs with lower Z-average and PdI, immediately post-thaw (T0). This apparent change of rate effectively 'inverted' the effects observed immediately post-thaw.

4.3 Validity of the Small-Scale Model to Understand the Behaviour of the Respective Full-Scale Commercial Process

The scalability of the small-scale experiments to commercial scale can be challenging due to the shorter freeze and thaw times. However, DLS and HPLC data support that changes in aggregation levels are equivalent between the full-scale control and the scaled-down experimental bottles both immediately post-thaw and over 4 weeks storage at 45 °C (**Figures 3-29 and 3-30**). In addition, fluorescence, near-UV CD and 2nd derivative UV data support that tertiary structure is not significantly affected by the differences of scale (**Figures 3-23, 3-26 and 3-28**).Determination of SA:V ratios for laboratory and commercial scale and use of the differential as a scaling factor resulted in reasonable prediction of expected freeze and thaw time for the commercial scale. While, the simplistic empirical model with a correction factor presented in this study

can provide some understanding, a better prediction of freezing time could potentially be achieved by the use of the model to determine freezing kinetics based on the principles established by Plank (López-Leiva and Hallström, 2003).

Studies designed to understand and model the freezing processes originally started with freezing of food and goes back to work performed by Plank. Originating from the basic heat transfer equations (Fourier's equation for heat transfer by conduction and the Prandtl concept of boundary layer for heat transfer by convection), Plank derived the following equation (López-Leiva and Hallström, 2003):

$$F = \frac{\rho \Delta H_f}{T_f - T_a}\left(P\frac{d}{h} + R\frac{d^2}{\lambda}\right) \qquad \textbf{[Equation 4-1]}$$

Where:

- F is freezing time ''according to Plank'' (sec),
- ρ is food density (kg/m^3),
- ΔH_f represents enthalpy change during freezing step (J/kg),
- T_f is initial freezing point (°C),
- T_a is temperature of the freezing medium (°C),
- d is sample thickness (=h_0) (m),
- h represents heat transfer coefficient (W/m^2 °C),
- λ is thermal conductivity of the frozen food (W/m °C), and
- P and R are parameters defining the geometry of the food.

Plank's analysis concluded that parameters P and R are functions of the geometry of the body. For the experiments reported in this thesis, the geometry of Protein Y FDS in a bottle, being frozen in a conventional freezer is best represented by a cube, as heat transfer can occur from three dimensions. From Planks derived equations the proposed P is 1/6 and R is 1/24. The P/R ratio is always equal to four irrespective of the

geometry of the shape for regular geometries. The 'freezing time according to Plank' specifically relates to the freezing plateau, where ice formation occurs.

Figure 4-1 provides a visual illustration of Protein Y freezing, in a 5 L polycarbonate bottles, along with variables to be considered to understand and model the freezing and thawing process.

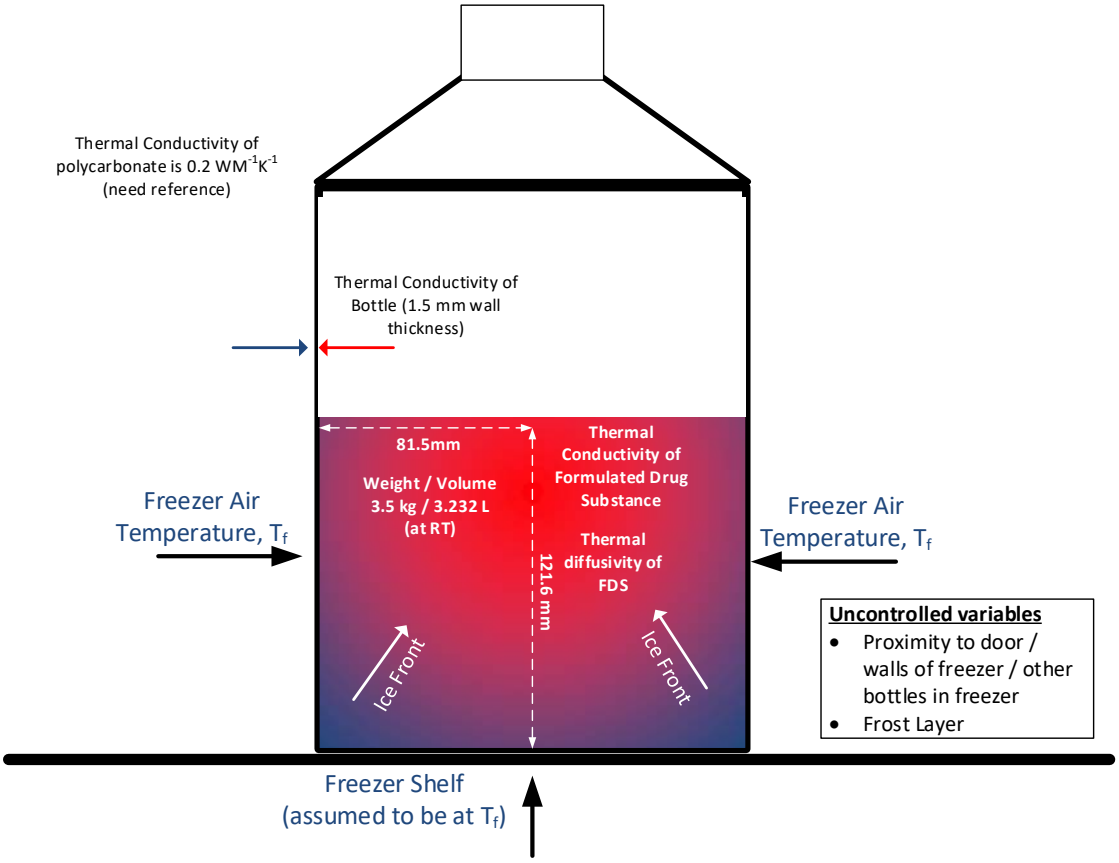


Figure 4-1: Visual graphic of freezing process for 5 L polycarbonate bottles

The freezing time according to Plank will be dependent on the rate of advancement of the ice front travelling through the solution, which will be defined by the efficiency of heat transfer of the freezing environment in which the solution is frozen. Considering the factors described in the Plank equation across the DoE runs, the key variable was the temperature of the freeze medium, as all other factors were constant between runs.

While the Plank equation can account for the freeze temperature, the factor of co-load is not accounted for, and would be difficult to describe and hence model.

Results highlight the robustness of the FDS to withstand stresses during freezing and thawing across DoE runs as demonstrated through the analytical data. This suggests that Protein Y is capable of being frozen and thawed through much quicker rates of temperature change than the current commercial process, and that faster freezing and thawing cycles could improve manufacturing efficiency and cycle times. Furthermore, the results show that cryo-concentration and the potential for changes in tertiary structure can be minimised with a faster freezing rate. This is consistent with similar conclusions reported by Miller et al. (Miller et al., 2013). Application of heat transfer through a water bath for thawing could potentially allow for a much quicker thaw. The process currently employed is uncontrolled because it relies on air contact as the medium for heat transfer/removal. Alternatively, the use of a controlled system, along with bag-based storage of the FDS, could allow for a combined system that both freezes and thaws the FDS and could increase freeze and thaw rates, as well as SA:V ratio.

5.0 PROPOSALS FOR FUTURE WORK

- **Investigate additional techniques to study protein aggregation and structural changes in freeze thaw samples**

The methods used to detect aggregation of Protein Y in the freeze-thaw experiments were SEC and DLS. These two methods can typically only detect particle sizes up to 100 nm and 500 nm respectively (Hamrang et al., 2015). It would be useful to employ a technique which count and classify particles for sizes greater than 500 nm to gain a better understanding of the type of aggregation observed.

Protein aggregates can be classified according to their size as visible (>100 μm), micron (1–100 μm), submicron (100–1000 nm), and nanometre particles (<100 nm). Aggregates in the micron and submicron size range raise concerns as they are potentially immunogenic, could coalesce to form larger particles over time, or function as nuclei for further aggregation. Even though the United States Pharmacopeia (USP) and the European Pharmacopoeia (Ph. Eur.) currently define concentration limits in parenteral solutions only for particles larger than 10 μm, regulatory authorities increasingly expect quantitative characterization of micron particles from 1 to 10 μm and qualitative characterization of submicron particles from 100 to 1000 nm, in early stages of the development phase (Weinbuch et al., 2013).

The techniques employed in this study were DLS which investigates particle sizes in the submicron range and SEC-HPLC which detects protein aggregates <100 nm. A study performed by Nidhi et al. compared the ability of Micro Flow Imaging (MFI) to detect protein aggregation versus SEC-HPLC during a monoclonal antibody freeze-thaw study. MFI was capable of detecting aggregated forms in the sub-visible particles range of 1-10 μm of protein and was shown to be more sensitive than SEC-HPLC (Nidhi et al., 2011). Future work would include MFI as a technique to compliment SEC-HPLC and DLS analysis of samples for aggregate detection. Fourier Transform

Infrared Spectroscopy (FT-IR) can be used for protein structural characterisation. Application is particularly pertinent to analysis of secondary structure in liquid and solid state. FT-IR has been widely used to characterise protein structure in precipitates, in amyloids and fibrils and in solid lyophilised state. It has also been useful to understand the mechanism of non-native aggregation as it can point to conformational changes that may take place prior to aggregation (Wang and Roberts, 2010). In that study all analysis of aggregation was performed in the thawed state. It would be interesting to study protein conformation and aggregation in the frozen solid state using a technique such as FT-IR.

- **Establish model based on the Plank equation to determine freezing time and investigate its ability to accurately predict freezing time**

The current study developed empirical models to predict freezing time, however fundamental theoretical models are considered to be advantageous as they can be extrapolated outside the set of experiments used to establish them. The Plank equation is a key equation used to predict freezing time and future experimental work is required to establish this equation for the freezers studied.

As described by Radmanovic et al. the freezing process can also be described as a one-dimensional heat transfer process or alternatively a thermal equilibrium between heat transferred by the cooling plates and the heat liberated during ice crystallization (Radmanovic et al., 2013).

$$t = \frac{s^2 \, Lf \, \rho}{\lambda d\vartheta} \qquad \textbf{[Equation 5-1]}$$

where:

- t is freezing time

- L_f represents the latent heat of fusion of the substance being 333.5 kJ/kg for water
- ρ is density of ice being 916.7 kg/m^3 at 0 ˚C
- λ is thermal conductivity of the system
- $d\vartheta$ is mean temperature difference between freeze container content and cooling plates and is calculated as difference between the mean cooling plate temperature over the course of freezing time and 0 ˚C
- s is pathlength or thickness of the dimensional object

Using this equation, the duration of freezing can be predicted with just one unknown parameter - the thermal conductivity, which can be empirically determined. Thermal conductivity depends on the freezing kinetics of the specific freezer and can be determined experimentally using water as the freezing medium as the latent heat of fusion is well known (333.5 J/g) (Radmanovic et al., 2013). Measurement of the temperature profiles and the actual freezer temperature as the water freezes would allow measurement of the freezing plateau time for each bottle/freezer combination. An overview of experiments to determine thermal conductivity has been outlined in **Table 5-1**. The set of experiments described cover the two freezers used for the freeze-thaw DoE conducted in this thesis. These freezers bracket the commercial scale freezer which has a set-point of -30 ºC.

Table 5-1: Experimental overview for determination of freezing kinetics and thermal conductivity for different freezers with different temperature set points

Bottle size (L) / fill (kg)	Number of bottles to be frozen per freezer		
	-20 °C (Lab Scale)	**-30 °C (Manufacturing Scale)**	**-80 °C (Lab Scale)**
0.125 / 0.0875	1	1	1
	9	9	9
1 / 0.7	1	1	1
	2	6	6
2 / 1.4	1	n/a	n/a
	2	4	4
	4	n/a	n/a
5 / 3.5	n/a	1	1
	n/a	4	4

Power is calculated as Joules per second. Therefore, the power of each freezer can be determined by multiplying the mass of ice frozen by the latent heat of fusion for ice and dividing by the freezing plateau time, as measured from the temperature profiles. Plotting the power versus observed freezer temperature allows an empirical correlation of the freezing time for each freezer that is equivalent to that determined by the Plank equation. The heat transfer coefficient (h) is calculated empirically, as the surface area, freezer temperature and power are all known or calculated values. This allows prediction of freezing time and temperature for any size and quantity of product using relatively simple algebraic equations.

6.0 CONCLUSIONS

This research project was conceived to perform a high-level experimental assessment of the freeze and thaw process for Protein Y FDS in polycarbonate bottles at a reduced scale (lower than commercial volumes) in order to evaluate the effect of freeze/thaw parameters on Protein Y aggregation and tertiary structure in a formulated therapeutic protein solution. The work was envisaged to assess the scalability of these experiments to the respective full-scale commercial process.

Analytical methods for characterisation of Protein Y were developed to detect changes in aggregation and tertiary structure of the protein. The methods were then utilised as responses, along with analysis of temperature/time profiles in a DoE study to assess the main process factors affecting these responses. The DoE demonstrated that the factors studied can have a statistically significant impact on temperature profile and consequently rate of heat transfer. The experiments showed that slower rates of freezing induced by co-loading of bottles, result in changes to the tertiary structure and subsequently in subtle aggregation changes as determined by DLS. Similarly, slower thaw rates were also shown to have more impact on changes in tertiary structure and aggregation as measured by DLS.

With respect to scalability of the experiments, despite the shorter freeze and thaw times, which would be expected with a smaller volume of FDS, the DLS data supports that levels of aggregation are equivalent to the bulk control FDS material over time. Also, while fluorescence, near-UV CD and 2nd derivative UV did show slight changes in protein tertiary structure. Determination of SA:V ratios for laboratory and commercial scale respectively, and the use of the differential as a scaling factor resulted in reasonable prediction of expected freeze and thaw time for the commercial scale using empirical models established using DoE results.

7.0 BIBLIOGRAPHY

Bhatnagar, B. S., Bogner, R. H.and Pikal, M. J. (2007). Protein stability during freezing: Separation of stresses and mechanisms of protein stabilization. *Pharmaceutical Development and Technology*, *12*(5), 505–523. https://doi.org/10.1080/10837450701481157

Bond, M. D., Panek, M. E., Zhang, Z., Wang, D., Mehndiratta, P., Zhao, H., Gunton, K., Ni, A., Nedved, M. L., Burman, S. and Volkin, D. B. (2010). Evaluation of a dual-wavelength size exclusion HPLC method with improved sensitivity to detect protein aggregates and its use to better characterize degradation pathways of an IgG1 monoclonal antibody. *Journal of Pharmaceutical Sciences*. https://doi.org/10.1002/jps.22034

Cao, E., Chen, Y., Cui, Z.and Foster, P. R. (2003). Effect of freezing and thawing rates on denaturation of proteins in aqueous solutions. *Biotechnology and Bioengineering*, *82*(6), 684–690. https://doi.org/10.1002/bit.10612

Chang, B. S. (1996). Surface-induced denaturation of proteins during freezing and its inhibition by surfactants. *Journal of Pharmaceutical Sciences*, *85*(12), 1325–1330. https://doi.org/10.1021/js960080y

Dill, K. A., and Shortie, D. (1991). Denatured states of proteins, *Annu. Rev. Biochem.* 795–825. https://doi.org/10.1146/annurev.bi.60.070191.004051

Dobson, C. (2003). Protein Folding and Misfolding, *Nature, 426*(6968), 884-890. https://doi.org 10.1038/nature02261

Dong, A., Prestrelski, S. J., Allison, S. D. and Carpenter, J. F. (1995). Infrared spectroscopic studies of lyophilization- and temperature-induced protein aggregation. *Journal of Pharmaceutical Sciences*. 84(4) 415-424 https://doi.org/10.1002/jps.2600840407

Eckhardt, B. M., Oeswein, J. Q., Bewley, T. A. (1991). Effect of freezing on aggregation of human growth hormone. *Pharmaceutical Research, (8)*11, 1360-1364. https://doi.org/10.1023/A:1015888704365

Fesinmeyer, R. M., Hogan, S., Saluja, A., Brych, S. R., Kras, E., Narhi, L. O., Brems, D. N. and Gokarn, Y. R. (2009). Effect of ions on agitation- and temperature-induced aggregation reactions of antibodies. *Pharmaceutical Research*, *26*(4), 903–913. https://doi.org/10.1007/s11095-008-9792-z

Gómez, G., Pikal, M. and Rodríguez-Hornedo, N. (2001). Effect of initial buffer composition on pH changes during far-from-equilibrium freezing of sodium phosphate buffer solutions. *Pharmaceutical Research, 18(1)*, 90-97. https://doi.org/10.1023/A:1011082911917

Hamrang, Z., Hussain, M., Tingey, K., Tracka, M., Casas-Finet, J. R., Uddin, S., Van Der Walle, C. F. and Pluen, A. (2015). Characterisation of stress-induced aggregate size distributions and morphological changes of a bi-specific antibody using orthogonal techniques. *Journal of Pharmaceutical Sciences*, *104*(8), 2473–2481. https://doi.org/10.1002/jps.24530

Hawe, A., Kasper, J. C., Friess, W. and Jiskoot, W. (2009). Structural properties of monoclonal antibody aggregates induced by freeze-thawing and thermal stress. *European Journal of Pharmaceutical Sciences*, *38*(2), 79–87. https://doi.org/10.1016/j.ejps.2009.06.001

Houde, D. J. and Berkowitz, S. A. eds. (2014). *Biophysical Characterization of Proteins in Developing Biopharmaceuticals*. Elsevier. https://doi.org/10.1016/C2012-0-01163-5

Hsu, C. C., Nguyen, H. M., Yeung, D. A., Brooks, D. A., Koe, G. S., Bewley, T. A. and Pearlman, R. (1995). Surface denaturation at solid-void interface - A possible pathway by which opalescent participates form during the storage of lyophilized tissue-type plasminogen activator at high temperatures. *Pharmaceutical Research: An Official Journal of the American Association of Pharmaceutical Scientists*. 12(1) 69-77 https://doi.org/10.1023/A:1016270103863

Hui, Y., Xue, X., Xuesong, Z. and Yan, W. U. (2015). Intrinsic fluorescence spectra of tryptophan, tyrosine and phenyloalanine, *5th International Conference on Advanced Design and Manufacturing Engineering* , 224–233. https://doi.org/ 10.1117/12.2268397

ICH. (2012). Development and manufacture of drug substances (chemical entities and biotechnological/ biological entities) Q11. *International Conference on Harmonisation*. https://doi.org/10.5639/gabij.2012.0103.025

Izutsu, K., Yoshioka, S. and Terao, T. (1993). Izutsu et al, 1993, Pharm Res, Decreased protein-stabilizing effects of cryoprotectants due to crystallization, *Pharmaceutical Research*, *10*(8), 1232–1237. https://doi.org/10.1023/A:1018988823116

Jagschies, G., Lindskog, E., Lacki, K. and Galliher, P. eds. (2018). *Biopharmaceutical Processing: Development, Design, and Implementation of Manufacturing Processes*. Elsevier. https://doi.org/10.1016/C2014-0-01092-1

Jiang, S. and Nail, S. (1998). Effect of process conditions on recovery of protein activity after freezing and freeze-drying. *European Journal of Pharmaceutics and Biopharmaceutics 45*(3), 249-257. https://doi.org/10.1016/S0939-6411(98)00007-1

Jiskoot, W., Bloemendal M., van Haeringen, B., van Grondellez, R., Beuvery, E. C., Herron, J. N. and Crommelin D. J. A. (1991). Non-random conformation of a mouse IgG2a monoclonal antibody at low pH. *European Journal of Biochemistry 201*(1) 223-232. https://doi.org/10.1111/j.1432-1033.1991.tb16278.x

Kantor, A., Warne, N. and Tchessalov, S. (2011). Quality-by-design for freeze-thaw of biologics: Concepts and application to bottles of drug substance. *American Pharmaceutical Review*, 1–14.

Katayama, D. S., Nayar, R., Chou, D. K., Campos, J., Cooper, J., Vander Velde, D. G., Villarette, L., Liu, C.P. and Cornell Manning, M. (2005). Solution behavior of a novel type 1 interferon, interferon-τ. *Journal of Pharmaceutical Sciences*, *94*(12), 2703–2715. https://doi.org/10.1002/jps.20461

Kelly, S. M., Jess, T. J., and Price, N. C. (2005). How to study proteins by circular dichroism. *Biochimica et Biophysica Acta - Proteins and Proteomics*, *1751*(2), 119–139. https://doi.org/10.1016/j.bbapap.2005.06.005

Kolhe, P. and Badkar, A. (2011). Protein and solute distribution in drug substance containers during frozen storage and post-thawing: A tool to understand and define freezing-thawing parameters in biotechnology process development. *Biotechnology Progress*, *27*(2), 494–504. https://doi.org/10.1002/btpr.530

Kueltzo, L. A., Wang, W., Randolph, T. W. and Carpenter, J. F., (2008). Effects of solution conditions, processing parameters, and container materials on

aggregation of a monoclonal antibody during freeze-thawing. *Journal of Pharmaceutical Sciences*, *97*(5), 1801–1812. https://doi.org/10.1002/jps.21110

Lam, X. M., Costantino, H. R., Overcashier, D. E., Nguyen, T. H., Hsu, C. C. (1996). Replacing succinate with glycolate buffer improves the stability of lyophilized interferon-7. *International Journal of Pharmaceutics, 142*(1), 85-95. https://doi.org/10.1016/0378-5173(96)04656-X

Lamanna, W. C., Holzmann, J., Cohen, H. P., Guo, X., Schweigler, M., Stangler, T., Seidl, A. and Schiestl, M. (2018). Maintaining consistent quality and clinical performance of biopharmaceuticals. *Expert Opinion on Biological Therapy*, *18*(4), 369–379. https://doi.org/10.1080/14712598.2018.1421169

López-Leiva, M. and Hallström, B. (2003). The original Plank equation and its use in the development of food freezing rate predictions. *Journal of Food Engineering*, *58*(3), 267–275. https://doi.org/10.1016/S0260-8774(02)00385-0

Lu, L., Jones Braun, L., Wang, W., Randolph, T. W. and Carpenter, J. F. (2014). Freezing-induced perturbation of tertiary structure of a monoclonal antibody. *Journal of Pharmaceutical Sciences*, *103*(7), 1979–1986. https://doi.org/10.1007/s11103-011-9767-z.Plastid

Miller, M. A., Rodrigues, M. A., Glass, M. A., Singh, S. K., Johnston, K. P. and Maynard, J. A. (2013). Frozen-state storage stability of a monoclonal antibody: Aggregation is impacted by freezing rate and solute distribution. *Journal of Pharmaceutical Sciences*, *102*(4), 1194–1208. https://doi.org/10.1002/jps.23473

Nema, S. and Avis, E. (1993). Freeze-thaw studies of a model protein, lactate dehydrogenase, in the presence of cryoprotectants. *Journal of Parenteral Science Technology*. 47(2),76-83 https://doi.org/10.1037//0003-066X.46.5.506

Nidhi, K., Indrajeet, S., Khushboo, M., Gauri, K. and Sen, D. J. (2011). Hydrotropy: A promising tool for solubility enhancement: A review. *International Journal of Drug Development and Research*, *3*(2), 26–33. https://doi.org/10.1002/jps

Padala, C., Jameel, F., Rathore, N., Gupta, K. and Sethuraman, A. (2010). Impact of uncontrolled vs controlled rate freeze-thaw technologies on process performance and product quality. *PDA Journal of Pharmaceutical Science and Technology / PDA*, *64*(4), 290–298.

Pikal-Clelend, K., Rodríguez-Hornedo N. G., Amidon, G, Carpenter, J. (2000). Protein denaturation during freezing and thawing in phosphate buffer systems: Monomeric and tetrameric β-galactosidase, *Archives of Biochemistry and Biophysics 384*(2) 398-406. https://doi.org/10.1006/abbi.2000.2088

Privalov, P. L. (1990). Cold denaturation of protein. *Critical Reviews in Biochemistry and Molecular Biology*, *25*(4), 281–306. https://doi.org/10.3109/10409239009090612

Radmanovic, N., Serno, T., Joerg, S. and Germershaus, O. (2013). Understanding the freezing of biopharmaceuticals: First-principle modeling of the process and evaluation of its effect on product quality. *Journal of Pharmaceutical Sciences*, *102*(8), 2495–2507. https://doi.org/10.1002/jps.23642

Rayfield, W. J., Kandula, S., Khan, H. and Tugcu, N. (2016). Impact of freeze/thaw process on drug substance storage of therapeutics. *Journal of Pharmaceutical Sciences*, *106*(8), 1944–1951. https://doi.org/10.1016/j.xphs.2017.03.019

Rupley, J. A., and Careri, G. (1991). Protein hydration and function. *Advances in Protein Chemistry*, *41,* 37-172. https://doi.org/10.1016/S0065-3233(08)60197-7

Sarciaux, J. M., Mansour, S., Hageman, M. J., and Nail, S. L. (1999). Effects of buffer composition and processing conditions on aggregation of bovine IgG during freeze-drying. *Journal of Pharmaceutical Sciences*, *88*(12), 1354-1361. https://doi.org/10.1021/js980383n

Shah, D. D., Zhang, J., Maity, H., and Mallela, K. M. G. (2018). Effect of photo-degradation on the structure, stability, aggregation, and function of an IgG1 monoclonal antibody. *International Journal of Pharmaceutics*, *547*(1–2), 438–449. https://doi.org/10.1016/j.ijpharm.2018.06.007

Shikama, K. and Yamazaki, T. (1961). Denaturation of catalase by freezing and thawing [18]. *Nature 190*(4770), 83-84. https://doi.org/10.1038/190083a0

Schwartz, P. L. and Batt, M. (1980). The aggregation of human growth hormone in response to freezing and thawing. Endocrinology 92: 1795–1798.

Singh, Satish K. and Nema, S. (2010). Freezing and thawing of protein solutions. In *Formulation and Process Development Strategies for Manufacturing Biopharmaceuticals.* John Wiley and Sons, 625–677. https://doi.org/10.1002/9780470595886.ch26

Strambini, G. B. and Gabellieri, E. (1996). Proteins in frozen solutions: evidence of ice-induced partial unfolding. *Biophysical Journal*, *70*(2), 971–976. https://doi.org/10.1016/S0006-3495(96)79640-6

Strambini, G. B. and Gonnelli, M. (2007). Protein stability in ice. *Biophysical Journal*, *92*(6), 2131–2138. https://doi.org/10.1529/biophysj.106.099531

Telikepalli, S., Kumru, O., Kalonia, C., Esfandiary, R., Joshi, S. B., Middaugh, C. R., and Volkin, D. B. (2014). Structural Characterization of IgG1 mAb Aggregates and Particles Generated Under Various Stress Conditions. *Journal of Pharmaceutical Sciences, 103*(3) 796-809. https://doi.org/10.1002/jps.23839

Vermeer, A. W. P. and Norde, W. (2000). The thermal stability of immunoglobulin: Unfolding and aggregation of a multi-domain protein. *Biophysical Journal*, *78*(1), 394–404. https://doi.org/10.1016/S0006-3495(00)76602-1

Vulto, A. G. and Jaquez, O. A. (2017). The process defines the product: what really matters in biosimilar design and production? *Rheumatology (Oxford, England), 56*(4), iv14-iv29. https://doi.org/10.1093/rheumatology/kex278

Walsh, G. (2018). Biopharmaceutical benchmarks 2018. *Nature Biotechnology*, *36*(12), 1136–1145. https://doi.org/10.1038/nbt.3040

Wang, W. (2000). *Lyophilization and development of solid protein pharmaceuticals. International Journal of Pharmaceutics, Vol. 203*, 1-60. https://doi.org/10.1016/S0378-5173(00)00423-3

Wang, W. and Roberts, C. eds. (2010). *Aggregation of Therapuetic Proteins*. John Wiley and Sons.

Wang, W., Nema, S. and Teagarden, D. (2010). Protein aggregation-pathways and influencing factors. *International Journal of Pharmaceutics*, *390*(2), 89–99. https://doi.org/10.1016/j.ijpharm.2010.02.025

Weinbuch, D., Zölls, S., Wiggenhorn, M., Friess, W., Winter, G., Jiskoot, W. and Hawe, A. (2013). Micro-flow imaging and resonant mass measurement (archimedes) - complementary methods to quantitatively differentiate protein particles and silicone oil droplets. *Journal of Pharmaceutical Sciences*, *102*(7), 2152–2165. https://doi.org/10.1002/jps.23552